Defence Research and Development Canada
Recherche et développement pour la défense Canada

DEFENCE R&D DÉFENSE

Missile flight control using micro-actuated flow effectors

-Review of fiscal year 2005/2006 progress

F.C. Wong
DRDC Valcartier

Defence R&D Canada – Valcartier
Technical Note
DRDC Valcartier TN 2006-178
August 2006

Canada

Missile flight control using micro-actuated flow effectors

– *Review of fiscal year 2005/2006 progress*

F.C. Wong
DRDC Valcartier

Defence R&D Canada – Valcartier

Technical Note

DRDC Valcartier TN 2006-178

August 2006

Author

Franklin Wong

Marc Lauzon

Interim Head/Precision Weapons

Approved for release by

Gilles Bérubé

Chief Scientist

This work was performed by DRDC – Valcartier and its collaborators between April 2005 and March 2006 under WBE 13eg16 Supersonic Missile Flight Control by Manipulation of the Flow Structure using Microactuated Surfaces. The project is financed by the DRDC Technology Investment Fund.

Abstract

Superior performance is a key goal in weapons design. Missiles must fly faster and farther, and be more agile, compact and lightweight. The United States have been very active in the development of smart structures for military applications such as missile guidance. For example, DARPA and the Air Force Office of Scientific Research are sponsoring the development of miniaturized active flow technologies to achieve far-term objectives for smart bombs and missiles. Their principal concepts for altering the flow around a body are centred on miniaturized devices that are embedded in the missile skin and/or airframe. The objective of this project is to demonstrate with hardware and software: 1) engineered micro-flow effectors of specific geometry and placement that are able to produce controllable aerodynamic forces on a missile under supersonic conditions or a delta wing under subsonic conditions, 2) microactuators that are able to meet the force, kinematic and thermal requirements set by the aerothermal environment, and 3) control algorithms running on non-flightweight electronics and feedback sensors that take in command signals and output appropriate actuator drive signals to produce the desired aerodynamic force on a wind or water tunnel delta wing model. This document records the progress made by the project members for fiscal year 2005/2006 in the areas of missile aerodynamics, delta wing aerodynamics, microactuator modeling, control synthesis and micro-fabrication.

Résumé

Une performance supérieure est un objectif fondamental dans la conception d'armes. Les missiles doivent voler plus rapidement, sur de plus grandes distances et être plus agiles, plus compacts et plus légers. Les États-Unis ont été très actifs dans le développement de structures intelligentes pour des applications militaires telles que le guidage des missiles. Par exemple, DARPA et l'*Air Force Office of Scientific Research* commanditent le développement de technologies d'écoulement actif en vue d'objectifs à long terme pour les bombes et missiles intelligents. Leurs principaux concepts pour modifier l'écoulement autour d'un corps portent sur les dispositifs miniaturisés qui font partie du revêtement et/ou de la cellule du missile. L'objectif de ce projet est de démontrer : 1) que les microsurfaces d'une forme particulière et leur mise en place peuvent produire des forces aérodynamiques contrôlables sur un missile dans des conditions supersoniques ou une aile delta dans des conditions subsoniques; 2) que les microactionneurs peuvent répondre aux exigences de force, cinématique et thermique; et 3) que les algorithmes de contrôle fonctionnant sur les équipements du laboratoire captent les signaux d'entrée et génèrent des signaux qui produisent la force aérodynamique désirée sur un modèle d'aile delta dans un tunnel aérodynamique ou hydrodynamique. Ce document fait état des progrès accomplis par les participants au projet durant l'année financière 2005-2006 dans les domaines de l'aérodynamique du missile, de l'aile delta, de la modélisation du microactionneur, de la synthèse du contrôle et de la microfabrication.

This page intentionally left blank.

Table of Contents

This page intentionally left blank.

1. Introduction

Superior performance is a key goal in weapons design. Missiles must fly faster and farther, and be more agile, compact and lightweight. The United States has been very active in the development of smart structures for military applications such as missile guidance. For example, DARPA and the Air Force Office of Scientific Research are sponsoring the development of miniaturized active flow technologies to achieve far-term objectives for smart bombs and missiles. Their principal concepts for altering the flow around a body are centred on miniaturized devices such as magnetic microflap actuators, bubble actuators, micro-synthetic jets, micro-jet actuators and Co-Located Actuator and Sensor (CLAS) units.

The success of using smart structures for active flow control depends on a micro-flow effector's ability to influence the macroscopic flow around the missile. Missiles with slender forebodies face significant yawing moments under asymmetric vortices. Controlling forebody vortex asymmetry is dependent on the sensitivity of the asymmetric flow to the distance between the micro-flow effector and the nose tip. The closer the micro-flow effector is to the nose tip, the lower the power required to trigger flow changes. Several techniques for manipulating forebody vortices have been investigated. Most methods are essentially steady schemes that produce quasi-steady loads by forcing the forebody vortices into desired positions.

The Defence R&D Canada project "Supersonic Missile Flight Control by Manipulation of the Flow Structure using Micro-Actuated Surfaces" was officially started on 1 April 2003. The project termination date is 31 March 2006. The objective of the project is to demonstrate with hardware and software the following items:

a) Engineered micro-flow effectors of specific geometry and placement that are able to produce controllable aerodynamic forces on a missile under supersonic conditions or a delta wing under subsonic conditions.

b) Microactuators that are able to meet the force, kinematic and thermal requirements set by the aerothermal environment. The availability of microactuators necessarily means that material and fabrication issues have been resolved to the extent that prototypes can be made.

c) Control algorithms running on non-flightweight electronics and feedback sensors that take in command signals and output appropriate actuator drive signals to produce the desired aerodynamic force on a wind or water tunnel delta wing model.

A meeting was held on 19 April 2006 at DRDC Valcartier to make formal presentations that informed the participants on the progress that was made from 1 April 2005 to 31 March 2006. As a secondary objective, the meeting was held to promote a better understanding on the technical issues that must be addressed in future work as the team works towards achieving the project objectives.

All participants were asked to provide a 250 word abstract and a PowerPoint presentation containing the following elements as they were applicable:

1) title page stating title of presentation, contributors, name of organization and date

2) previous studies in the open literature,
3) geometry studied,
4) test set up and instrumentation,
5) modeling assumptions,
6) governing equations of phenomenon,
7) parametric study,
8) major observations and problems,
9) conclusions,
10) future work.

This documents collects the presentations made by the project members in the areas of missile aerodynamics, delta wing aerodynamics, microactuator modeling, control synthesis and micro-fabrication. The abstracts provided by the participants precede their presentations.

2. Lessons Learned about Multi-disciplinary Interaction

Development of active flow control technology requires advances in the areas of aerodynamics, microactuator design and fabrication and control synthesis to construct a workable active flow control system. The hierarchy shown in Figure 1 described best the interrelationships and flow of the development process. Because active flow attempts to alter the flow structure, the fundamental problem in the case of aerovehicles is one of aerodynamics. The success of active flow control technology rests on the proper understanding of the interaction between parameters

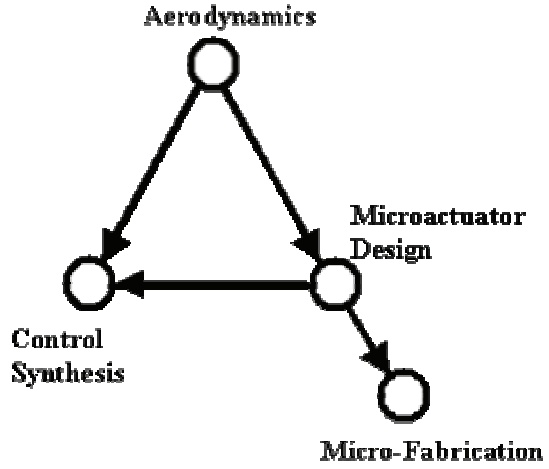

Figure 1. Information flow between technologies

that affect the nonlinear flow phenomenon and the resultant aerodynamic forces. The microactuator design can proceed once the aerodynamic loads and the required deflections and actuation frequencies are known. Actuator modeling activities are centred on materials selection, characterization and mechanism synthesis. Control synthesis necessarily requires a mathematical description of the processes that it aims to control. In this case, control algorithm development aims to optimize a highly nonlinear, time-dependent airflow-microactuator response to a given command input. The system model is used to evaluate the performance of a proposed aero-mechanical-control system and can provide insight as to the areas where performance gains can be obtained. The micro-fabrication activity is dependent on the progress made in the microactuator design. With the great strides made in the fabrication of micro-electromechanical systems, the problem for active flow control devices is centred on the development of machining and joining techniques to make a miniature multi-material, multi-component device.

The progress in the second year of the project has been steady though arduous. Each technology group worked in semi-isolation in order to concentrate on the detailed model development or experimental measurement particular to the technology. This step was necessary so that there is a high confidence in the data and tools that will be used in the system level trade-off studies.

In the final year, the experimental missile aerodynamic work was reduced to allow the CFD studies time to examine the flow physics in detail. With the position and geometry of the flow effectors determined, it was possible to design a dynamic flow effector because the capability of the SMA actuator was also known. The process followed a linear progression moving from flow effector design to micro-fabrication to sub-scale assembly and then to control synthesis. The preliminary studies carried out for micro-fabrication and control algorithm development permitted insights to be made into the factors that affected the performance in each of the technology areas.

2.1 Participant Impressions

At the end of the 2005/2006 review meeting, a questionnaire was given to the participants to record their impressions on lessons learned, group interaction and ideas for potential follow-on projects. The following paragraphs summarize their assessments.

1. What were the 'lessons learned' for your particular technology?

The flow effector position can influence the vortex system so differently. Excellent project to have multiple disciplines together to understand the problem/project in a comprehensive way.

CFD results are dependent on the turbulence model used. A more exhaustive study using different turbulence models and CFD codes would provide a greater level of confidence in the results.

You never know until you try but all reasonable results come from careful thinking and deep understanding of the principles of flow behaviour.

From the aerodynamic point of view, the application of the micro-flow effector to a supersonic missile appears limited. Vortices can only be affected at low speeds or low supersonic Mach number. Vortices form at angles of attack between 10 and 20 deg. It is not obvious to have a missile flying at such an attitude. Micro-flow effectors might have more application for cancelling side forces than to generate side forces.

For SMA's, cooling time constants of the material limit the actuation frequency. Forced cooling can be used however the actuator then loses its simplicity of design.

To achieve a high actuation rate, the configuration of the actuator must be considered in addition to actuator material. The antagonistic arrangement is a good example. Maybe another arrangement could be better.

Experimentation for SMA control was the main issue. Several iterations between theory and practice were and are still necessary.

Require experimental results for control proofs. Sophisticated control methods are needed to achieve satisfactory performance. Delta wing problem is a good demonstration of control synthesis development.

Experimentation is very important for active flow control development.

Timely development of micro-milling technology allowed fabrication of flow effectors with desired accuracy. For higher production rates, laser and milling technique would work effectively. For features sizes less than 100 micron and acute angles, lasers may still be an effective tool.

2. What were the 'lessons learned' while working in a multi-disciplinary group?

Could start with CFD conceptual computations then design experiments for several typical cases. Detailed CFD could be re-run afterwards to corroborate results.

The flow of information begins with the aerodynamic results. A viable aerodynamic control method is required to set the context for the structures, controls and fabrication efforts.

Two heads are better than one. It is very important to have a multi-disciplinary team in one group to make a project work and to ensure that people are benefitting from each other's expertise.

It is important to start the integration of the various technologies early on in the project in order to have enough time to face the inherent problems associated with the various technologies.

Controlling the actuator depends on the mechanical/electrical design, the aerodynamics and the control algorithms. Integrated design is necessary to achieve good performance of multi-component systems.

It is difficult to work on a problem with variables that depend on other technology domains especially when those variables are essential to advance our own work.

It was interesting to see how other disciplines approached technical problems.

Early development of the delta wing vortex breakdown model was very useful for the development of roll control algorithms.

Difficult to understand other technologies. Not everyone understood the need for dynamic feedback control. Sometimes, each technology assigned different meanings to similar words.

Understanding of the aerodynamics, modeling the flow patterns and the design and control of the actuators laid out a clear path towards product development although there is still significant practical work that remains to be done.

3. What could the group have done better during the past three years to advance the technology beyond the point that we are at today?

Some flow visualization studies in addition to CFD analyses would have helped understand the flow mechanism better.

The decision to carry out CFD studies on the missile and delta wing configuration allowed us to minimize the risks associated with the project. However, a review after the first year's effort to decide which platform to focus on could have permitted greater comprehension of the flow physics on the chosen platform.

Have group review meetings twice a year instead of just one meeting.

A better literature review on missile aerodynamics could have allowed a better application of the micro-flow effector to be developed.

A common analysis model covering the aerodynamic-flow effector interaction, the compliant mechanism-SMA dynamics and the control algorithm synthesis would have permitted more concepts and systems issues to be examined.

The group worked well together during the last three years to achieve the objectives. However, the time required to complete all objectives may have been underestimated which would explain why the project could not be completely finished by 31 March 2006.

Having monthly review meetings is required to stay on schedule.

More interaction between the design of the compliant mechanism and the control group would have been helpful.

More understanding of other people's technologies. A more focused approach with fewer topics would have helped.

A student internship program could have been helpful.

Early input on aerodynamics and modeling studies would have taken the project further in the completion of the first prototype integrated device. Most the results achieved remain at the fundamental understanding/scientific level.

4. What follow-on studies can you forsee as a result of the technology developed in this project?

Continue to examine the flow effector and missile fin configuration to examine the interaction between the fin and the vortex caused by the flow effector. Look at Reynolds and Mach number effects. Continue CFD study of delta wing.

Control of the boundary layer on flapping wings or delta wings.

Drag reduction of projectiles at high angles of attack.
Application of micro-flow effectors to low velocity ammunition.

Long range unspun artillery projectile control.

Actuators for munitions must remain compact yet be able to produce displacements in the millimeter range at frequencies up to 100 Hz. Piezoceramic materials coupled to a compliant mechanism is an area that could be investigated.

Investigate MEMS to speed up dynamic response.

Solenoid actuators for flow control and further experimentation on the delta wing.

Outer loop flow control integrated with NRC delta wing testbed.

Examine implementation issues such as real-time performance of receding horizon control for outer loop control of delta wing.

Would like to see the validation of the prototype missile flow effector device.

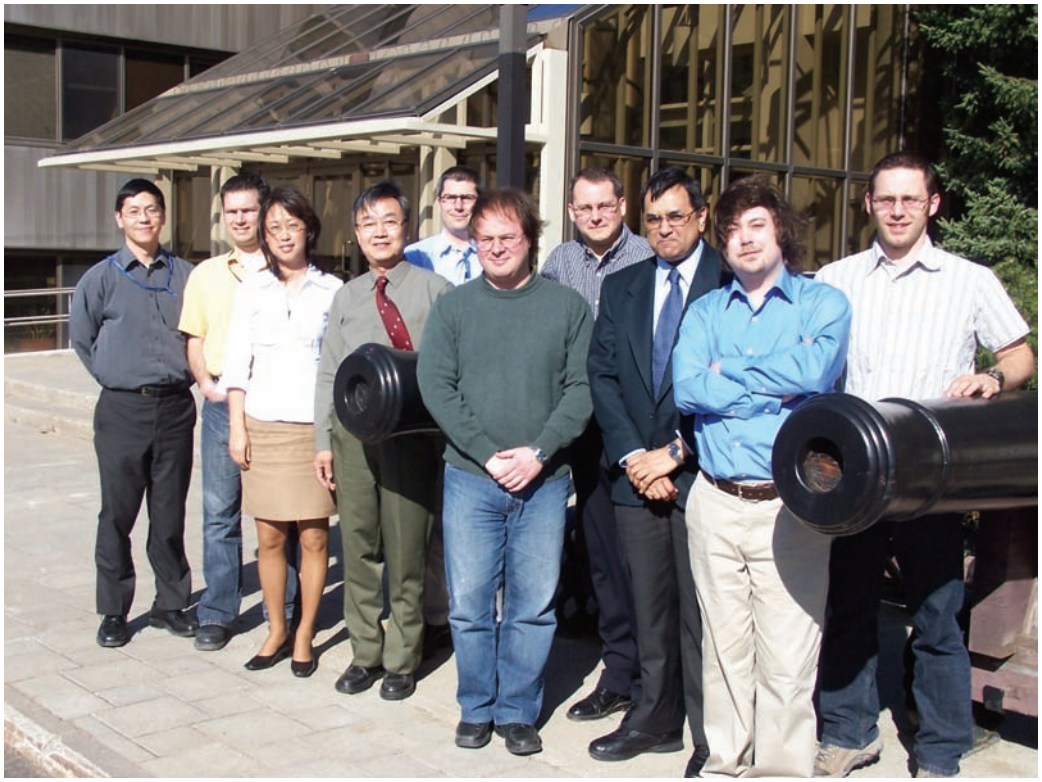

Figure 2. Project participants (r to l) Olivier Boissonneault, Brandon Gordon, Suwas Nikumb, Daniel Corriveau, Nicolas Léchevin, Camille Alain Rabbath, Xingzhong Huang, Suzhen Chen, Nicolas Hamel, Frank Wong

This page intentionally left blank.

3. Cumulative Action Items

Legend for groups:
DRDC-aero: Daniel Corriveau, Nicolas Hamel, François Lesage
DRDC-struct: Frank Wong, Olivier Boissonneault (ETS)
Numerica: Pierre Antoine Ranville, Pierre Gosselin
IAR-cfd: Suzhen Chen, Stuart McIlwain, Mahmood Khalid
IMTI: Suwas Nikumb, Dan Zhang
ETS: Patrick Terriault
Concordia: Wei Wei Liu, Brandon Gordon

Legend for individuals:
IAR-xzh: Xing Zhong Huang
IAR-sc: Suzhen Chen
IMTI-sn: Suwas Nikumb
DRDC-dc: Daniel Corriveau
DRDC-car: Camille Alain Rabbath
DRDC-fw: Frank Wong

April 2005 Action Items

Y0405-1. Continue with pressure measurements and oil or vapor screen visualization studies on the DRDC-B1AC2R model with and without fins. Determine how separation line changes with flow effector position.
Action: **DRDC-dc** (May-Sep 2005)

Y0405-2. Compare pressure measurements and flow visualization results with current set of CFD results.
Action: **DRDC-dc, DRDC-nh, IAR-sc** (May-July 2005)

Y0405-3. Carry out additional CFD analysis for the finless DRDC-B1AC2R between 15 deg. to 20 deg. to determine where the peak side force is situated. Compare pressure distribution with IAR results.
Action: **DRDC-nh** (April-May 2005)

Y0405-4. Produce joint DRDC-IAR paper comparing CFD to wind tunnel results. Propose explanation on how the flow effector generates the observed side forces.
Action: **DRDC-dc, IAR-sc**

Y0405-5. Produce joint DRDC-IAR paper comparing results from Fluent and SPARC CFD codes and various turbulence models.

Action: **DRDC-nh, IAR-sc**

Y0405-6. Carry out CFD study on DRDC-B1AC2R with fins. Decide on analysis matrix. Coordinate with wind tunnel test matrix.
Action: **DRDC-nh**

Y0405-7. Decide on the best way to visualize the separation line from the CFD results.
Action: **DRDC-nh, IAR-sc** (May 2005)

Y0405-8. Characterize Dynalloy SMA. Construct small-scale test bench.
Action: **DRDC-ob** (May 2005)

Y0405-9. Examine ability of SMA model to predict response under complex force profile.
Action: **DRDC-ob** (June-July 2005)

Y0405-10. Investigate methods to increase frequency response of the SMA wire given force requirements.
Action: **DRDC-ob, DRDC-fw** (Aug-Sep 2005)

Y0405-11. Examine impact on the control strategy for a semi-active actuator. Aeroloading is assumed negligible. F. Wong will provide spring constant.
Action: **DRDC-nl, DRDC-car** (May 2005)

Y0405-12. Clarify what aerodynamic data was provided to Concordia and agree on what additional data will be provided.
Action: **Concordia, IAR-xzh**

Y0405-13. Develop method to analyze compliant beam. Integrate method with SMA model to determine appropriate size for beam elements.
Action: **DRDC-fw, DRDC-ob** (May-June 2005)

Y0405-14. Develop manufacturing plan for micro-flow effector.
Action: **DRDC-fw, IMTI-sn** (June 2005)

Y0405-15. Preliminary test to integrate MatLab control law in LabView.
Action: **DRDC-nl, DRDC-car** (May-June 2005)

Y0405-16. Integrate control law in macro- and micro-test bench environment. Explore ability to track command signal.
Action: **DRDC-car, DRDC-nl, DRDC-fw, DRDC-ob** (July 2005)

Y0405-17. Micro-PIV study on 2D wing with pressure taps.

Action: **IAR-xzh** (May 2005)

Y0405-18. Provide delta wing drawings to DRDC. DRDC will provide minimum wing thickness based on actuator requirements.
Action: **IAR-xzh, DRDC-fw** (May 2005)

Y0405-19. Coordinate fabrication of delta wing between IAR and IMTI.
Action: **DRDC-fw**

Y0405-20. Investigate possibly of loaning U. Laval micro-PIV system to IAR to continue delta wing study.
Action: **DRDC-nh** (April 2005)

Y0405-21. Prepare validation test plan for missile model with micro-actuated flow effectors.
Action: **DRDC**

Y0405-22. Prepare validation test plan for delta wing model with micro-actuated leading edge fence.
Action: **DRDC-fw, DRDC-car, IAR-xzh**

Y0405-23. Provide list of papers that will be produced for 2005/2006 including conference details.
Action: **All**

April 2004 Action Items

Y0304-1. Advance individual technology development from April 2004 to February 2005 to the point that integration issues can be addressed in March 2005.
Action: **All**

Y0304-2. Missile geometry will be referred to as the DRDC-B1AC2R geometry. Flow alteration devices will generally be referred to as flow effectors.
Action: **All**

Y0304-3. A common definition for the missile coordinate system will be agreed upon.
Action: **DRDC-aero, Numerica, IAR-cfd**

Y0304-4. A standard, compact nomenclature to describe missile flow effector number, placement and orientation will be developed for use by all participants.
Action: **DRDC-dc**

Y0304-5. DRDC will continue using blunt-edged rectangular flow effectors in its wind tunnel tests unless CFD studies show there is an advantage to using a knife-edged flow effector.

Action: **DRDC-dc**

Y0304-6. Verify Numerica results and the impact of knife-edged flow effectors.

Action: **DRDC-nh, Numerica, IAR-cfd**

Y0304-6.1 Common conditions: 15 deg AOA, flow effector placed at front station, no base drag, freestream conditions M = 1.5, 26kPa, 206K

Y0304-6.2 DRDC will perform a grid refinement study of the short conical nose body with one flow effector at 45 deg orientation to verify if the Numerica CFD result is grid independent.

Y0304-6.3 Numerica will modify the CFD mesh for the short conical nose body with one flow effector at 45 deg orientation to include a knife-edge on the leading and trailing edges of the flow effector. Each knife-edge will occupy one-third of the flow effector chord.

Y0304-6.4 IAR will verify the Numerica blunt-edged flow effector result by analyzing a short conical nose body with one blunt-edged rectangular flow effector oriented at 45 deg.

Y0304-7. If CFD studies show there is no difference between a blunt-edged and knife-edge flow effector, decide whether it is acceptable to compare CFD results derived from a knife-edged flow effector with wind tunnel data derived from a blunt-edged flow effector.

Action: **DRDC-aero, IAR-cfd**

Y0304-8. Determine through wind tunnel and CFD analyses on DRDC-B1AC2R with flow effectors whether it is separation or vortex phenomenon or a combination of the two that produces the observed side forces.

Action: **DRDC-aero, Numerica and IAR-cfd**

Y0304-9. CFD results will be produced for the test cases shown in Table 1. The results will be compared and conclusions on their consistency and trends will be made. We wish to gain confidence that the CFD analyses are able to predict the observed wind tunnel trends so that missile flow effector specifications can be generated for microactuator development.

Action: **DRDC-aero, Numerica and IAR-cfd**

Table 1 – CFD analysis matrix	
Nose	short conical
Body	finless cylindrical
Flow Effectors: number, placement, orientation	 0 (baseline) 1 front at 0 deg 1 front at 45 deg 3 front at 0 deg with 30 deg separation
Angle of attack	0, 10, 15, 20 deg
Freestream conditions	M = 1.5, 26kPa, 206K
Required results	integrated forces streamlines pressure contours C_p profiles at DRDC specified x/L intervals velocity profiles skin friction for whole body

Y0304-10. Complete SMA linear actuator model and assemble test bench for validation and closed-loop control tests.

Action: **DRDC-struct, DRDC-car**

Y0304-11. Reformulate SMA linear actuator model into a form suitable for control synthesis development.

Action: **DRDC-struct, DRDC-car**

Y0304-12. Discuss collaboration on development of compliant mechanism algorithms, compliant mechanism design and prototype fabrication.

Action: **DRDC-struct, IMTI, IAR-sc**

Y0304-13. Discuss plan of work for SMA machining and joining studies.

Action: **DRDC-fw, IMTI-sn, ETS**

Y0304-14. IAR to provide load, deflection, frequency requirements for delta wing to DRDC so that DRDC can examine implications for SMA actuator design.

Action: **IAR-xzh, DRDC-struct**

Y0304-15. DRDC-aero to provide DRDC-struct with preliminary load estimate and deflection requirement for missile flow effector.

Action: **DRDC-aero**

Y0304-16. IAR will provide C_L database to Concordia for further development of delta wing plant model.

Action: **IAR-xzh, Concordia**

Y0304-17. Determine what information aerodynamicists need to provide for control synthesis in a wind tunnel setting.

Action: **DRDC-aero, DRDC-car, DRDC-fw**

Y0304-18. Determine what a closed loop control of a wind tunnel missile equipped with microactuated flow effector experiment would look like.

Action: **DRDC-aero, DRDC-fw, DRDC-car**

Y0304-19. Prepare global timeline to coordinate the rate of progress in the individual technologies.

Action: **DRDC-fw**

Y0304-20. Examine possibility of performing trajectory simulations using force information from microactuated flow effectors to determine their system effectiveness.

Action: **DRDC-fw**

4. Missile and Delta Wing Aerodynamics

4.1 CFD and Experimental Investigation on Side-Force Generation

presented by N. Hamel, DRDC – Valcartier

Using nose-mounted micro-structures, it was shown experimentally and computationally in earlier studies that a significant side force could be generated at moderate angles-of-attack and in supersonic flow on a generic missile configuration. Under these flow conditions, a "clean" slender body would not normally experience any lateral or side forces.

In these earlier investigations, the side force induced by the presence of the micro-structures was shown to peak for angles-of-attack between 15 and 20 degrees. Furthermore, it was found that the magnitude of the side force generated was maximized by positioning the flow effectors at an angular position close to 135 or 225 degrees.

For the current study, surface pressure measurements in the DRDC trisonic wind tunnel as well as additional numerical simulations using FLUENT® were made in order to determine the mechanism by which the nose-mounted micro-structures contributed to the generation of a side force at moderate angles-of-attack where otherwise no side force would be present.

A vortex shed off from the flow effector entrains the matching leeside vortex to eventually merge into a single stronger vortex. The newly formed vortex, being stronger than the opposite side vortex, is forced to move upward above the missile's leeside. The formation of the flow effector vortex arises because of the pressure differential on either side of the flow effector. This pressure difference causes the flow to wrap around the top edge of the flow effector, thus resulting in a vortical flow.

DEFENCE R&D DÉFENSE

CFD and Experimental Investigation on Side-Force Generation

Nicolas Hamel & Daniel Corriveau
Defence R&D Canada – Valcartier

Final Meeting on Missile Control using Micro-actuated Flow Effectors

19 April 2006

Defence Research and Development Canada | Recherche et développement pour la défense Canada

Canada

Presentation Overview

- Objectives
- Missile Configuration
- Test and CFD Setup
- Side Force Generation Mechanism
- Comparison of Results
- Conclusions

Objectives

- Determine the mechanism by which the nose-mounted micro-structures contributed to the side force generation
- Support the wind tunnel test results and help in the interpretation of the results

Missile Configuration

Baseline Geometry With Conical Nose

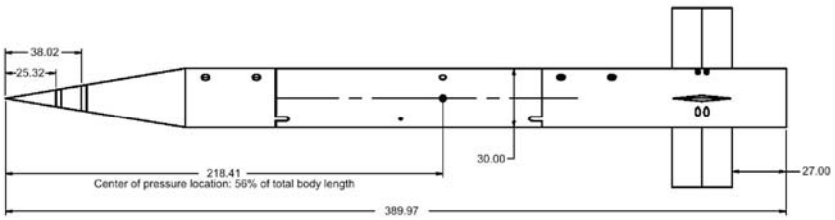

All dimensions in mm

- Aspect Ratio L/D = 13.0
- Nose Aspect Ratio $L_N/D = 3.0$
- Conical Nose
- 4 Fins in + Configuration (Removable)

Missile Configuration

Flow Effector Geometry

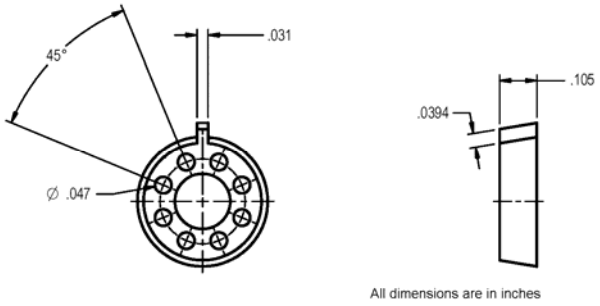

Test Setup and Instrumentation

DRDC Trisonic Wind Tunnel

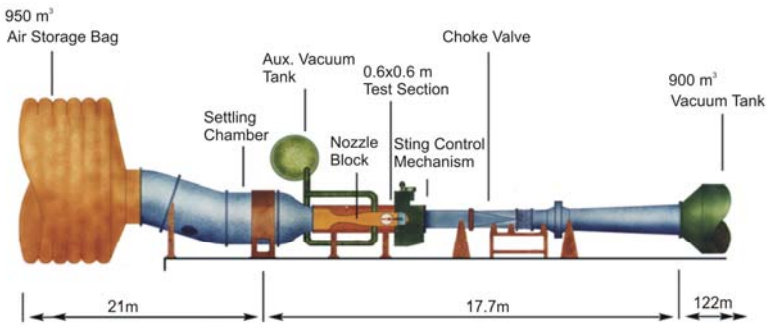

- **Indraft wind tunnel**
- **Test section: 2'x 2'**
- **0.2 < Ma < 4.0**
- **-20° < AOA < +20 °**
- **Test duration: 5 – 11 sec**
- **Turnaround time: 30 min.**

CFD Set-up

- Fluent 6.1
  - RANS with the coupled explicit solver
  - Realizable k-epsilon viscous model
  - Enhanced wall treatment with pressure option
- Wind tunnel freestream conditions
  - Mach Number: 1,5
  - Static Pressure: 26 000 Pa

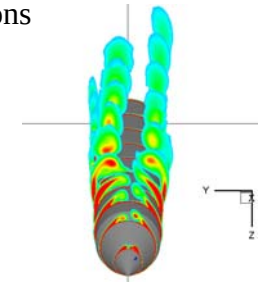

Grid Topology

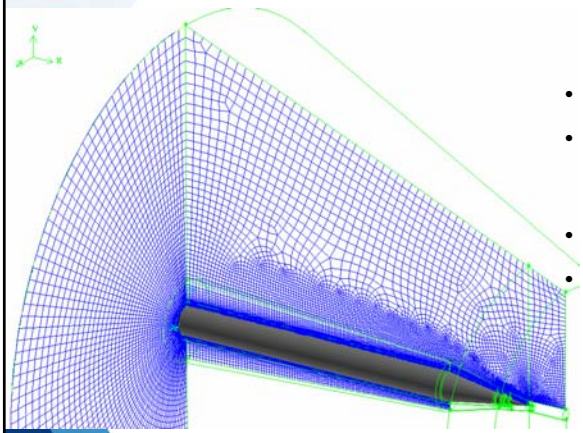

- All Hexahedral
- Structured in the boundary layer and in the vicinity of the model
- Wall Y+ around 1
- 3.3 Million Cells

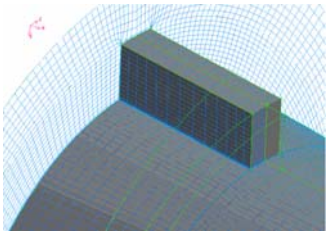

Surface Static Pressure Coefficient

$$C_p = \frac{P_x - P_\infty}{1/2\,\gamma P_\infty M_\infty{}^2}$$

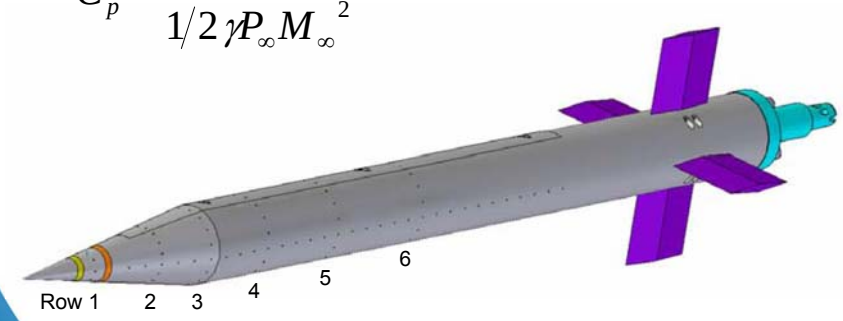

Surface Static Pressure Coefficient

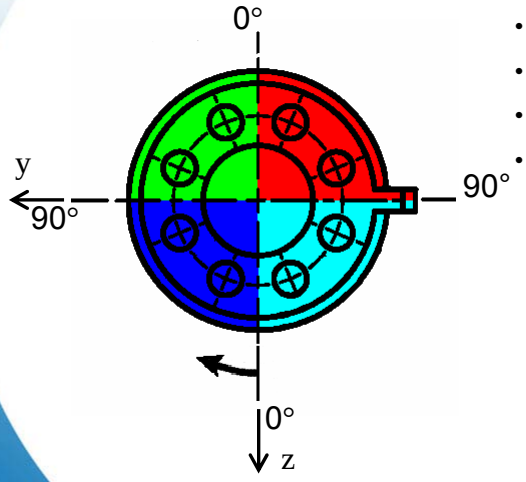

- No fins
- Conical nose L/D= 3
- 1 FE on the front row
- NED coordinate system
  - Blue 0° to 90°
  - Green 90° to 180°
  - Red 180° to 270°
  - Cyan 270° to 360°

Side Force Generation Mechanism

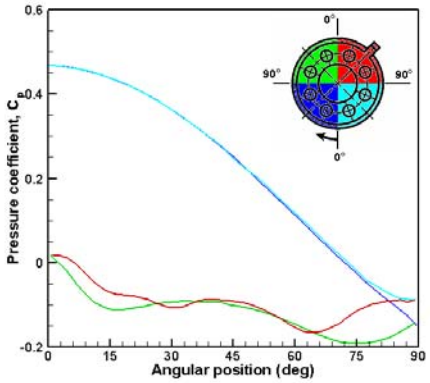

- No fins
- Conical nose L_N/D= 3.0
- Flow effectors centered at 225°
- Front row
- Ma= 1.5 AoA= 20°
- Re/m= 15.2×10^6
- Row 3

Side Force Generation Mechanism

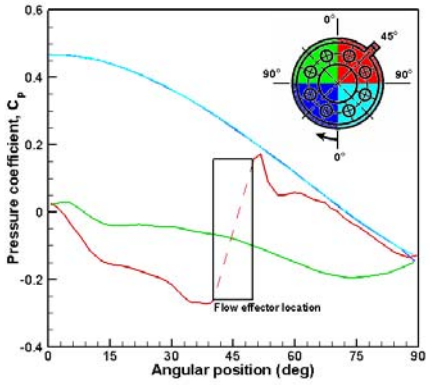

- No fins
- Conical nose L_N/D= 3.0
- Flow effectors centered at 225°
- Front row
- Ma= 1.5 AoA= 20°
- Re/m= 15.2×10^6
- Middle of the FE

Side Force Generation Mechanism

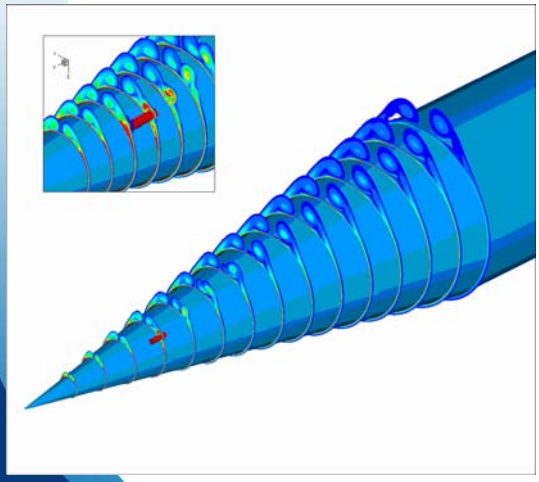

- No fins
- Conical nose L_N/D= 3.0
- Flow effectors centered at 225°
- Front row
- Ma= 1.5 AoA= 20°
- Re/m= 15.2×10^6

Comparison of Results

Surface Static Pressure Coefficient

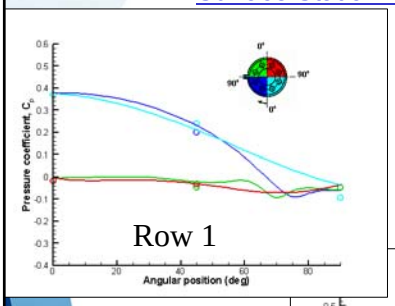

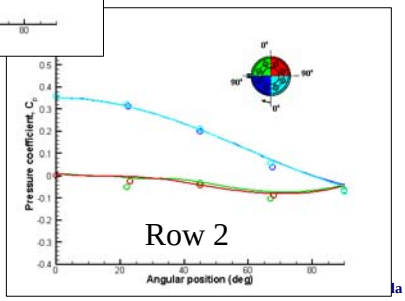

- No fins
- Conical nose L_N/D= 3.0
- Flow effectors centered at 90°
- Front row
- Ma= 1.5 AoA= 15°
- Re/m= 15.2×10^6

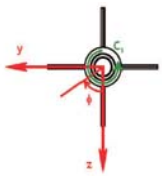

Comparison of Results

Surface Static Pressure Coefficient

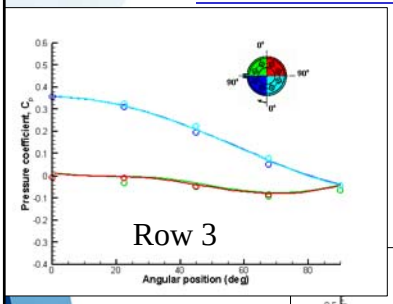

- No fins
- Conical nose L_N/D= 3.0
- Flow effectors centered at 90°
- Front row
- Ma= 1.5 AoA= 15°
- Re/m= 15.2x10^6

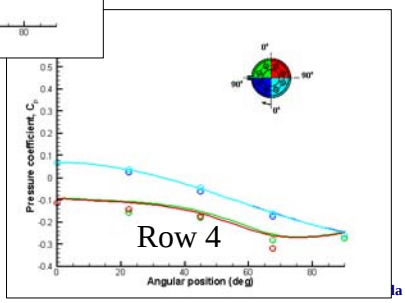

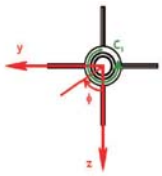

Comparison of Results

Surface Static Pressure Coefficient

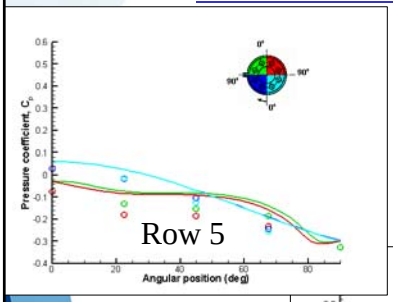

- No fins
- Conical nose L_N/D= 3.0
- Flow effectors centered at 90°
- Front row
- Ma= 1.5 AoA= 15°
- Re/m= 15.2x10^6

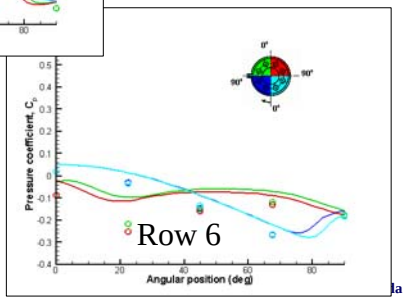

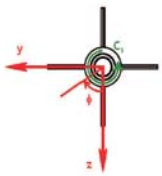

Comparison of Results

Surface Static Pressure Coefficient

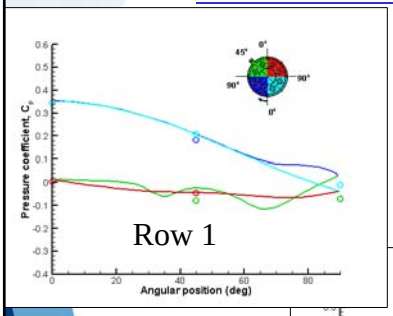

- No fins
- Conical nose L_N/D= 3.0
- Flow effectors centered at 135°
- Front row
- Ma= 1.5 AoA= 15°
- Re/m= 15.2x10^6

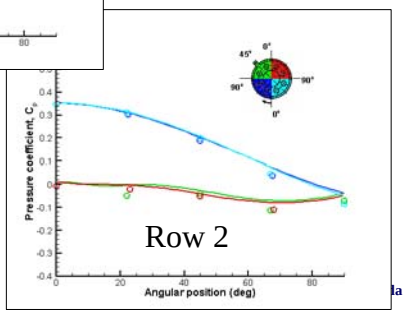

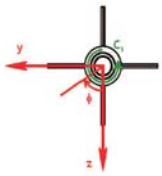

Comparison of Results

Surface Static Pressure Coefficient

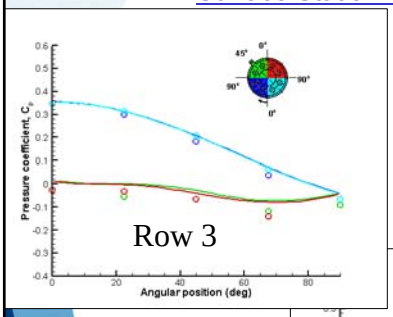

- No fins
- Conical nose L_N/D= 3.0
- Flow effectors centered at 135°
- Front row
- Ma= 1.5 AoA= 15°
- Re/m= 15.2x10^6

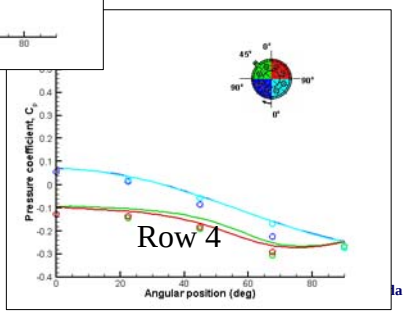

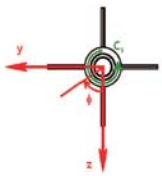

Comparison of Results

Surface Static Pressure Coefficient

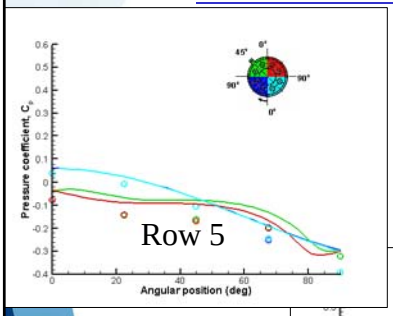

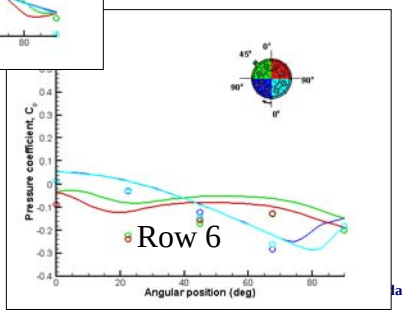

- **No fins**
- **Conical nose L_N/D= 3.0**
- **Flow effectors centered at 135°**
- **Front row**
- **Ma= 1.5 AoA= 15°**
- **Re/m= 15.2x10^6**

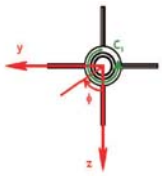

Conclusion

- CFD is able to match the wind tunnel pressure coefficient (clean body)
- CFD is able support the wind tunnel test and help in the interpretation of the results
- The nose-mounted micro-structures contribution to the side force generation is now understand

4.2 A CFD Parametric Study on Missile Yawing Control using Nose-Mounted Flow Effectors

presented by S. Chen, IAR/NRC

IAR has performed a CFD investigation of the aerodynamic performance of blunt-edged rectangular key-shaped flow effectors mounted at the nose of a supersonic flight missile. The flow effectors (FEs) were situated at the front row position, located at x/D = 0.844 from the nose tip. The study focused on four FE configurations. They were: a single FE situated at $\phi = 225°$ (RFE1-225), a single FE situated at $\phi = 270°$ (RFE1-270), triple FEs spaced 30o apart from the middle one situated at $\phi = 225°$ (RFE3-225), triple FEs situated at $\phi = 270°$ (RFE3-270). Parametric studies were also performed considering the effects of the locations (azimuthal angle and axial locations), numbers and dimensions (heights) of the flow effectors on the side force performance. The freestream flow conditions were Mach number $M\infty = 1.5$, pressure $P\infty =$ 26000 Pa and temperature $T\infty = 206$ K for all simulations. The computations were run at angles of attack (AOA) of 0°, 10°, 15°, 17°, 19° and 20°.

Multi-block structured meshes were produced using ICEM-CFD HEXA. Fine grids were used to resolve the viscous boundary layer above the missile surface. The average dimensionless normal distance of the first grid point from the wall, y+, was less than 2. The total number of grid points was about 3 millions. Steady-flow numerical solutions were obtained using the CFD code SPARC with the Spalart-Allmaras one-equation turbulence model.

The numerical results indicated that the maximum peak side forces occurred at AOA = 17° for all the configurations with flow effectors at the front axial location x/D = 0.844. Among the configurations studied, the single FE situated at an azimuthal angle of 225° was the most efficient in generating the side forces. The side force gradually decreased as the FE position moved to the horizontal symmetry plane of the body ($\phi = 270°$). The front configuration was more efficient than the back configuration in influencing the vortex system behaviour. The side force did increase with the number of FEs, however, the advantage was not dramatic. These quantitative observations agreed with the wind tunnel results obtained from DRDC-Valcartier. Regarding the quality of the comparison, the side force coefficients on the starboard side of the body agreed well with the wind tunnel data, but those on the port side of the body, which had identical numerical counterparts, were consistently lower than the wind tunnel data. The asymmetrical features of the wind tunnel data might have been caused by the understandable imperfections in the experimental models or the facilities, which could be significant for the small magnitude of the side force coefficients. The numerical normal and axial forces agreed with the wind tunnel data well.

Both numerical and experimental studies concluded that for the studied cases, the location of FEs was more important than the number of FEs in terms of their contribution to the side force. The numerical study also showed that the side forces generated by the RFE1-225 configuration were on average about 25% of the normal forces. The side force gain was quite remarkable with such a small device installed at the nose of the body. This re-confirms the feasibility of using small devices at the nose of the slender body to control the side forces.

NRC·CNRC
NRCaerospace.com

A CFD PARAMETRIC STUDY ON MISSILE YAWING CONTROL USING NOSE-MOUNTED FLOW Effectors

S. Chen
IAR/NRC

4th Meeting on Missile Control using Micro-actuated Flow Effectors
DRDC-Valcartier, April 19th, 2006

National Research Council Canada | Conseil national de recherches Canada

Canada

NRC·CNRC
NRCaerospace.com

Outline

- Introduction
- Numerical Description
- Grid Generation
- Results and Discussion
- Conclusions

Numerical Descriptions

Geometry and flight conditions

- FEs located at *L/D=0.844 (Front row) or x/D=1.269 (back row).*
- Shape: Rectangular key
- *M=1.5, P=26000Pa, T=206K,*
  R_e/m = 15.2×10⁶.

  AOA = 0° to 20°.

h/D = 0.033
w/D = 0.089
t/D = 0.026

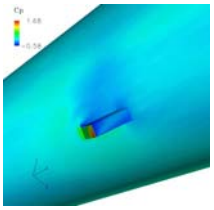

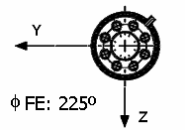

RFE1-225

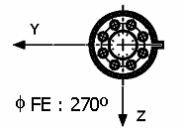

RFE1-270

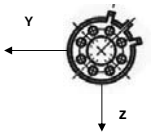

RFE3-225

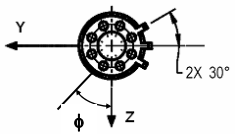

RFE3-270

Numerical Descriptions

- CFD Solver: SPARC
- SPARC:
  - Developed by University of Karlsruhe, Germany
  - A multi-block structured code
  - Multigrid strategy is available
  - Parallelized code
  - Turbulence models: **Spalart-Allmaras**, Baldwin-Lomax, Lauder and Sharma's *k-τ* model and Spezial's non-linear *k-τ* model
- LU-SSOR implicit scheme
- Artificial dissipation term

Grid Generations

- *Structured grids*
- *ICEMCFD HEXA 4.3*
- *Average $y^+ < 2.0$*
- *Number of grid points: about 3 million*
- *Base flow: neglected*

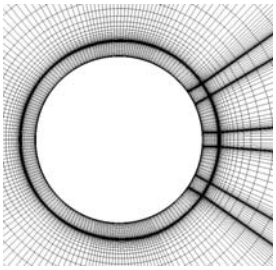

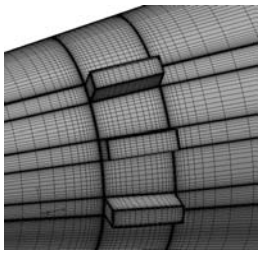

RFE3

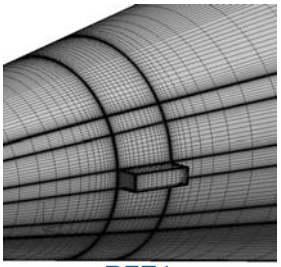

RFE1

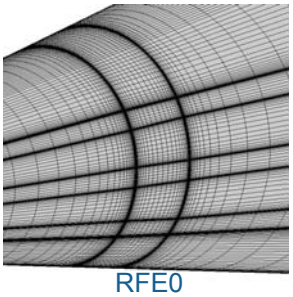

RFE0

Results and Discussion

- *Numerical errors*
- *Effect of the Azimuthal Location of the Flow Effectors*
- *Effect of the Axial Location of the Flow Effectors*
- *Effect of the Height of the Flow Effectors*
- *Effect of the Number of Flow Effectors*
- *Comparison with wind tunnel test data*
- *Efficiency of the flow effectors*

Results and Discussion

Residual histories of case RFE1-225 at AOA = 17°

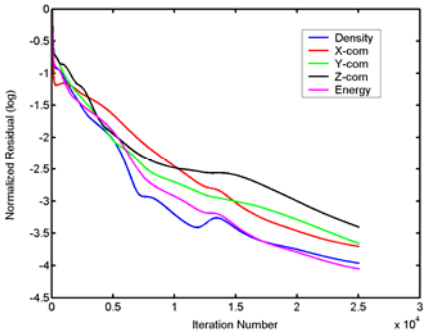

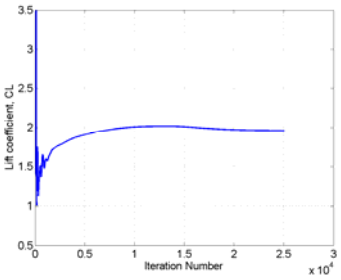

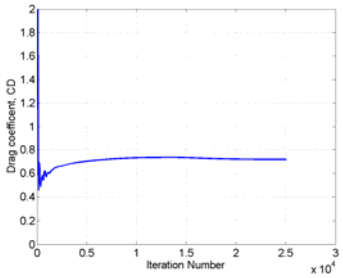

Results and Discussion

Effect of grid distribution for the body-alone configuration

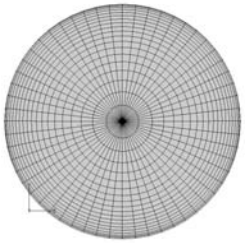

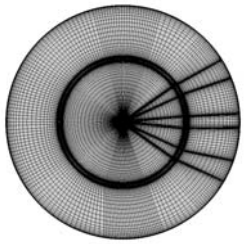

	Uniform Mesh		Non-uniform Mesh	
AOA = 15°	C_Y = 0.00358	C_Y/C_Z = 0.00280	C_Y = 0.02033	C_Y/C_Z = 0.01288
AOA = 17°	C_Y = 0.00567	C_Y/C_Z = 0.00335	C_Y = 0.03043	C_Y/C_Z = 0.01455

Results and Discussion

- ***Effect of the Azimuthal Location of the Flow Effectors***

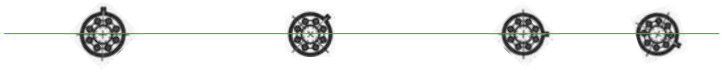

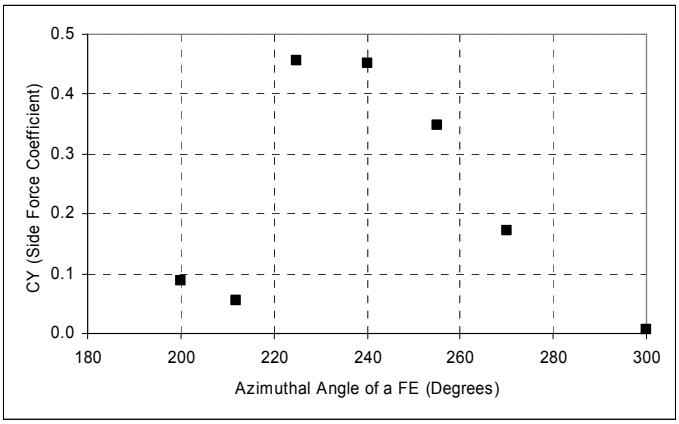

Single FE, Front location, AOA=17°

Effect of the Azimuthal Location of the Flow Effectors

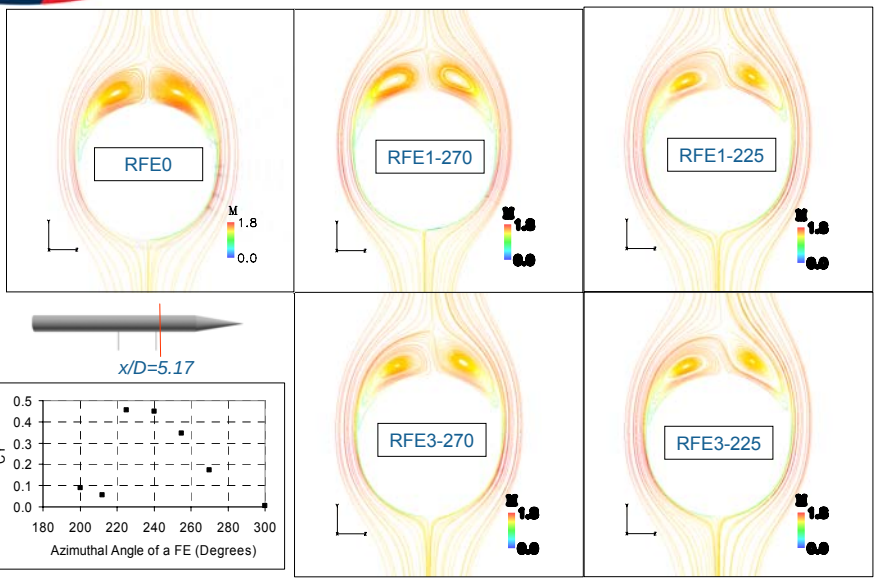

Effect of the Azimuthal Location of the Flow Effectors

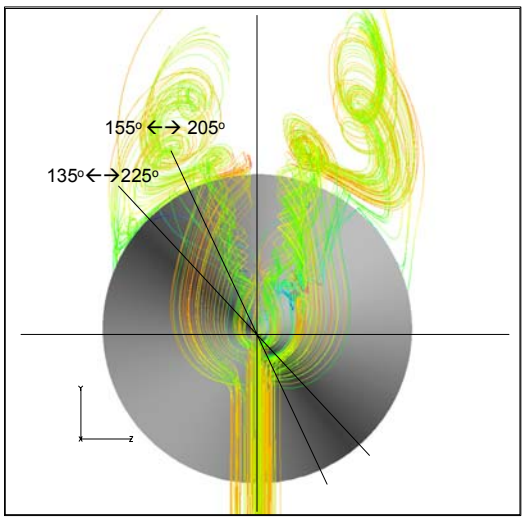

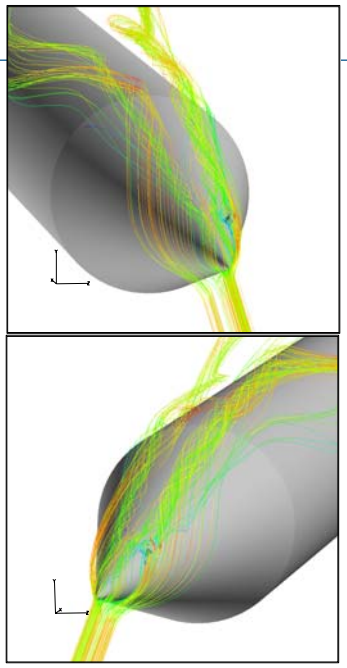

Effect of the Azimuthal Location of the Flow Effectors

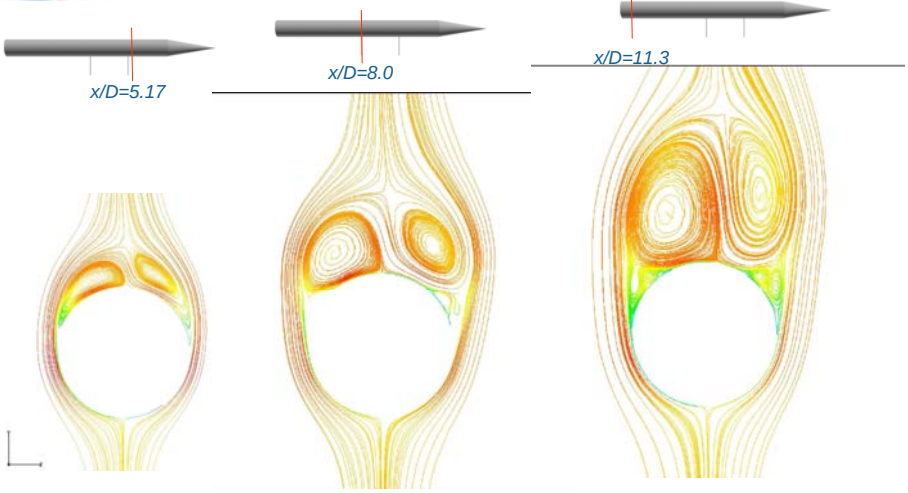

RFE1-225, AOA=17°

Effect of the Azimuthal Location of the Flow Effectors

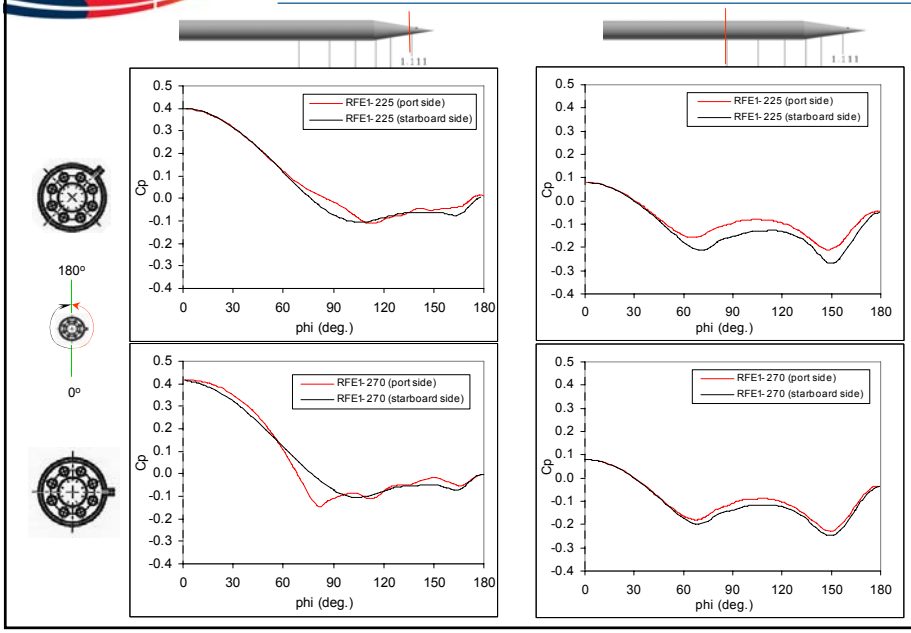

Effect of the Azimuthal Location of the Flow Effectors

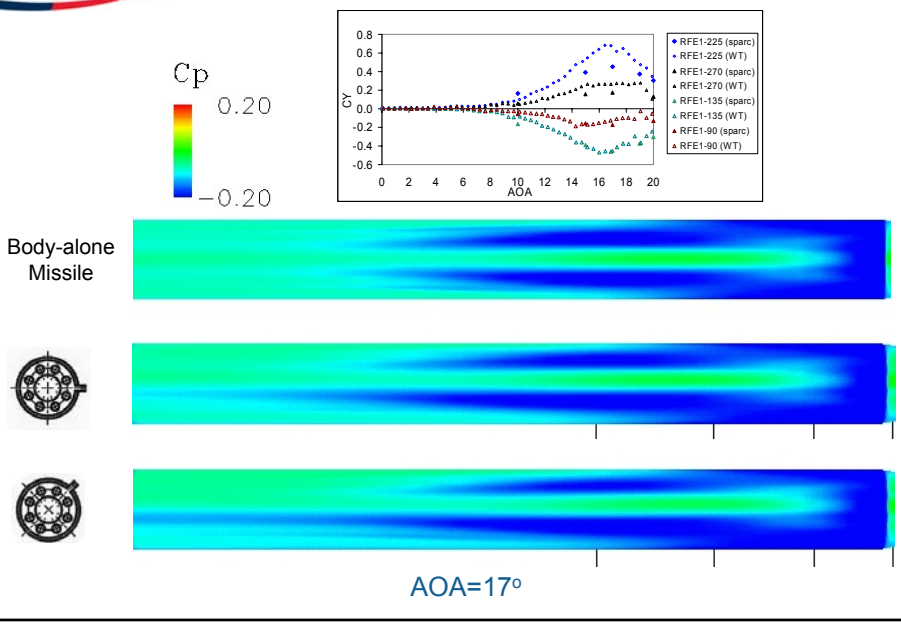

Results and Discussion

- ***Effect of the Axial Location of the Flow Effectors***

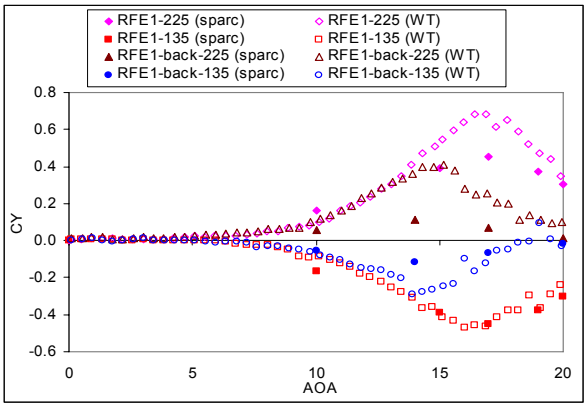

Front location:
x/D=0.844

Back location:
x/D=1.286

Single FE, AOA=17°

Results and Discussion

- ***Effect of the Height of the Flow Effectors***

FE Height	*0.5H*	*1H*	*1.5H*	*2H*
C_Y/C_Z	*6.43%*	*21.34%*	*30.77%*	*35.02%*

H/D=0.033

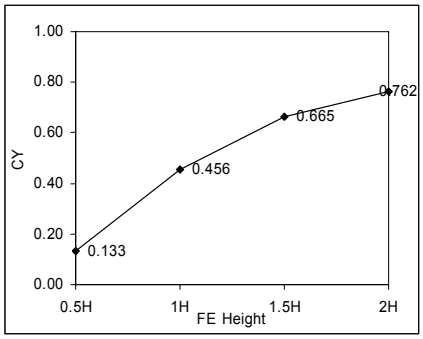

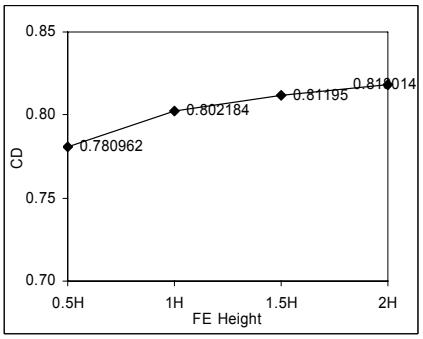

Results and Discussion

- ***Effect of the Number of Flow Effectors***

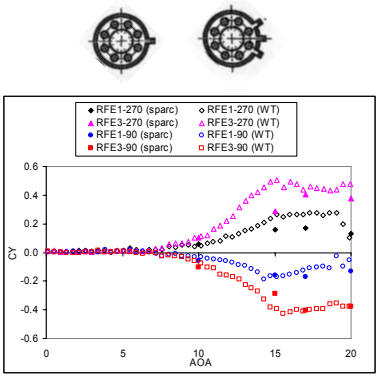

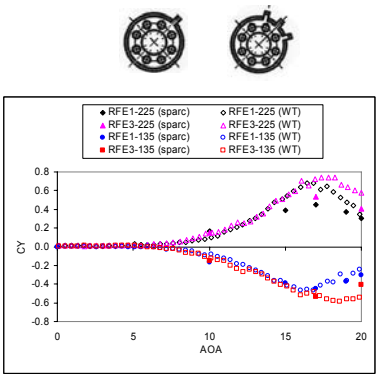

Results and Discussion

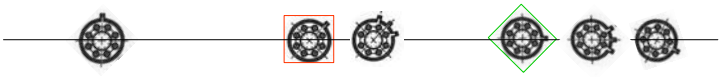

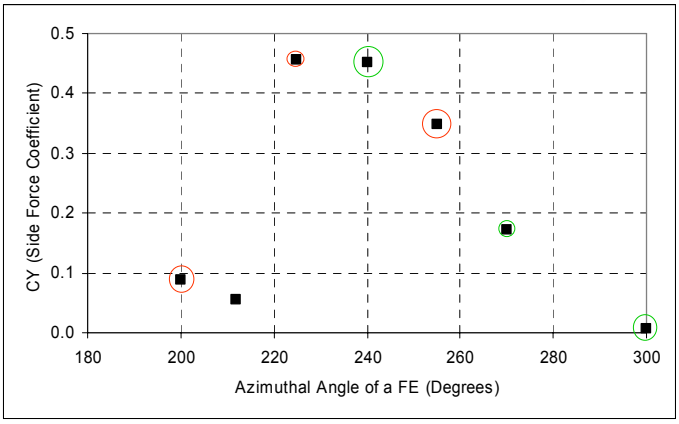

Single FE, Front location, AOA=17°

Results and Discussion

- ***Comparison with wind tunnel test data***
  - Normal and axial force coefficients

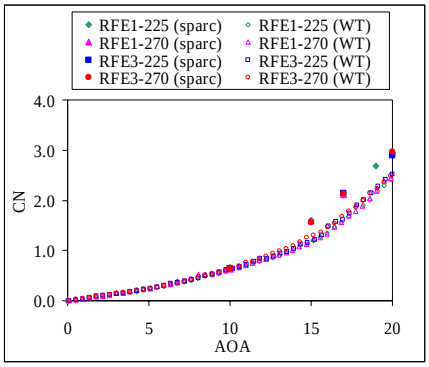

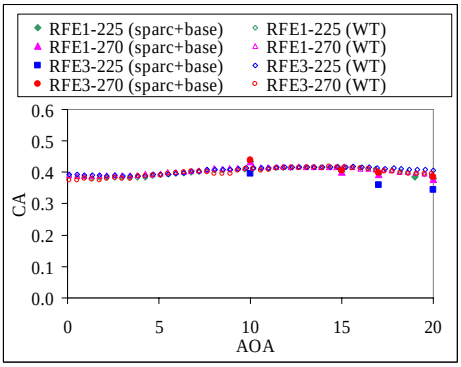

Results and Discussion

- ***Comparison with wind tunnel test data***
  – side force coefficients

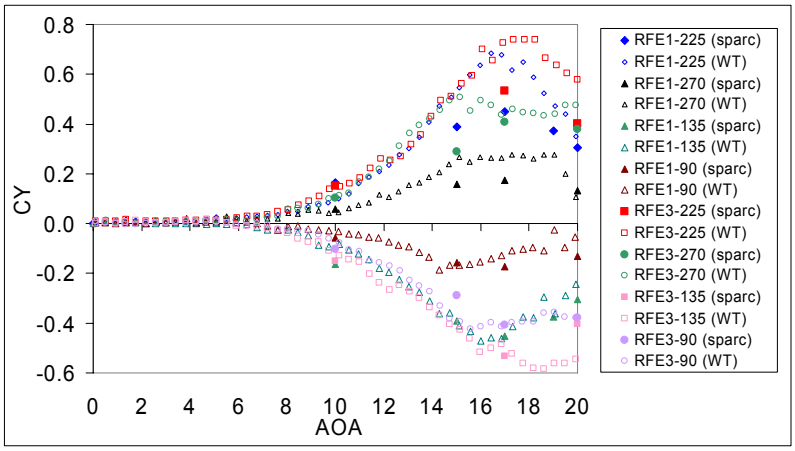

Results and Discussion

- ***Comparison with wind tunnel test data***
  – moment coefficients

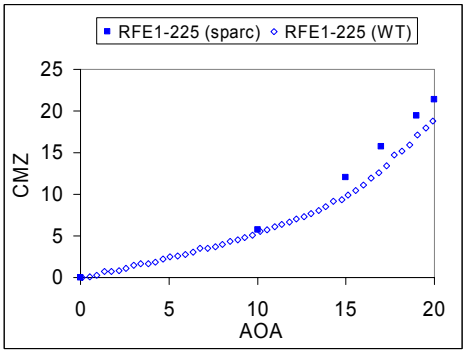

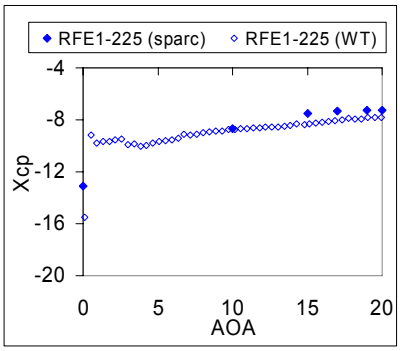

Results and Discussion

- ***Efficiency of the flow effector***
  - side/normal force coefficients

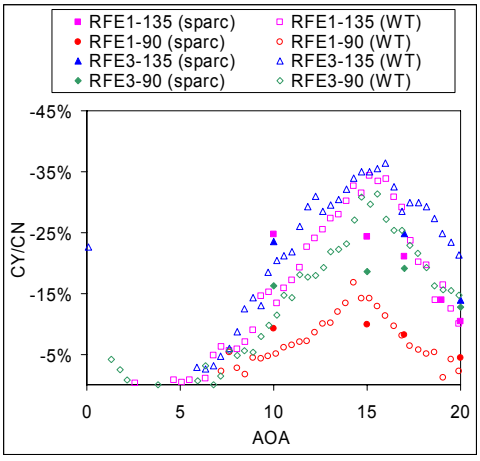

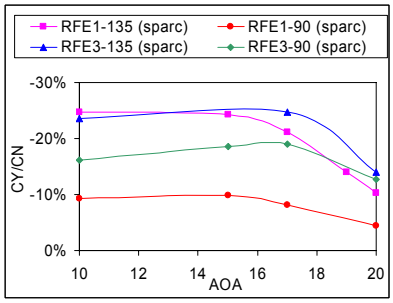

Lauder and Sharma's k-τ model

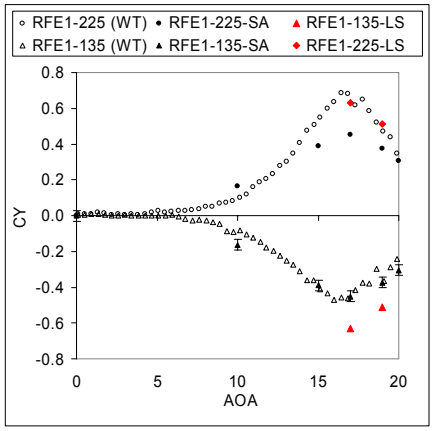

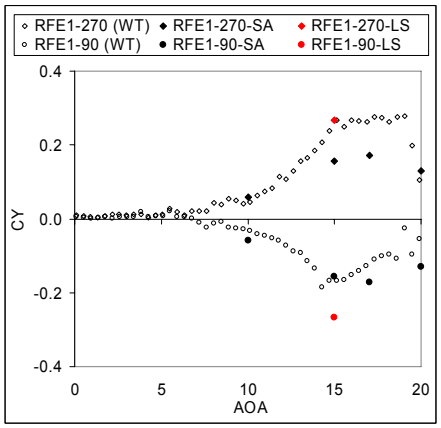

Conclusions

- The maximum peak side forces occurred at AOA = *17*^{o} for all the configurations with flow effectors at the front axial location *x/D = 0.844*.
- Among the configurations studied, the single FE situated at an azimuthal angle of *225*^{o} was the most efficient in generating the side forces.
- The side force gradually decreased as the FE position moved to the horizontal symmetry plane of the body.
- The front configuration was more efficient than the back configuration in influencing the vortex system behaviour.
- The side force did increase with the number of FEs; however, the advantage was not dramatic.

Conclusions

- the side force coefficients on the starboard side of the body agreed well with the wind tunnel data, but those on the port side of the body, which had identical numerical counterparts, were consistently lower than the wind tunnel data. The numerical normal and axial forces agreed with the wind tunnel data well.
- The numerical study showed that the lateral forces generated by case RFE1-225 were on average about *25%* of the normal forces. **With such a small device installed at the nose of the missile, the lateral force gain was quite remarkable**. This re-confirms that the concept of using small devices at the nose of the missile to control the lateral forces is feasible.

4.3 Impact of Nose-mounted Micro-structures on the Aerodynamics of a Generic Finned Missile

presented by D. Corriveau, DRDC – Valcartier

Balance force measurements were performed on a generic missile configuration with finned mounted in cruciform configuration. The baseline experimental model used consists in a finned missile having a conical nose and an aspect ratio (L/D) of 13. Tests were performed in the DRDC indraft wind tunnel at a free stream Mach number of 1.5 and for angles-of-attack varying between 0.0° and 20.0°. Several configurations of the nose-mounted flow effectors were investigated. The results show that no peak in the side force generated is attained for angles of attack up to 20.0°. It was also found that the side force is higher when the flow effectors are located closer to the nose tip. By indexing the flow effectors to various roll positions on the nose, it was determined that the maximum side force occurs at an angular position of 225°. On the downside, for missile equipped with fins, the side force generated by the flow effectors is relatively small in comparison to the normal force.

DEFENCE R&D DÉFENSE

Impact of Nose-Mounted Micro-Structures on the Aerodynamics of a Generic Finned Missile

Dr. Daniel Corriveau and Nicolas Hamel
Flight Mechanics Group
Precision Weapons Section
April 19th, 2006

Defence Research and Development Canada
Recherche et développement pour la défense Canada
Canada

Presentation Overview

- Objectives
- Background
- Test setup and instrumentation
- Missile configuration
- Experimental results
- Conclusions

Presentation Overview

- Objectives
- Background
- Test setup and instrumentation
- Missile configuration
- Experimental results
- Conclusions

Objectives

- Determine: Optimum flow effector configurations
- Determine: Range of AOA for which a side force is generated
- Understand: Mechanisms through which the flow effectors impact on the side force's magnitude
- Evaluate: Use of vortex-induced side force to achieve yaw control

Presentation Overview

- Objectives
- Background
- Test setup and instrumentation
- Missile configuration
- Experimental results
- Conclusions

Background

Slender Body Vortex Shedding

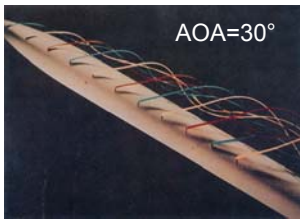

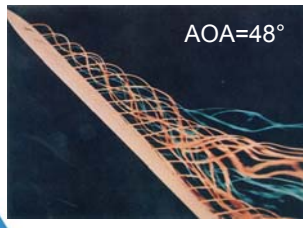

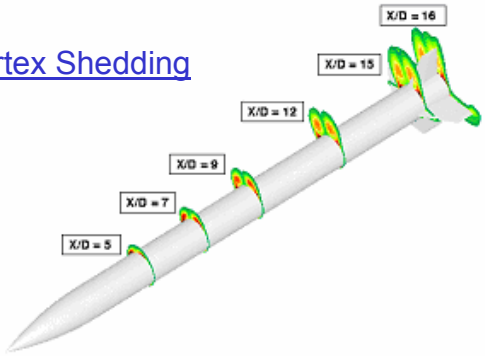

- Vortices form on the missile's leeside operating at AOA
- Early studies dates back to the 50's
- Early concerns related to vortex interactions with the control surfaces

Background

Slender Body Vortex Shedding

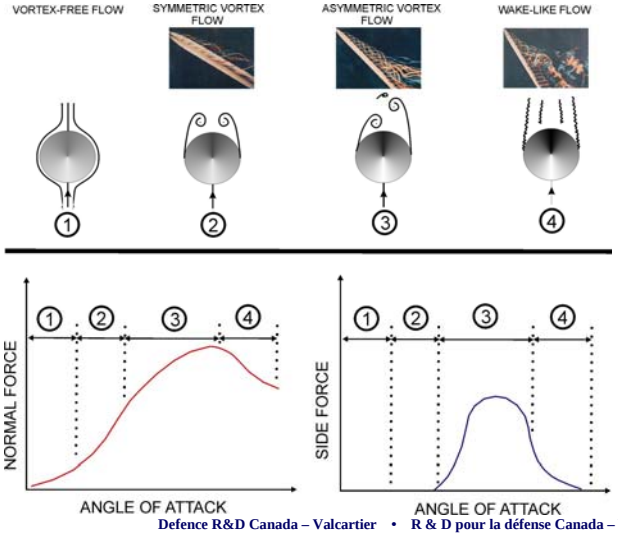

Background

Side Force Control Using Micro-Structures

- AFRL MN (2003)
  - Air Force Basic Research Shape
  - A/B range tests
  - Wind tunnel test DRDC Valcartier

- Orbital Research / DARPA (2002)
  - High AOA (+30° to +60°)
  - Low aspect ratio model (l/d = 4.5)
  - Incompressible subsonic flow
  - Control existing side force

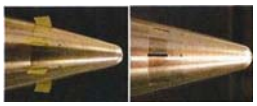

- Leu et al. (2005)
  - Low AOA (0° to +60°)
  - Low aspect ratio model (l/d = 5.0)
  - Incompressible subsonic flow
  - Control existing side force

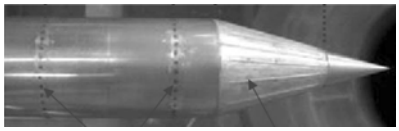

Background

Side Force Control Using Micro-Structures

- Current Study (2004)
  - Low AOA (0° to +20°)
  - Medium aspect ratio model (l/d = 13)
  - Supersonic flow (M = 1.5)
  - Generate side force for yaw control

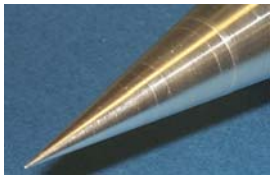

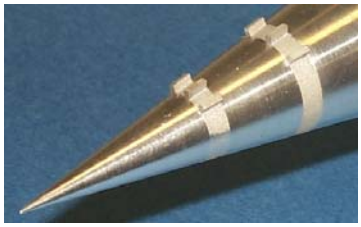

Presentation Overview

- Objectives
- Background
- Test setup and instrumentation
- Missile configuration
- Experimental results
- Conclusions

Test Setup and Instrumentation

DRDC Trisonic Wind Tunnel

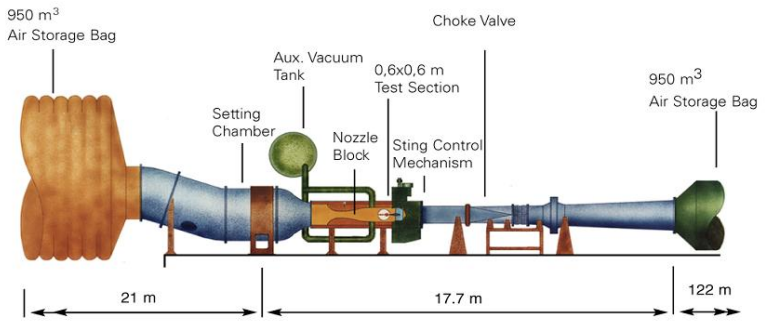

- **Indraft wind tunnel**
- **Test section: 2'x 2'**
- **0.2 < Ma < 4.0**
- **-20° < AOA < +20 °**
- **Test duration: 5 – 11 sec**
- **Turnaround time: 30 min.**

Missile Configuration

Baseline Geometry With Conical Nose

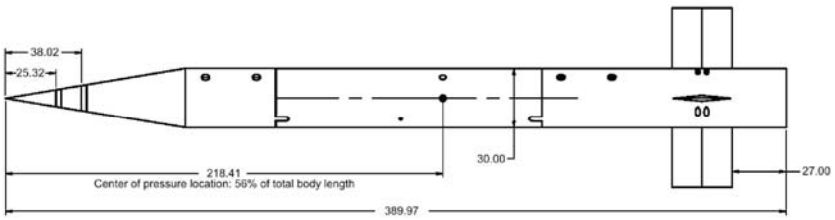

All dimensions in mm

- Aspect Ratio L/D = 13.0
- Nose Aspect Ratio L_N/D = 3.0
- Conical Nose
- 4 Fins in + Configurations (Removable)

Missile Configuration

Baseline Geometry With Conical Nose

Missile Configuration

Baseline Geometry With Conical Nose

Defence R&D Canada – Valcartier • R & D pour la défense Canada – Valcartier

Missile Configuration

Nose Arrangement

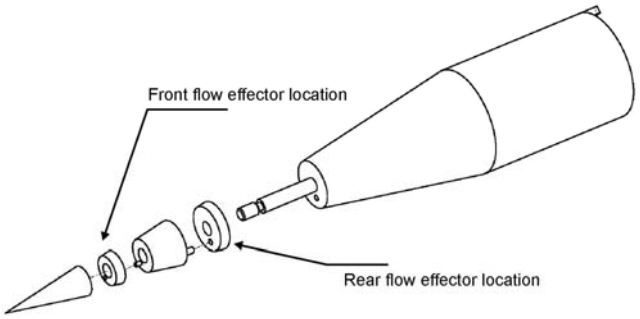

Missile Configuration

Flow Effector Geometries

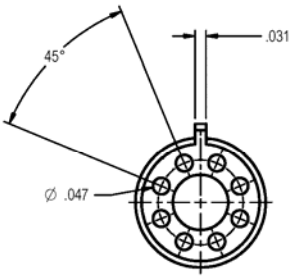

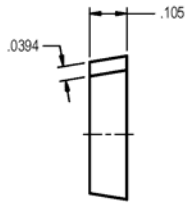

All dimensions are in inches

Missile Configuration

Flow Effector Configurations

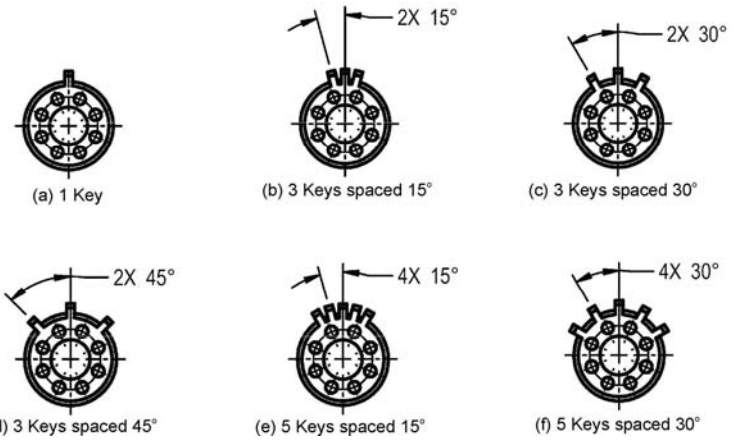

Missile Configuration

Flow Effector Configurations

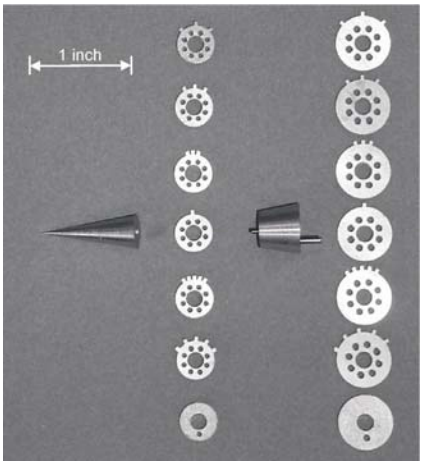

Missile Configuration

Nomenclature: North East Down Coordinate System

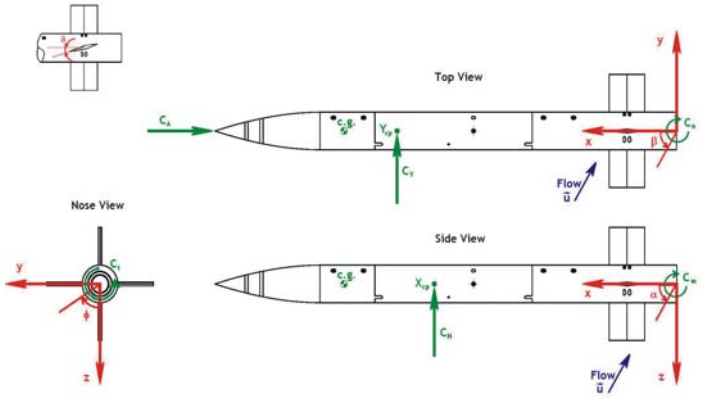

Presentation Overview

- Objectives
- Background
- Test setup and instrumentation
- Missile configuration
- Experimental results
- Conclusions

Experimental Results

Lateral Force Coefficient vs AOA

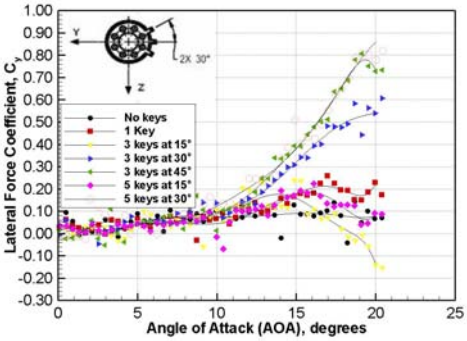

- 4 fins in + configuration
- Conical nose L_N/D= 3.0
- Flow effectors centered at 270°
- Front row
- Ma= 1.5
- Re/m= 15.2x10^6

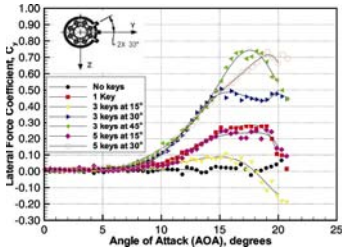

Experimental Results

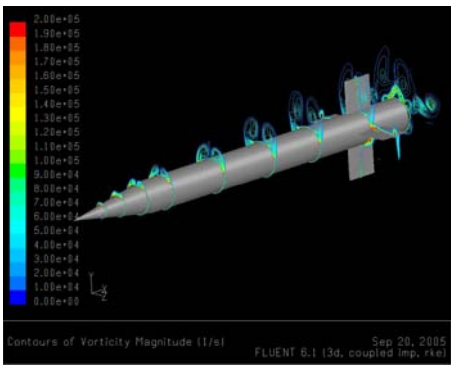

- 4 fins in + configuration
- Conical nose L_N/D= 3.0
- Flow effectors centered at 270°
- Front row
- Ma= 1.5
- Re/m= 15.2x10^6

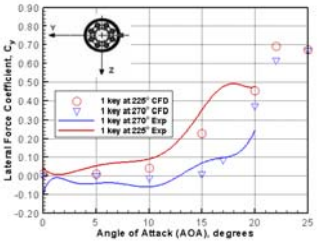

Experimental Results

Lateral Force Coefficient vs AOA

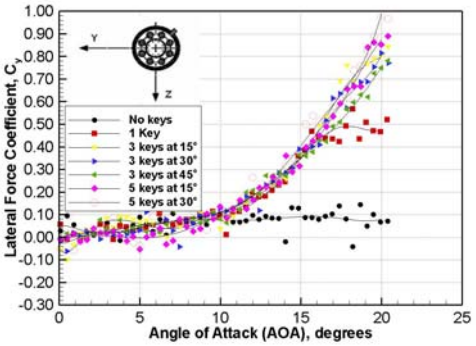

- 4 fins in + configuration
- Conical nose L_N/D= 3.0
- Flow effectors centered at 225°
- Front row
- Ma= 1.5
- Re/m= 15.2×10^6

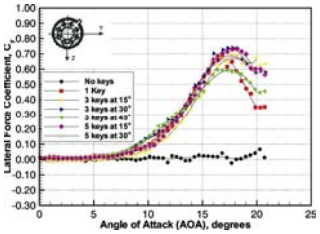

Experimental Results

Lateral Force Coefficient vs AOA

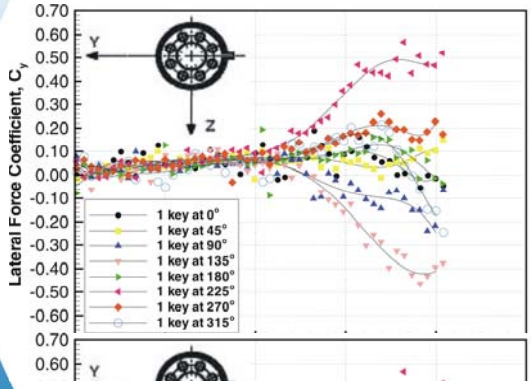

- 4 fins in + configurations
- Conical nose L_N/D= 3.0
- Flow effector: 1 key
- Front row
- Angular position: 0° - 360°
- Ma= 1.5
- Re/m= 15.2×10^6

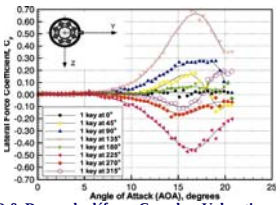

Experimental Results

Lateral Force to Normal Force Coefficient Ratio vs AOA

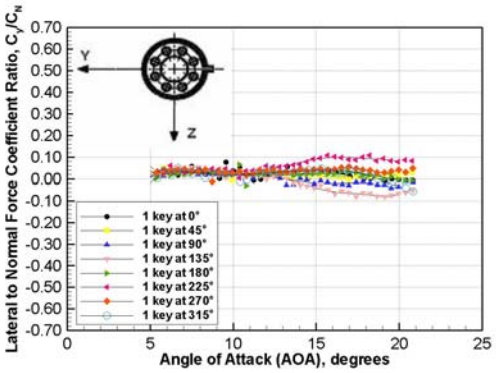

- 4 fins in + configuration
- Conical nose L_N/D= 3.0
- Flow effector: 1 key
- Angular position: 0° - 360°
- Front row
- Ma= 1.5
- Re/m= 15.2×10^6

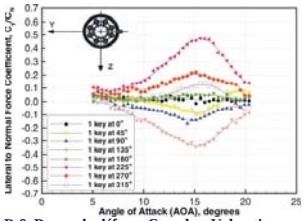

Experimental Results

Lateral Force Coefficient vs AOA

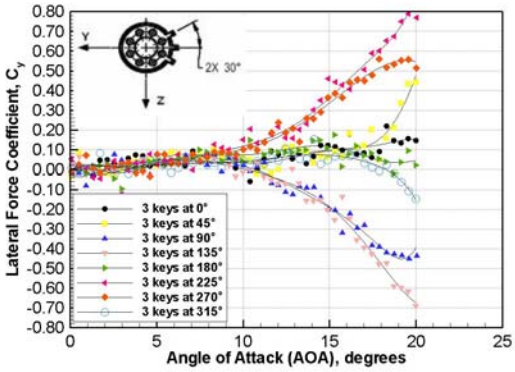

- 4 fins in + configuration
- Conical nose L_N/D= 3.0
- Flow effector: 3 keys spaced at 30°
- Front row
- Angular position: 0° - 360°
- Ma= 1.5
- Re/m= 15.2×10^6

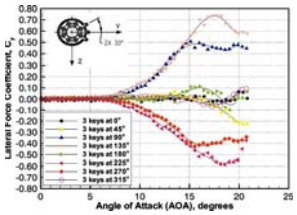

Experimental Results

Lateral Force to Normal Force Coefficient Ratio vs AOA

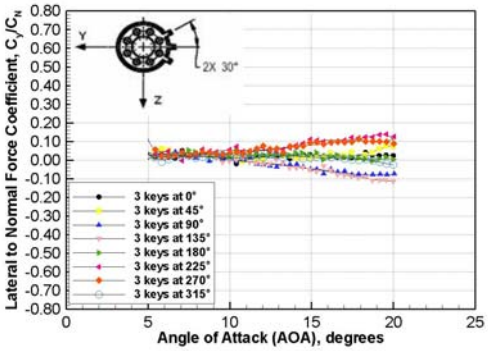

- 4 fins in + configuration
- Conical nose L_N/D= 3.0
- Flow effector: 3 keys spaced at 30°
- Angular position: 0° - 360°
- Front row
- Ma= 1.5
- Re/m= 15.2×10^6

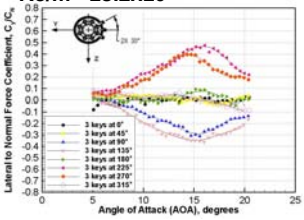

Experimental Results

Lateral Force Coefficient vs AOA

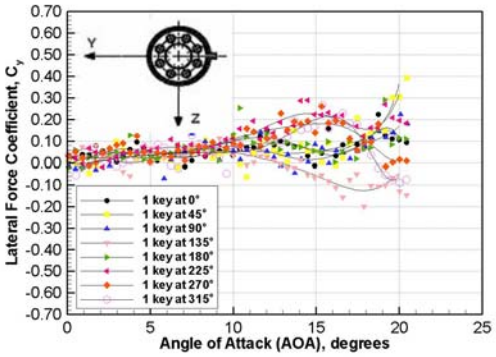

- 4 fins in + configuration
- Conical nose L_N/D= 3.0
- Flow effector: 1key
- Angular position: 0° - 360°
- Aft row
- Ma= 1.5
- Re/m= 15.2×10^6

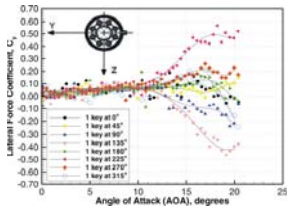

Experimental Results

Axial Force Coefficient vs AOA

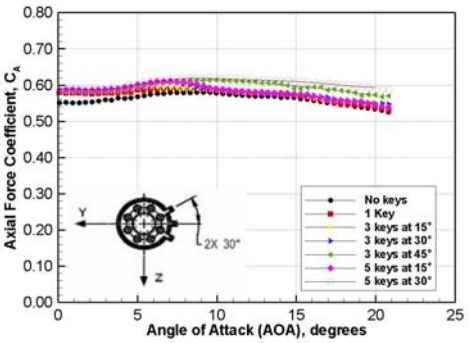

- 4 fins in + configuration
- Conical nose L_N/D= 3.0
- Flow effectors centered at 270°
- Front row
- Ma= 1.5
- Re/m= 15.2×10^6

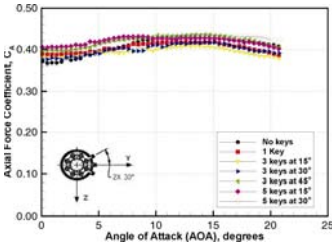

Experimental Results

Axial Force Coefficient vs AOA

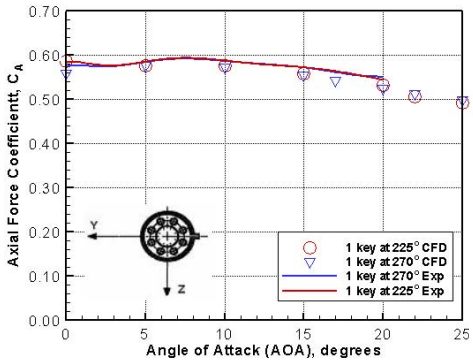

- 4 fins in + configuration
- Conical nose L_N/D= 3.0
- Flow effectors centered at 270°
- Front row
- Ma= 1.5
- Re/m= 15.2×10^6

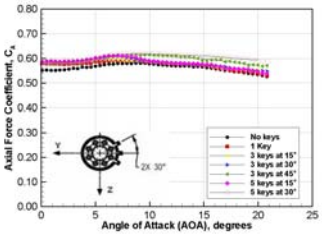

Experimental Results

Normal Force Coefficient vs AOA

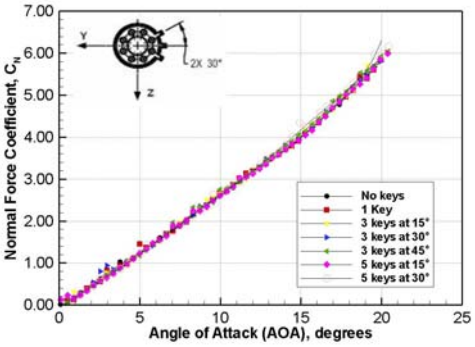

- 4 fins in + configuration
- Conical nose L_N/D= 3.0
- Flow effectors centered at 270°
- Front row
- Ma= 1.5
- Re/m= 15.2×10^6

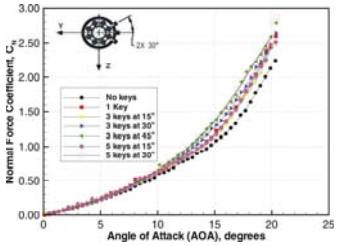

Experimental Results

Normal Force Coefficient vs AOA

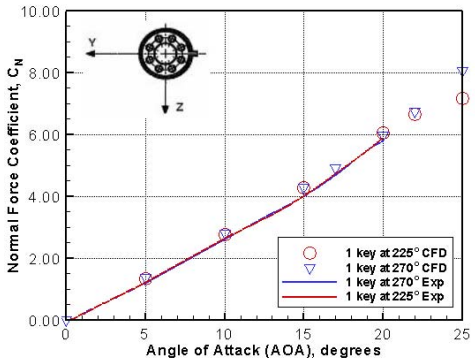

- 4 fins in + configuration
- Conical nose L_N/D= 3.0
- Flow effectors centered at 270°
- Front row
- Ma= 1.5
- Re/m= 15.2×10^6

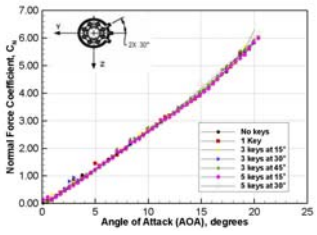

Presentation Overview

- Objectives
- Background
- Test setup and instrumentation
- Missile configuration
- Experimental results
- Conclusions

Conclusions

- Peak Side force magnitude measured between AOA of 15.0° and 20.0°
- Locating the flow effectors closer to the nose tip results in higher side forces
- Maximum side forces measured at an angular position of 225°
- Side forces generated by the micro-structures are symmetric for complementary flow effectors angular position
- Apart from side force, the nose-mounted micro-structures have little impacts on the other aerodynamic coefficients

4.4 Mini-scale PIV Measurements during Unsteady Excitation of Mini-Leading Edge Flaps Used for Separation Control and Development of a Bi-fold Five Component Force Balance

presented by X-Z. Huang, IAR/NRC

Reduction of boundary separation is a key issue to increase lift and control power especially at take-off, landing and post-stall flight conditions. Leading-edge flaps, either static or dynamic, are one of the promising methods that has been studied. Miniature flaps activated by micro-actuators may reduce power demands of such devices. A clear understanding on how aerodynamic forces can be altered by manipulating the micro-flow effectors is a prerequisite for its application. To this end, an unsteady excitation of a micro-leading-edge flap concept was introduced and studied at IAR. The experiments were conducted in the IAR 1520 water tunnel with a two dimensional wing profile (NACA 0012) as test model. Mini-scale PIV measurements showed that when the leading-edge was oscillating, the boundary layer separation area was reduced dramatically. Parameter studies found that when the non-dimensional frequency, $fc/U_\infty > 1$, the effectiveness becomes smaller as the frequency increased. An analysis shows that the effectiveness of the moving surface is related to the increased viscosity present in the sub-layer with the increment in effectiveness being related to the frequency of the moving wall.

In a connected activity, a five-component, bi-fold force balance was developed for data measurement in water/wind tunnel open test sections. Since the two dimensional profile wing is a half-model where only the wing is immersed in the water tunnel, a short balance is needed because the center pressure of the model should be as close to the pivot of the motion control system as possible. On the other hand, requirements for sensitivity, linearity and gauge space does not allow the balance elements to be too short. The bi-fold concept keeps the length of each element as long as possible while shortening the total length of the balance. Numerical calculations based on the finite element method were conducted and compared with data measured from a prototype bi-fold balance. The experimental results confirmed that the concept could be successfully used in half-model experiments.

Progress Review

Experimental Investigations of Micro-Flow Effectors on Aerodynamic Behavior of Lifting Surfaces

X. Z. Huang IAR/NRC Canada
April 19, 2006, Quebec City Canada

This work was supported by the DRDC TIF through DRDC - Valcartier
and
the Aerodynamics Laboratory of the Institute for Aerospace Research (IAR)

Content

Topic 1

Development of a New Concept of Bi-Fold, Five-Component, Half-Model Balance used in IAR Water Tunnel

- Introduction
- Principle of bi-fold balance
- Geometrical description of initial balance
- Gauges and bridges
- Calibration results
- Further configuration studies and recommendations

Advantage of bi-fold balance

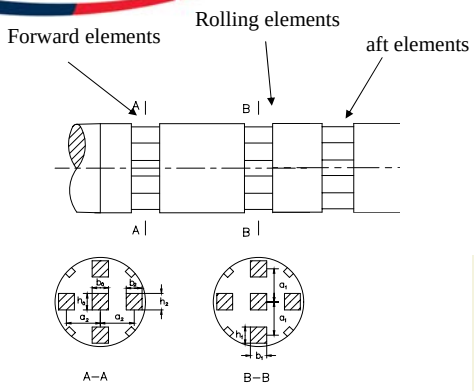

Normal balance

Bi-fold balance

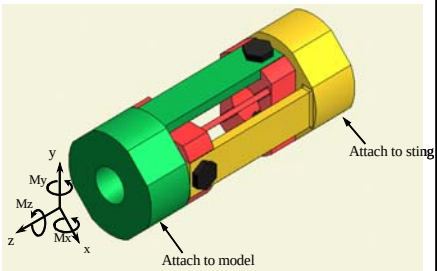

Principle of bi-fold balance

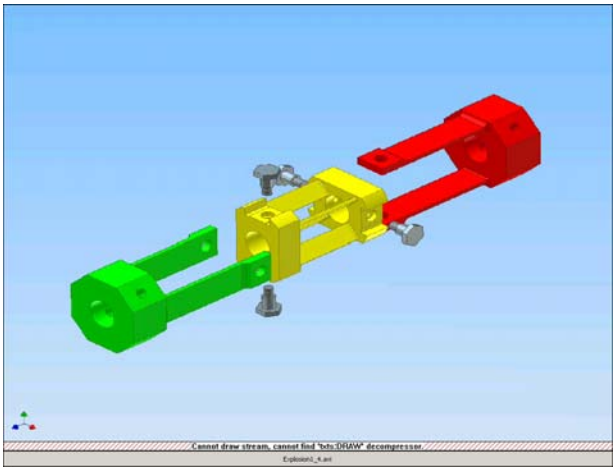

Gauges and bridges

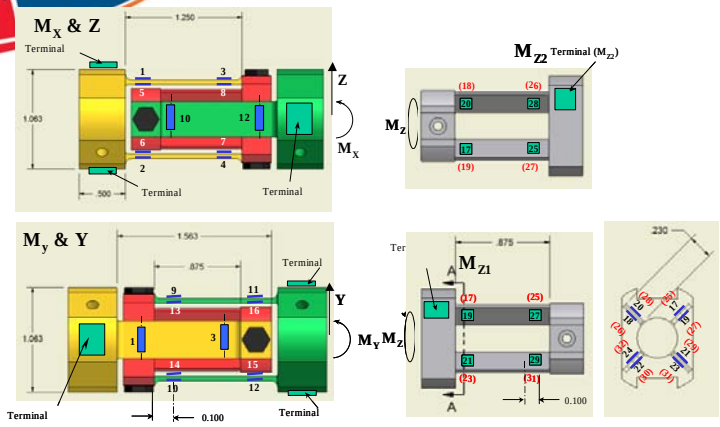

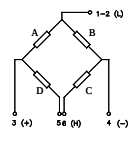

Bridge	Lead color	A	B	C	D	Ω
M_X	Black	1	2	3	4	1000
Z	White	5	6	7	8	1000
M_Y	Yellow	9	10	11	12	1000
Y	Blue	13	14	15	16	1000
M_{Z1}	Red	17, 18	19, 20	21, 22	23, 24	1000+1000
M_{Z2}	Brown	25, 26	27, 28	29, 30	31, 32	1000+1000

NRC·CNRC
NRCaerospace.com

FEM results

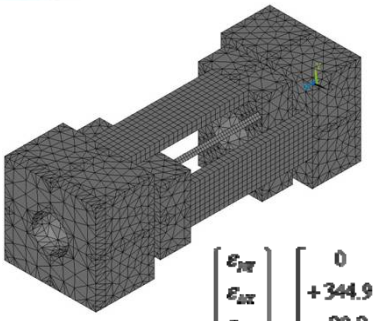

$$\begin{Bmatrix} \varepsilon_{1M} \\ \varepsilon_{2M} \\ \varepsilon_{M1} \\ \varepsilon_{M2} \\ \varepsilon_{M21} \\ \varepsilon_{M22} \end{Bmatrix} = \begin{bmatrix} 0 & -345.1 & -0.7 & 0 & 0 & 0 \\ +344.9 & 0 & 0 & +0.6 & 0 & 0 \\ -20.2 & 0 & 0 & -38.5 & 0 & 0 \\ 0 & +14.5 & -38.7 & 0 & 0 & 0 \\ 0 & 0 & 0 & 0 & +3239 & -3239 \\ 0 & 0 & 0 & 0 & +3239 & -3239 \end{bmatrix} \begin{Bmatrix} N_1 \\ N_2 \\ M_1 \\ M_2 \\ M_{21} \\ M_{22} \end{Bmatrix}$$

NRC·CNRC
NRCaerospace.com

Further configuration studies and recommendations

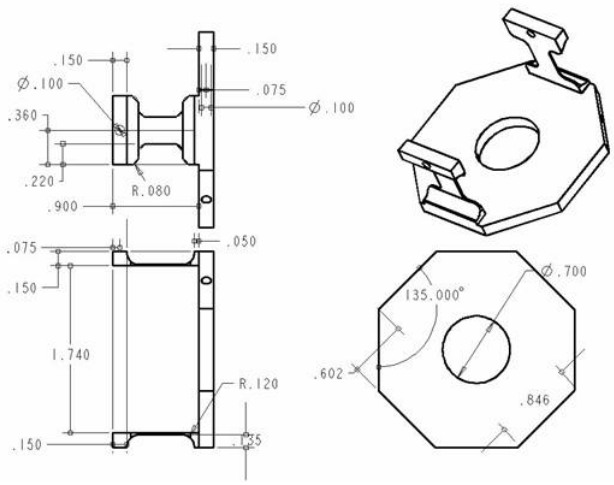

Development of Mini-Scale PIV Methodology and its Applications on Wall-Bounded Flows

- Introduction
- Experimental set-up
- Experimental results
- Analysis and conclusions

Development of Mini-Scale PIV Methodology and its Applications on Wall-Bounded Flows

Introduction

- Wall-bounded flow is full of vorticities
- Aerodynamic behavior is mainly determined by vorticity generation in boundary layer and convection downstream
- Leading-edge area is crucial for voticity generation and convection downstream
- The effectiveness of mini flow effectors depends on the studying of the mini-scale wall-bounded flow, especially at leading-edge area

NRC·CNRC
NRCaerospace.com

Turbulence structure at various heights in a low-Re boundary layer condition

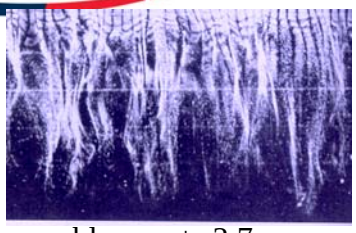

sublayer y+=2.7

wake region y+=407

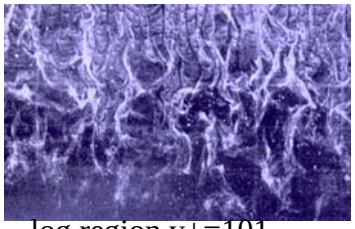

log region y+=101

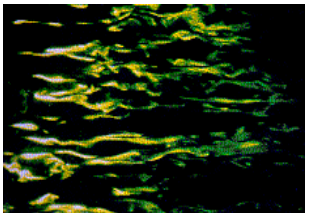

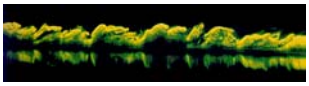

Top and side views of wall-bounded flow

NRC·CNRC
NRCaerospace.com

Mini-PIV set-up on Wall-Bounded Flow Experiments

IAR Water tunnel

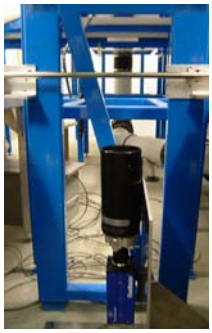

Long-range mini-scale PIV system

NRC·CNRC
NRCaerospace.com

Mini-scale PIV measurements on wall-bounded flow at the mid chord of NACA 0012, U∞=2.7in/sec, Re=13450

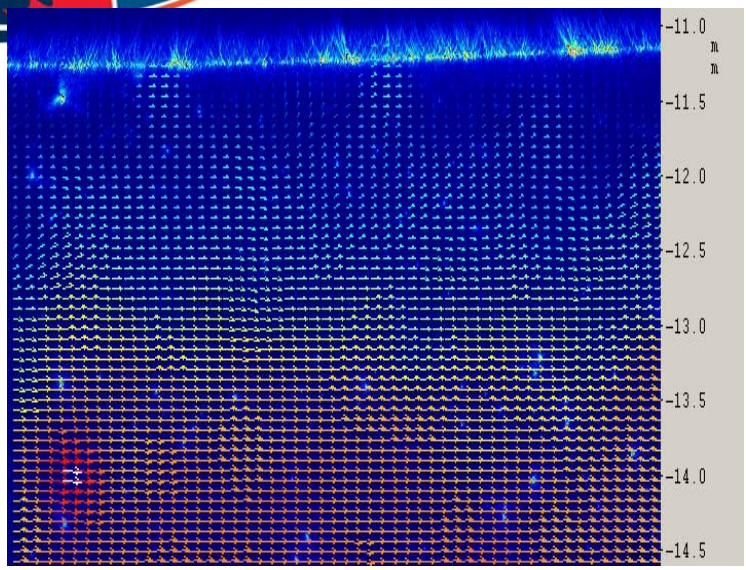

NRC·CNRC
NRCaerospace.com

Mini-scale PIV measurements of wall-bounded flow on the mid chord of NACA 0012, U∞=5.3in/sec, Re=26900

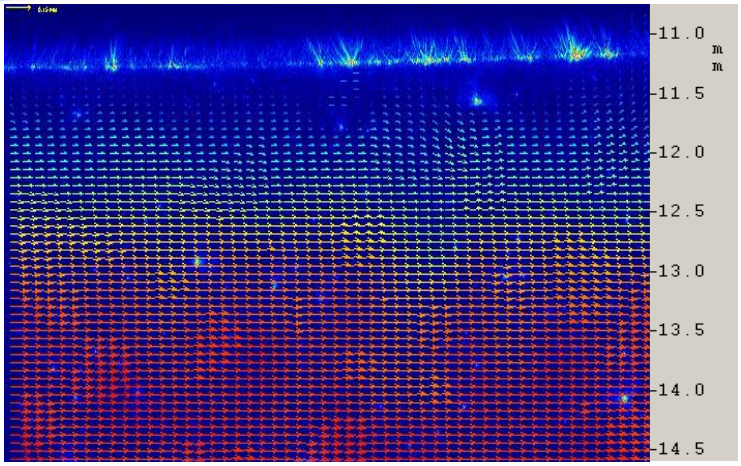

NRC·CNRC
NRCaerospace.com

Mini-scale PIV measurements of wall-bounded flow on the mid chord of NACA 0012, U∞=7.9in/sec, Re=40350

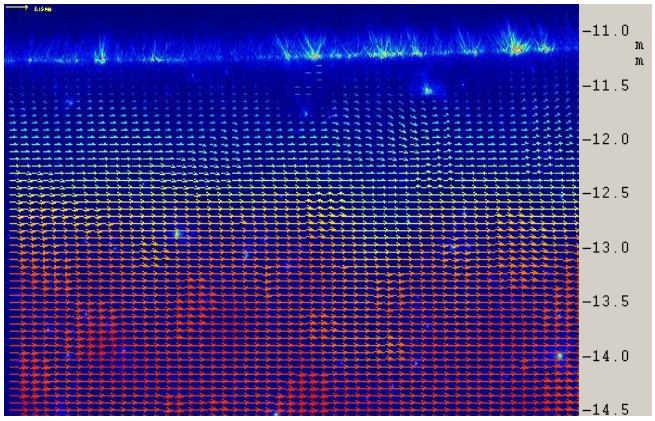

NRC·CNRC
NRCaerospace.com

Mini-scale PIV measurements of wall-bounded flow at the leading-edge of NACA 0018, U∞=2.7in/sec, Re=13450

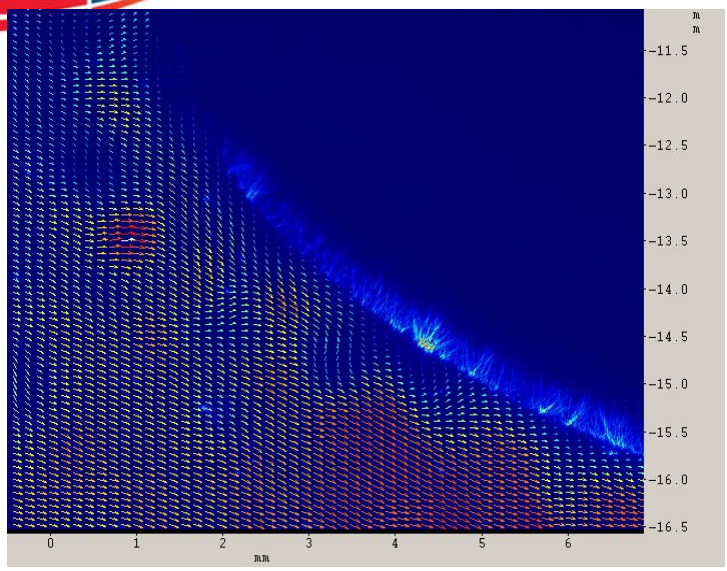

Topic 2

Conclusion and discussions

- The resolution could reach 50μm and view area could be 2~5 mm
- The instability in the open shear flow may be classified as either *noise* ***amplifiers*** with ***extrinsic dynamics*** or as ***oscillators*** with ***intrinsic dynamics***
- For the wall-bounded flows, the velocity gradient at the wall is the highest one resulting in the maximum production of turbulent energy
- That energy source is exported to the rest of the flow as a spatial energy flux. When the flow velocity is very low and the outside flow is in laminar state, the outside flow acts as energy sinks. The dissipation process will absorb the energy flux. At this situation the flow acts as a *noise amplifiers* and the flow will be back to laminar eventually as observed in the experiments.
- If the flow velocity is high enough and the flow state crosses the border of the ***oscillators*** with ***intrinsic dynamics***, those small eddies may trigger large flow instability

Topic 3

Boundary layer separation control by unsteady excitation of mini-scale leading-edge flaps

Topic 3

Boundary layer separation control by unsteady excitation of mini-scale leading-edge flaps

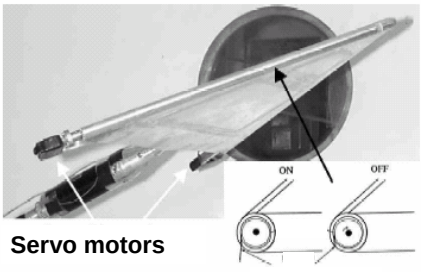

Servo motors

Mechanical actuator

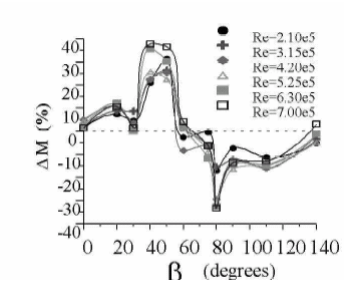

Rolling moment produced by leading-edge flap actuators

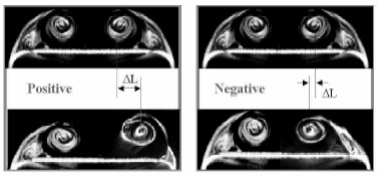

Smoke flow visualization on different leading-edge flap angles

Leading/-edge vortex flap

Boundary layer separation control by unsteady excitation of mini-scale leading-edge flaps

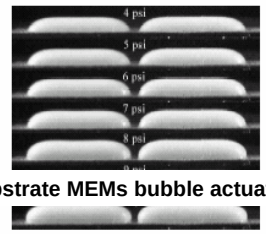

Silicon substrate MEMs bubble actuators

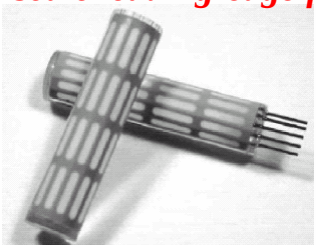

Flexible MEMs metal substrate MEMs bubble actuators

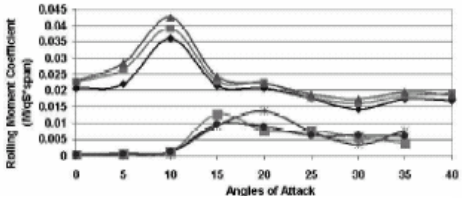

Rolling moment comparisons between conventional and MEMs bubble actuators

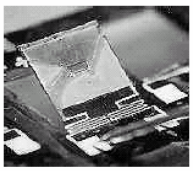

Permalloy flap actuators

electromagnetic coil actuators

Different actuators used in leading-edge vortex flap

Boundary layer separation control by unsteady excitation of mini-scale leading-edge flaps

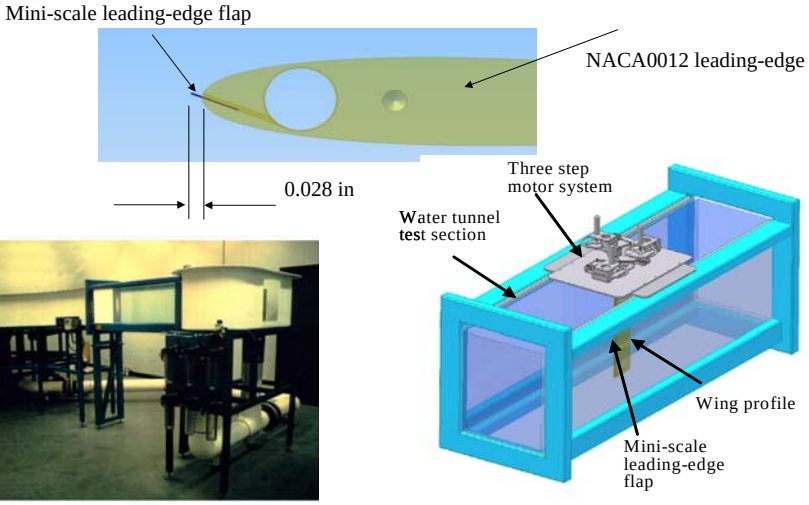

IAR Water tunnel

Three-leading-edge flaps

Topic 3

Boundary layer separation control by unsteady excitation of mini-scale leading-edge flaps

Video records

Boundary layer separation control by unsteady excitation of mini-scale leading-edge flaps

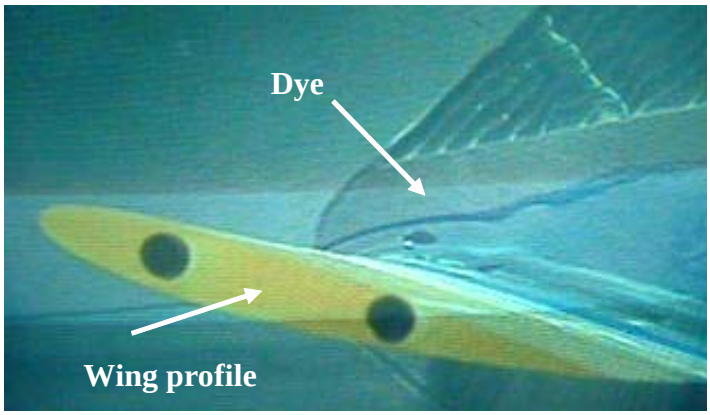

Mini-scale leading-edge flap inside (static)

Boundary layer separation control by unsteady excitation of mini-scale leading-edge flaps

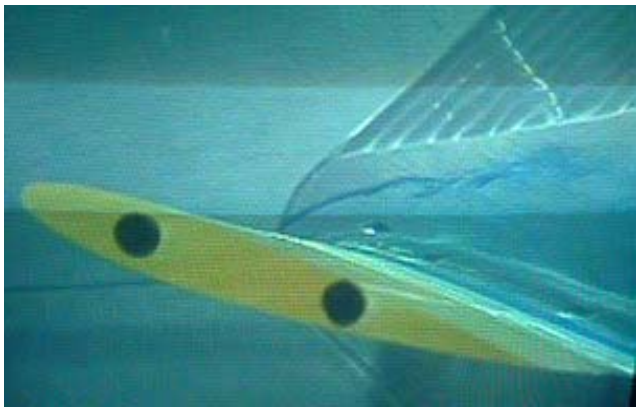

Mini-scale leading-edge flap outside (static)

Boundary layer separation control by unsteady excitation of mini-scale leading-edge flaps

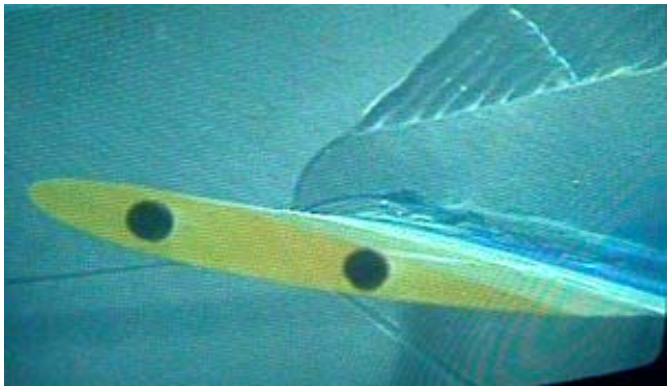

Mini-scale leading-edge flap oscillating at 0.5 Hz

Boundary layer separation control by unsteady excitation of mini-scale leading-edge flaps

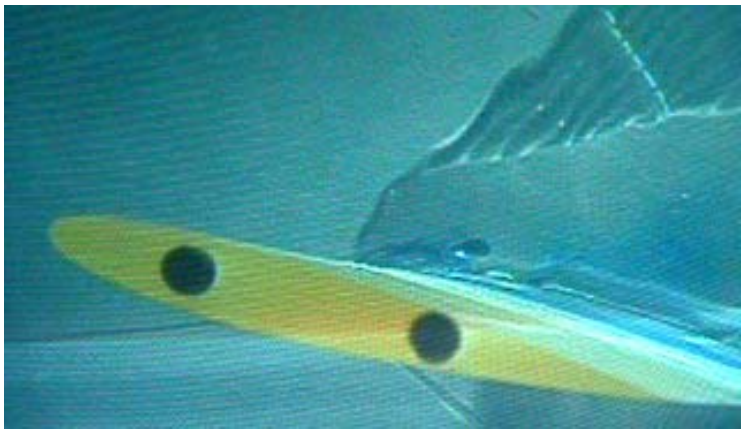

Mini-scale leading-edge flap oscillating at 1 Hz

- Video records

Mini-scale PIV measurement for mini-scale leading-edge flap inside the wing profile (static)

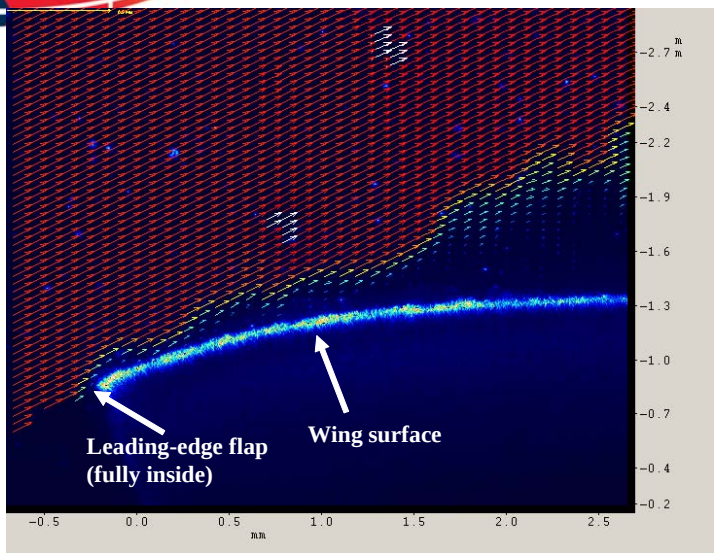

Mini-scale PIV measurement for mini-scale leading-edge flap outside the wing profile (static)

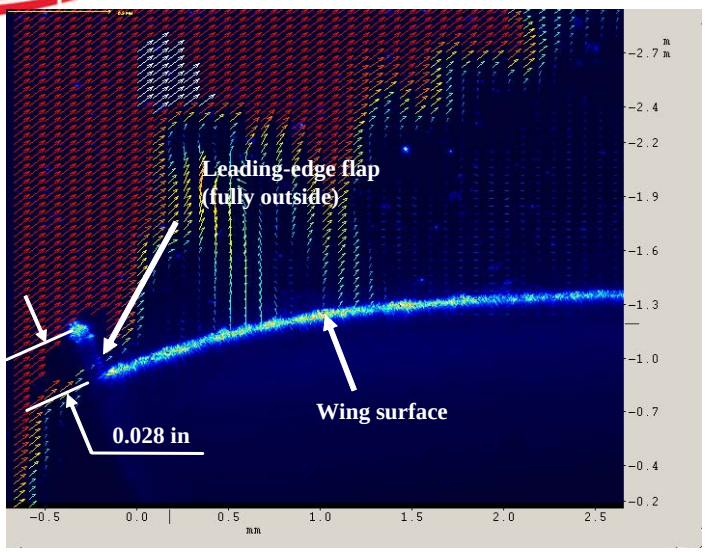

Mini-scale PIV measurement for leading-edge oscillating at 1Hz

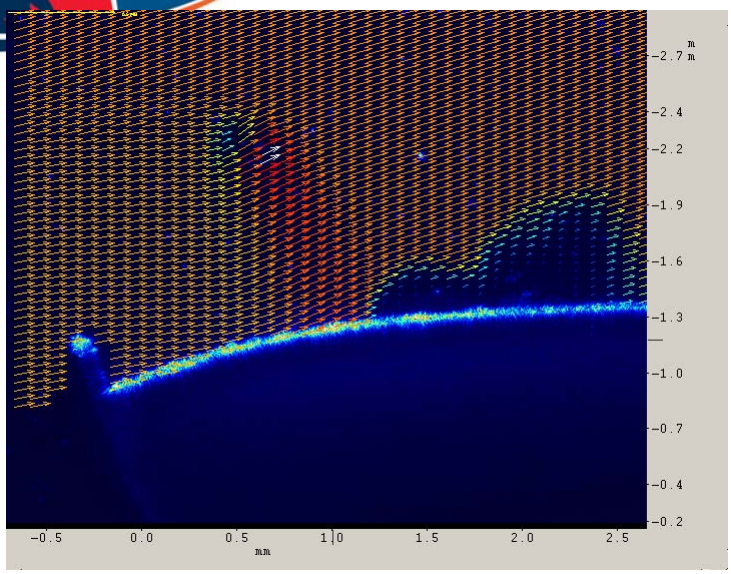

NRC·CNRC
NRCaerospace.com

Future work

NRC·CNRC
NRCaerospace.com

Future work

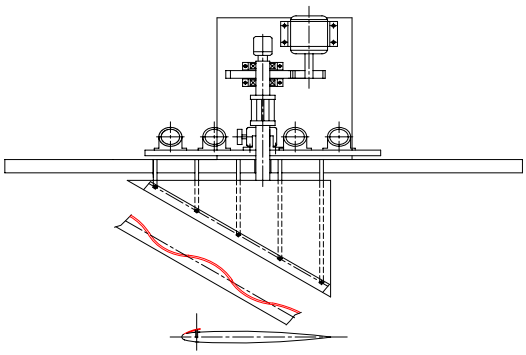

NRC·CNRC
NRCaerospace.com

Future work

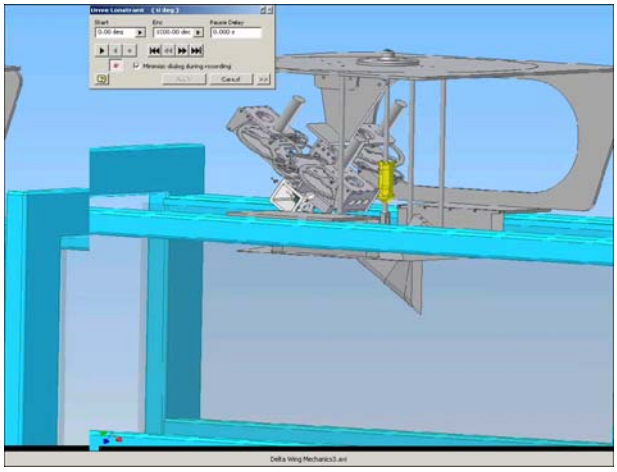

NRC·CNRC
NRCaerospace.com

Conclusion

1. New concept of bi-fold balance has been developed and constructed
2. Mini-scale PIV method can be used to visualize wall-bounded flow field
3. Unsteady excitation of mini-scale leading-edge flaps are able to create enough control force on boundary layer separation
4. Full model experiments remain to be completed

5. Microactuator Development

5.1 SMA Antagonistic Actuator Modeling and Validation Results

presented by O. Boissonneault, Numerica

In the field of micro-machines, shape memory alloys (SMA) are receiving increased attention because of their high power-to-volume ratio and large recoverable deformation. However, these materials have a complex thermomechanical behavior due to the hysteresis related to stress, strain and temperature. A constitutive model that can consider thermal or mechanical loads or a combination of loads was developed in order to predict shape memory effect as well as superelasticity.

The parameters for the constitutive model in the form of a phase diagram is required. They were measured using a 0.1 mm diameter SMA wire with a Rheometrics (RSA-II) Dynamic Mechanical Analyser in a series of isothermal tensile tests. All tests were in the range of 30°C to 130°C.

A small test bench was built to compare the predicted and experimental results. SMA wire measuring approximately 100 mm in length was excited by short and intense voltage pulses measuring between 4.5 to 10 volts. The contraction of the SMA was used to lift a constant 150 g load.

An another test bench was built to study the performance of SMA wire in an antagonistic set-up. A series of 2 or 3 volt step inputs were alternately injected into each wire to characterize the peak-to-peak displacement and the motion time constant. An antagonistic actuator model based on the hybrid SMA model predicted reasonably well the displacement-time results.

SMA Actuator Modeling and Validation Results

Olivier Boissonneault, RDDC-NUMERICA

Action list

8 – Characterize Dynalloy SMA wire and construct a small-scale test bench

9 – Examine ability of SMA model to predict response under complex force profile

10 – Investigate methods to increase frequency response of the SMA wire given force requirements

13 – Develop method to analyse compliant beam. Integrate method with SMA model to determine appropriate size for beam elements.

16 – Integrate control law in test bench environment. Explore ability to track command signal.

Characterization of the SMA wire

Characterization of the SMA wire

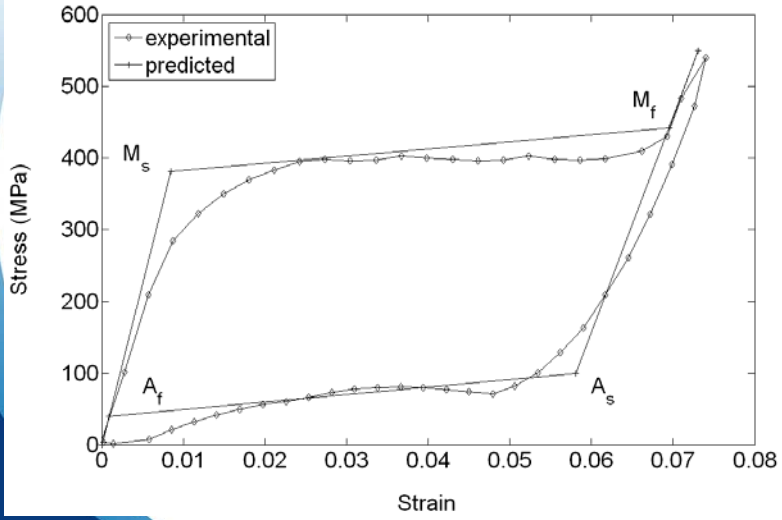

Characterization of the SMA wire

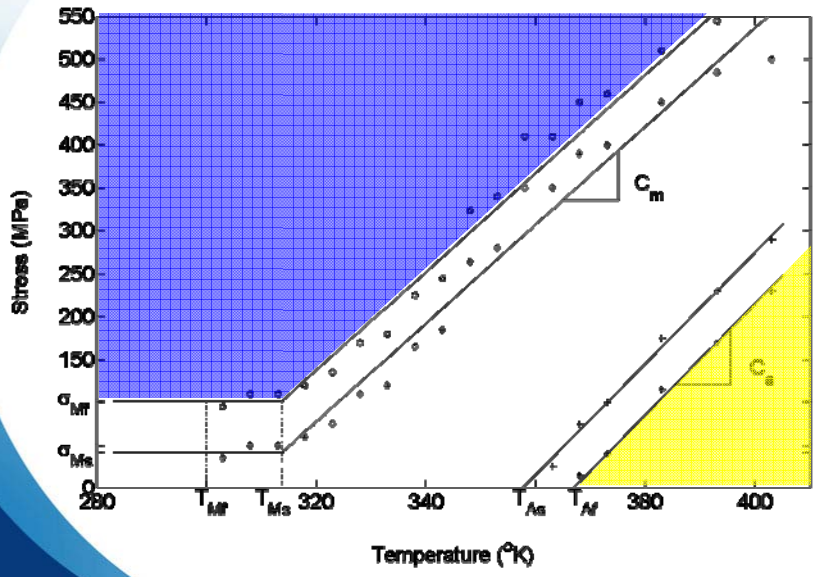

Small test bench

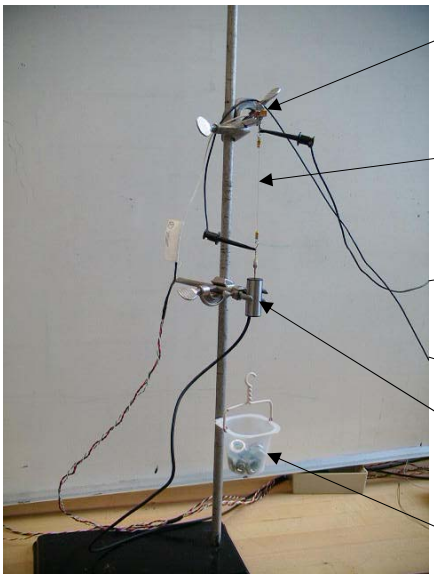

Results for 4.5 volts

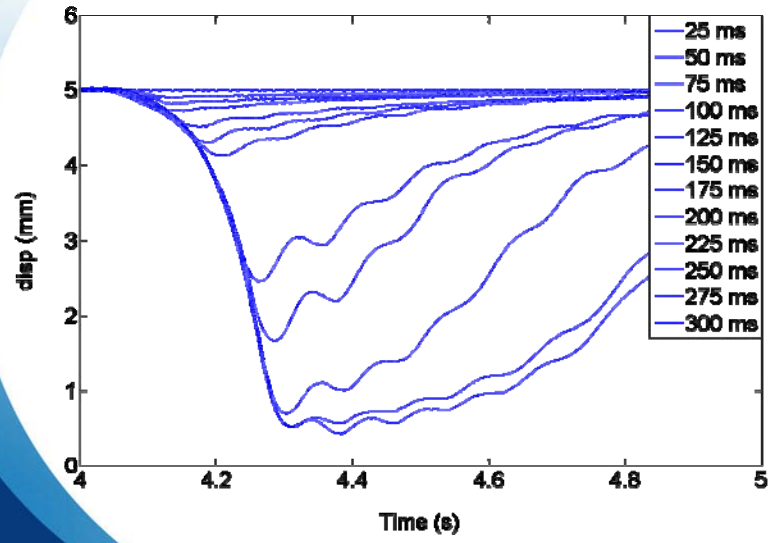

Results for 10 volts

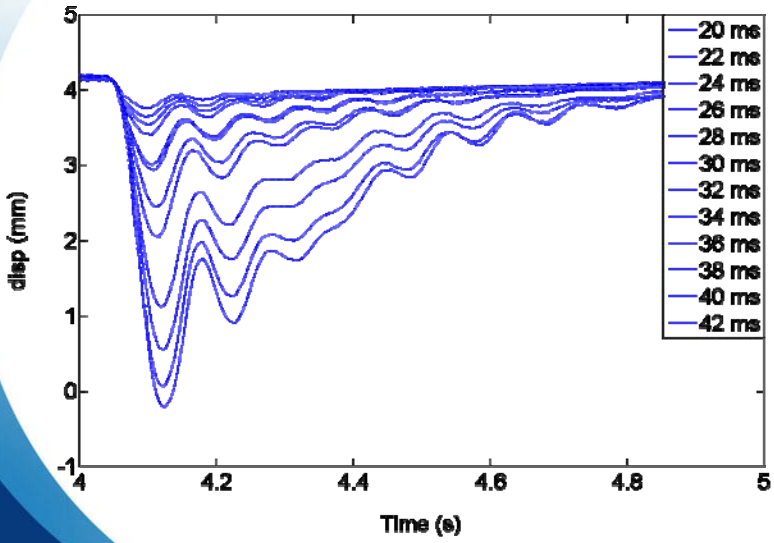

Displacement of 1 mm

Voltage (V)	Heating (ms)	Cooling (ms)	Total Time (ms)	Oscillations	Power (W)	Energy (J)
10	26	1070	1096	++++	10	0.26
8	40	1210	1250	+++	6.4	0.256
6	100	1160	1260	++	3.6	0.36
4.5	175	1140	1315	+	2.03	0.304

$$P = \frac{E^2}{R}$$

* Hypothesis : the electrical resistance is 10 ohms

Action list

8 – Characterize Dynalloy SMA wire and construct a small-scale test bench

9 – Examine ability of SMA model to predict response under complex force profile

10 – Investigate methods to increase frequency response of the SMA wire given force requirements

13 – Develop method to analyse compliant beam. Integrate method with SMA model to determine appropriate size for beam elements.

16 – Integrate control law in test bench environment. Explore ability to track command signal.

Antagonistic test bench

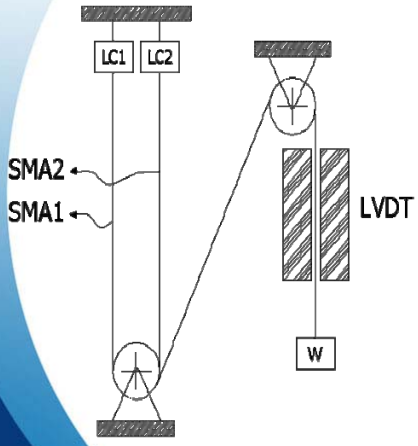

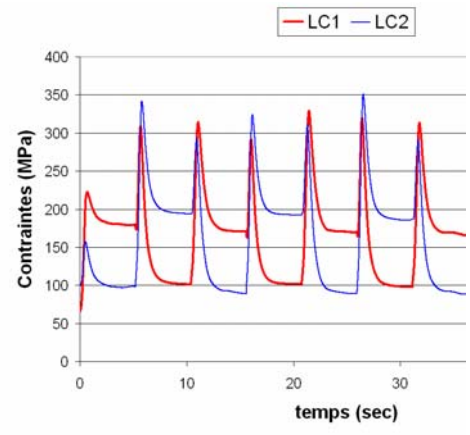

Antagonistic test bench

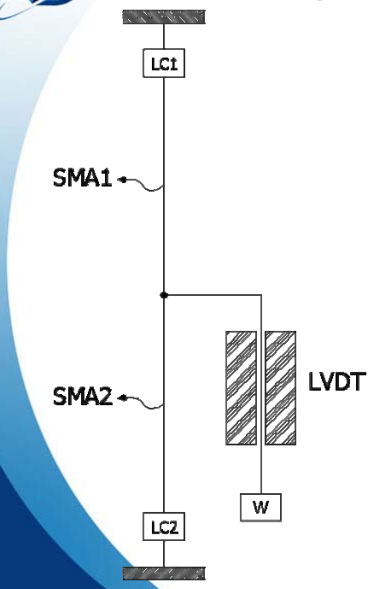

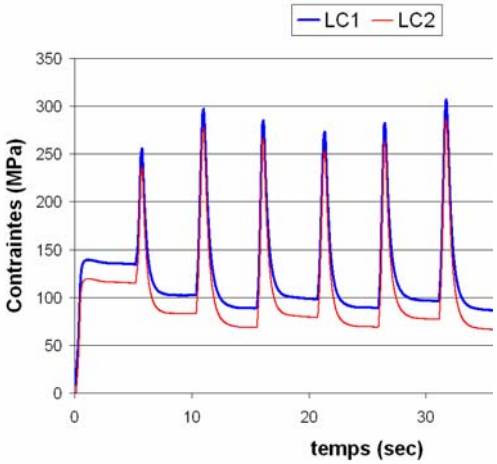

Modification of the model hybrid

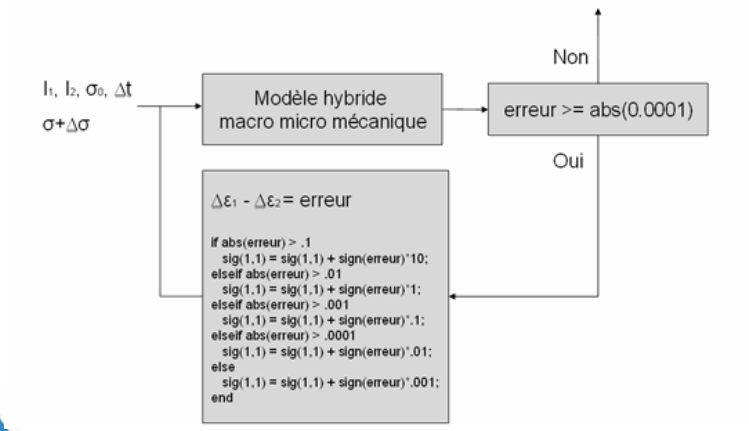

Experimental VS Predicted

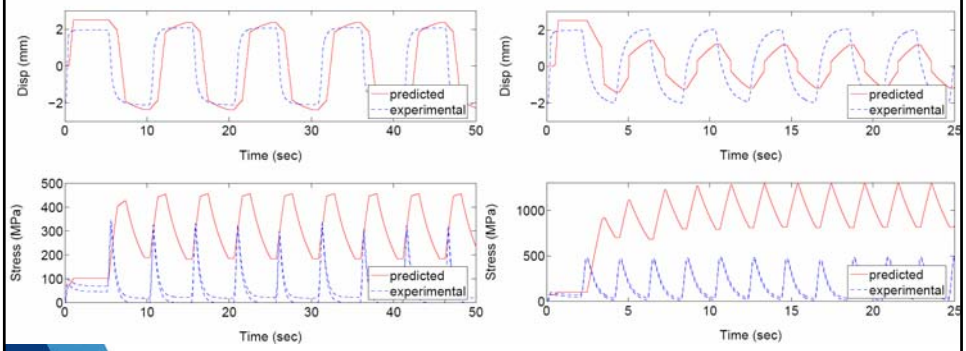

square 2 V -- 0.1 Hz

square 3 V -- 0.25 Hz

Action list

8 – Characterize Dynalloy SMA wire and construct a small-scale test bench

9 – Examine ability of SMA model to predict response under complex force profile

10 – Investigate methods to increase frequency response of the SMA wire given force requirements

13 – Develop method to analyse compliant beam. Integrate method with SMA model to determine appropriate size for beam elements.

16 – Integrate control law in test bench environment. Explore ability to track command signal.

Compliant actuator

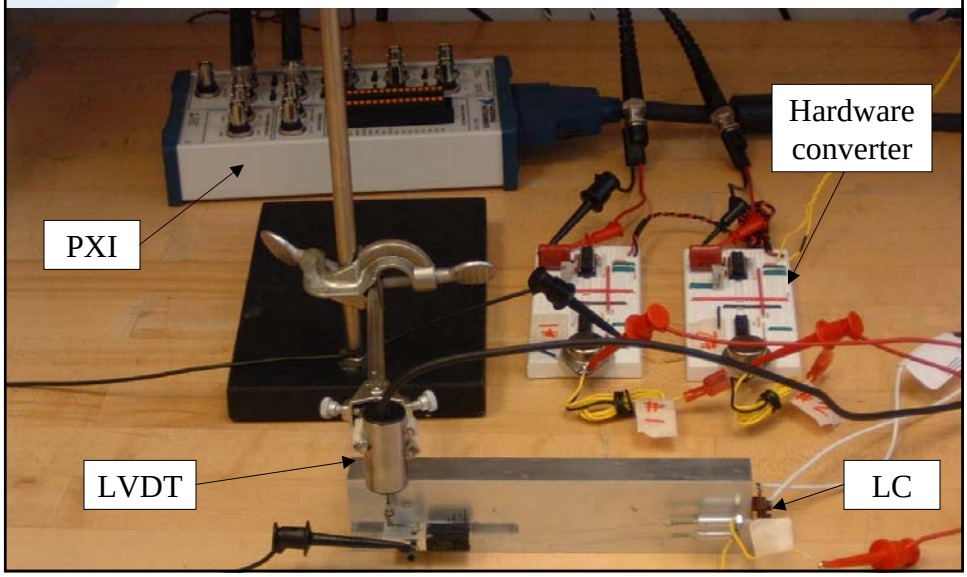

Compliant actuator

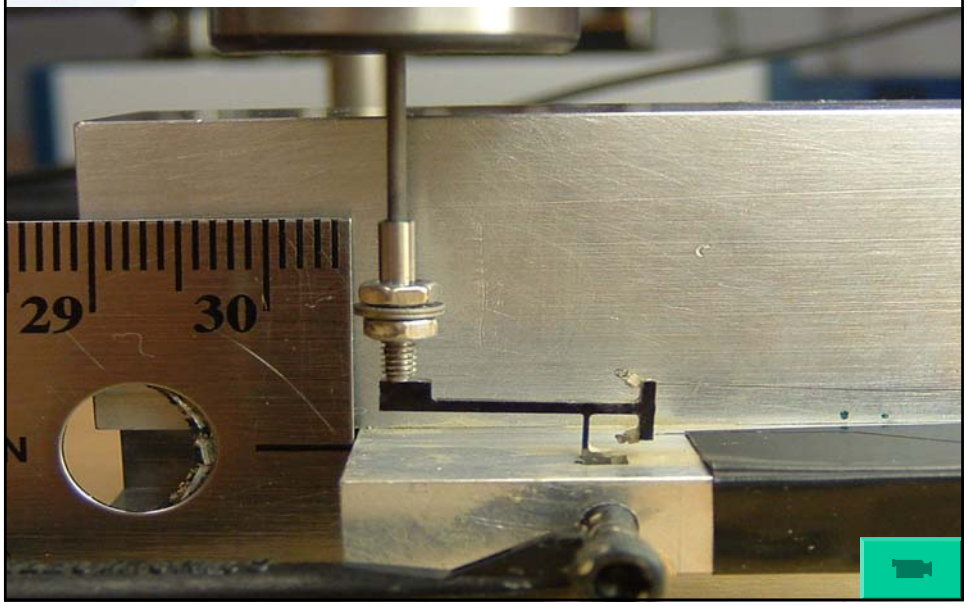

Results close loop

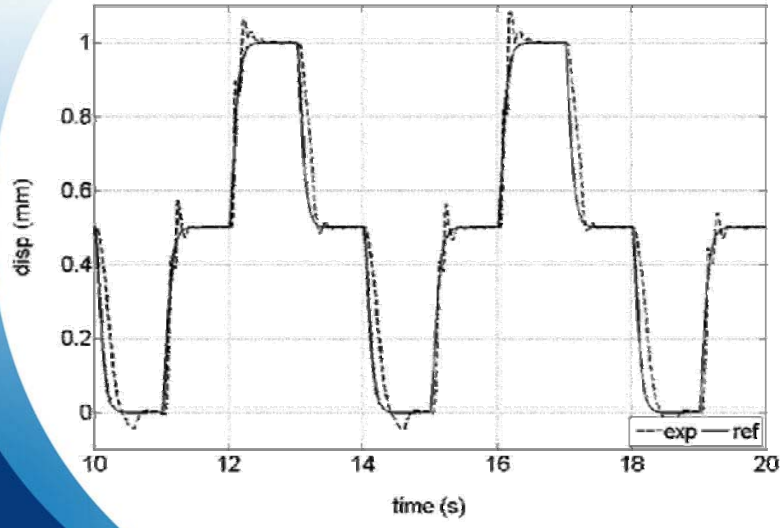

Future works

- Calibration of flow effectors strain gage (last generation)
- System identification of the actuators for control
- Validation of the closed loop control
- Validation in the wind tunnel

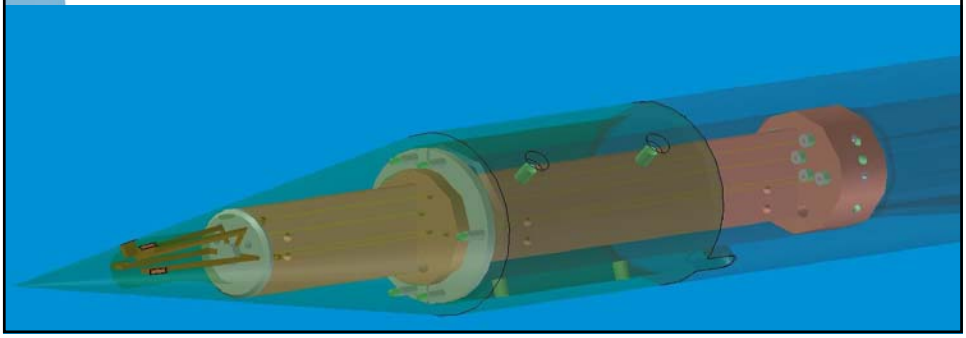

Question ?

5.2 Compliant Flow Effector Design for Missile Side Force Control

presented by F. Wong, DRDC – Valcartier

Active flow control can be used in a control actuation system to generate control authority for supersonic missiles. Placing small flow effectors close to the nose tip permits modulation of vortex shedding to generate controllable side forces and moments. The lack of volume for an actuator in the missle nose necessitates a different approach be taken for its design. To this end, an actuator comprised of a shape memory alloy actuator (SMA) coupled to a compliant mechanism was conceived. The mechanism acts as a transmission to convert the force-displacment characteristics of the SMA wire to the displacement characteristics required to generate control forces.

Three compliant mechanisms were studied. Pivot, Trapezoid and Inverted Trapezoid geometries were selected for their simplicity. The main constraints for a viable mechanism geometry were maximizing the tip displacement while keeping the post base stresses below the structure's yield stress. It was found that a trapezoid mechanism gave a tip displacement of 870 micron while remaining within the yield stress limits of the material. The Pivot and Inverted Trapezoid geometries could not transform the SMA force and displacement input without yielding the structure.

DEFENCE R&D DÉFENSE

Compliant Flow Effector Design for Missile Side Force Control

F. Wong, Precision Weapons Section

4th Meeting on Missile Control using Microactuated Flow Effectors

April 2006

Defence Research and Development Canada
Recherche et développement pour la défense Canada

Canada

Background

- Wind tunnel studies on finless missile showed that the magnitude of the side force can be modulated by positioning micro-flow effectors at different angular positions around central axis.
- Shape memory alloy study developed a constitutive model that captures the temporal thermomechanical behavior of the material.
- Control algorithm was synthesized to compensate for hysteretic behaviour and provide good tracking performance at moderately high frequencies.

Compliant Mechanism Requirements

Flow effectors: 1 mm x 2.67 mm x 0.76 mm
Diameter at 1st row: 10 mm
Operating parameters:
a) 1 mm flow effector deflection
b) 150-200 g SMA applied force
c) no yielding of material
d) 1 Hz operation

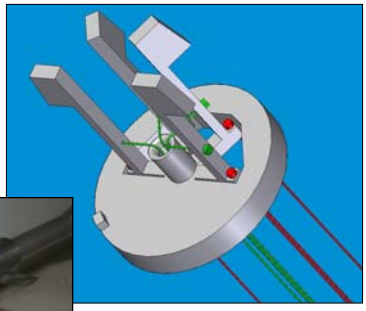

Problem Statement

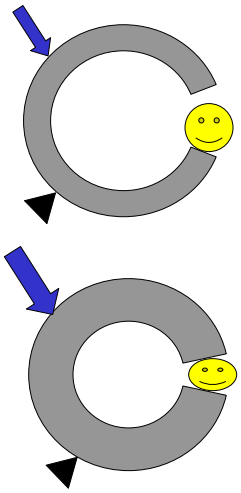

- Seek a structure that will meet kinematic requirements while at the same time meet mechanical requirements.
- Too flexible a structure will not support loads.
- Too rigid a structure will require high forces to achieve motion.
- Synthesis procedure finds an optimum structure that satisfies both requirements.

Synthesis Criteria

- Required kinematic motion
- Available design space
- Desired geometric or mechanical advantage
- Material properties
- Stress or strain limitations

Current synthesis methods address these criteria.

- Buckling instabilities
- Weight limitations
- Dynamic behaviour

Pivot Concept

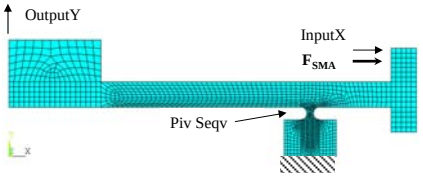

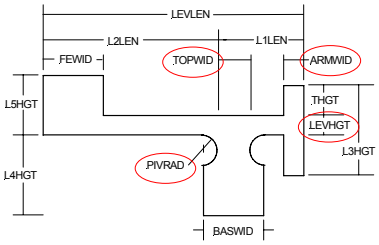

	1		2		3		4		5	
TOPWID	203.2	(micron)	**152.2**	(micron)	203.0	(micron)	203.2	(micron)	203.2	(micron)
PIVRAD	191.0	(micron)	191.0	(micron)	**762.0**	(micron)	**381.0**	(micron)	**444.5**	(micron)
ARMWID	508.0	(micron)	508.0	(micron)	**762.0**	(micron)	**762.0**	(micron)	**762.0**	(micron)
LEVHGT	508.0	(micron)	508.0	(micron)	508.0	(micron)	**762.0**	(micron)	**762.0**	(micron)
InputX	45.0	(micron)	75.5	(micron)	46.2	(micron)	69.5	(micron)	76.0	(micron)
OutputY	169.8	(micron)	330.3	(micron)	192.0	(micron)	278.5	(micron)	301.5	(micron)
Piv Seqv	546.2	(MPa)	926.1	(MPa)	616.7	(MPa)	619.4	(MPa)	648.8	(MPa)
Out/In Disp	3.8		4.4		4.2		4.0		4.0	
Seqv/SY	1.10		1.86		1.24		1.25		1.31	

L1LEN	(micron)	3505.0
L2LEN	(micron)	8839.0
L3HGT	(micron)	2540.0
L4HGT	(micron)	1499.0
L5HGT	(micron)	2032.0
ARMWID	(micron)	508.0
LEVHGT	(micron)	508.0
TOPWID	(micron)	203.0
BASWID	(micron)	1575.0
FEWID	(micron)	2794.0
LEVLEN	(micron)	12344.0
FETHK	(micron)	787.0
THGT	(micron)	1016.0
PIVRAD	(micron)	191.0
SY allow	(MPa)	497.0
Modulus	(MPa)	72.0
FSMA	(g)	150.0

Inverted Trapezoidal Post

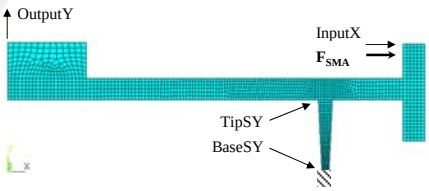

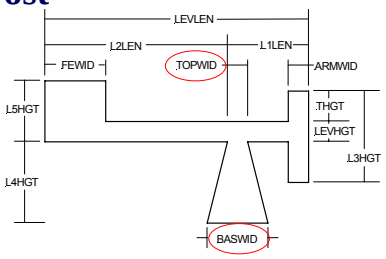

	1		2		3	
TOPWID	508.0	(micron)	**787.4**	(micron)	**787.4**	(micron)
BASWID	787.4	(micron)	**508.0**	(micron)	**254.0**	(micron)
InputX	21.3	(micron)	22.9	(micron)	56.4	(micron)
OutputY	41.3	(micron)	44.3	(micron)	154.8	(micron)
BaseSY	57.5	(MPa)	167.8	(MPa)	713.7	(MPa)
TipSY	54.9	(MPa)	16.1	(MPa)	14.1	(MPa)
Out/In Disp	1.9		1.9		2.7	
BaseSY/SY	0.12		0.34		1.44	
TipSY/SY	0.11		0.03		0.03	

L1LEN	(micron)	3759.0
L2LEN	(micron)	8839.0
L3HGT	(micron)	2540.0
L4HGT	(micron)	1498.6
L5HGT	(micron)	2032.0
TOPWID	(micron)	508.0
BASWID	(micron)	787.0
ARMWID	(micron)	762.0
LEVHGT	(micron)	508.0
FEWID	(micron)	2794.0
LEVLEN	(micron)	14760.0
FETHK	(micron)	787.0
THGT	(micron)	1016.0
SY allow	(MPa)	497.0
Modulus	(MPa)	150.0
FSMA	(g)	150.0
FAERO	(N)	0.172

Trapezoidal Post

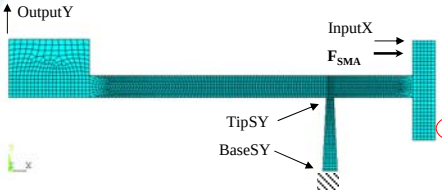

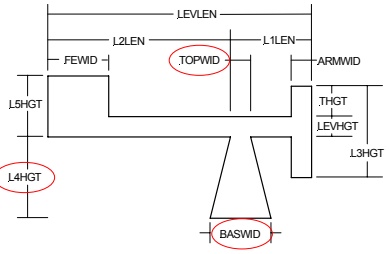

	1		2		3		4		5		6	
TOPWID	508.0	(micron)	**254.0**	(micron)	**254.0**	(micron)	**254.0**	(micron)	**254.0**	(micron)	**254.0**	(micron)
BASWID	787.0	(micron)	**254.0**	(micron)	**304.8**	(micron)	**304.8**	(micron)	**304.8**	(micron)	**304.8**	(micron)
L4HGT	1498.6	(micron)	**2540.0**	(micron)	**2540.0**	(micron)	**2540.0**	(micron)	**2540.0**	(micron)	**2540.0**	(micron)
L3HGT	2540.0	(micron)	2540.0	(micron)	2540.0	(micron)	**3429.0**	(micron)	**3429.0**	(micron)	**3175.0**	(micron)
L2LEN	8839.0	(micron)	8839.0	(micron)	8839.0	(micron)	8839.0	(micron)	**10998.2**	(micron)	**11000.0**	(micron)
LEVHGT	508.0	(micron)	508.0	(micron)	508.0	(micron)	508.0	(micron)	508.0	(micron)	**762.0**	(micron)
FAERO	0.0	(N)	0.0	(N)	0.0	(N)	0.172	(N)	0.172	(N)	0.172	(N)
InputX	21.3	(micron)	414.3	(micron)	296.8	(micron)	321.0	(micron)	282.7	(micron)	275.4	(micron)
OutputY	41.3	(micron)	1217.0	(micron)	896.7	(micron)	770.8	(micron)	814.0	(micron)	870.3	(micron)
BaseSY	57.5	(MPa)	786.4	(MPa)	545.0	(MPa)	510.9	(MPa)	477.2	(MPa)	477.3	(MPa)
TipSY	54.9	(MPa)	211.4	(MPa)	212.9	(MPa)	164.8	(MPa)	120.1	(MPa)	130.5	(MPa)
Out/In Disp	1.9		2.9		3.0		2.4		2.9		3.2	
BaseSY/SY	0.12		1.58		1.10		1.03		0.96		0.96	
TipSY/SY	0.11		0.43		0.43		0.33		0.24		0.26	

L1LEN	(micron)	3759.0
L2LEN	(micron)	8839.0
L3HGT	(micron)	2540.0
L4HGT	(micron)	1498.6
L5HGT	(micron)	2032.0
TOPWID	(micron)	508.0
BASWID	(micron)	787.0
ARMWID	(micron)	762.0
LEVHGT	(micron)	508.0
FEWID	(micron)	2794.0
LEVLEN	(micron)	14760.0
FETHK	(micron)	787.0
THGT	(micron)	1016.0
SY allow	(MPa)	497.0
Modulus	(MPa)	150.0
FSMA	(g)	150.0
FAERO	(N)	0.172

Validation of Analysis

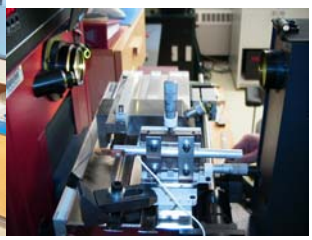

- Measured flow effector tip and T-section displacements and compliant link strains.

Displacement Results

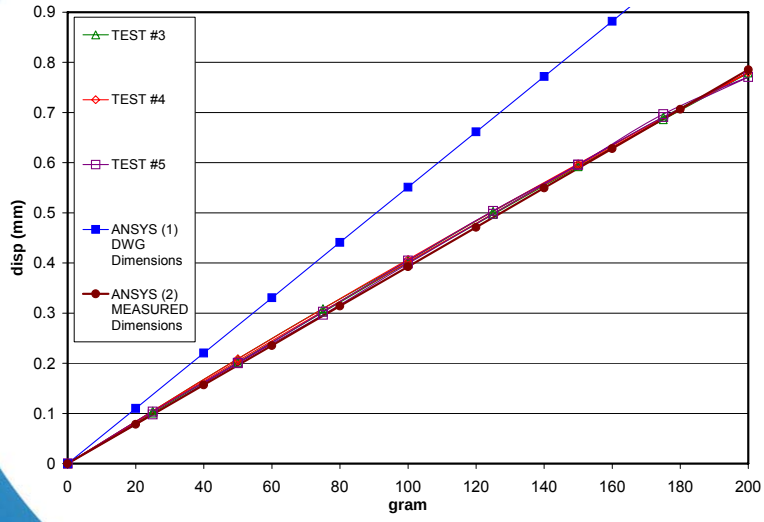

Compliant Link Strain Results

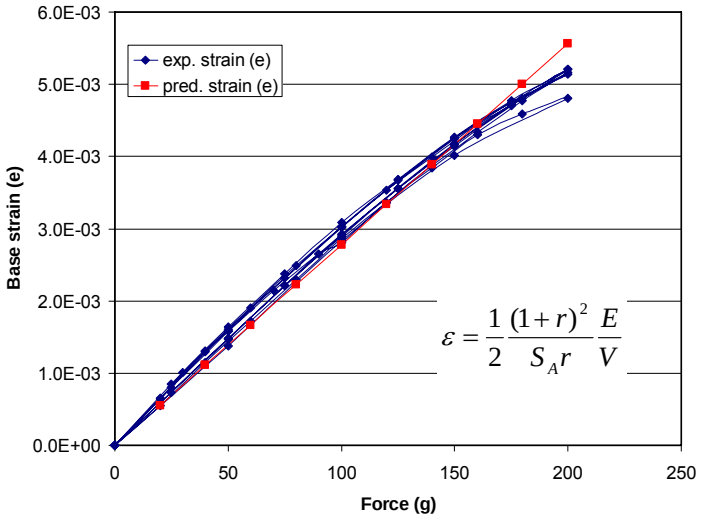

Final Configuration

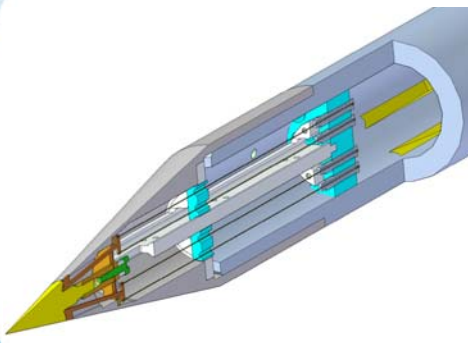

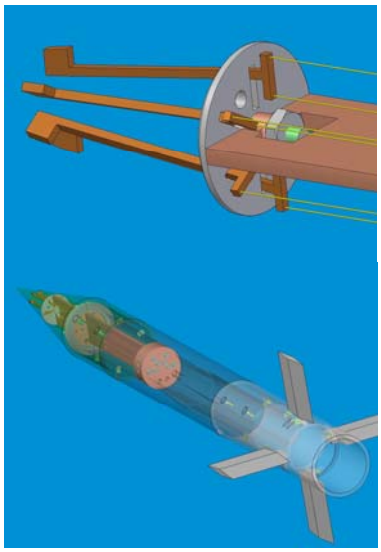

Final Flow Effector Geometry

L1LEN	(micron)	3607.0
L2LEN	(micron)	21158.0
L3HGT	(micron)	3429.0
L4HGT	(micron)	2540.0
L5HGT	(micron)	2286.0
TOPWID	(micron)	254.0
BASWID	(micron)	279.0
ARMWID	(micron)	762.0
LEVHGT	(micron)	762.0
FEWID	(micron)	2667.0
LEVLEN	(micron)	24765.0
FETHK	(micron)	787.0
THGT	(micron)	1207.0
SY allow	(MPa)	882.0

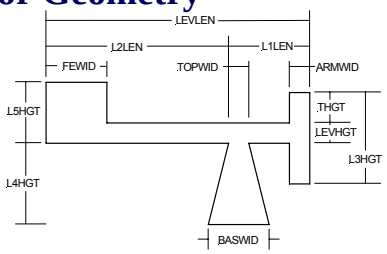

FSMA Top	(g)	150.0	0.0	150.0	0.0	185.0	185.0	(g)
FSMA Bot	(g)	0.0	150.0	0.0	150.0	0.0	150.0	(g)
FAero	(N)	0.172	0.172	0.0	0.0	0.172	0.172	(N)
SMA Top X	(micron)	154.7	-189.2	367.2	23.3	240.4	263.6	(micron)
SMA Top Y	(micron)	-136.2	202.7	-345.1	-6.2	-216.7	-222.9	(micron)
SMA Bot X	(micron)	16.7	14.5	23.3	21.1	22.2	43.2	(micron)
SMA Bot Y	(micron)	-135.9	203.0	-344.8	-5.9	-216.3	-222.3	(micron)
FE Frt X	(micron)	51.8	-40.9	112.1	19.4	78.0	97.4	(micron)
FE Frt Y	(micron)	662.4	-1351.6	2078.1	64.2	1147.3	1211.4	(micron)
FE Bck X	(micron)	60.7	-61.4	142.4	20.3	93.9	114.2	(micron)
FE Bck Y	(micron)	586.5	-1175.1	1817.7	56.1	1010.6	1066.7	(micron)
Link Tip X	(micron)	59.7	-49.2	128.8	19.9	89.8	109.6	(micron)
Link Tip Y	(micron)	4.7	-6.8	12.1	0.5	7.6	8.1	(micron)
Link Base SY	(MPa)	449.0	-100.5	798.8	249.3	635.4	884.6	(MPa)
Link Tip SY	(MPa)	19.1	-481.8	344.4	-156.4	99.4	-57.0	(MPa)
Link Base ey	(--)	0.0032	-0.0012	0.0059	0.0016	0.0045	0.0061	(--)
Out/In Disp		4.3	7.1	5.7	2.8	4.8	4.6	

Summary

- Compliant mechanism principles used to develop a transmission mechanism to transform the force-displacement characteristics of the actuator to the required force-displacement characteristics of the flow effector.
- Initial mechanism produced 90% of the desired displacement without yielding the material.
- Design validated with displacement and strain data under applied forces.
- Design revised to produce 1 mm displacement and adjusted for missile model envelope constraints.
- Design of four flow effector assembly produced.

6. Micro-Fabrication Technology

6.1 Precision Fabrication of Active Flow Effectors for Supersonic Missile Control

presented by S.K. Nikumb, IMTI/NRC

Development of highly precise flow effectors based on the results of studies in aerodynamics, control system requirements and design specifications, posed significant challenges to manufacture them. In this presentation, we report our results on the precision fabrication of the test bench and final optimum geometries of the flow effectors. To achieve desired geometric tolerances, repeatability and good surface finish, different machining methods were employed and their relative performance was evaluated. The machining method was optimized during the fabrication of four versions of the flow effectors made from Aluminum, Brass, Shape Memory Alloy (SMA) and Titanium materials. Laser machining, micro-hole drilling, laser-milling as hybrid process and micro milling processes were used in the fabrication of the flow effectors. Based on the results obtained from the initial bench tests, several samples of Titanium flow effectors were successfully fabricated with high dimensional accuracy, <6 micron tolerance and with a cut edge surface finish down to several tens of nanometers. The samples were measured and characterized using optical inspection techniques SEM, Microscopes, WYKO and shadow graph instruments. Interesting observations were made on tool wear and its effect on the cut edge surface finish.

NRC·CNRC
Integrated Manufacturing Technologies Institute

Precision Fabrication of Flow Effectors for Supersonic Missile Control

SUWAS NIKUMB
NRC-IMTI
Suwas.nikumb@nrc.ca

National Research Council Canada | Conseil national de recherches Canada | Canada

DRDC Final Meeting April 19th, 2006

NRC·CNRC
Integrated Manufacturing Technologies Institute

Introduction

Precision Fabrication of the Flow Effector

Objective: To achieve high dimensional tolerances, repeatability, and good edge surface finish

Version 1: Process selection, Parameters development, Laser cutting of flow effectors out of Al, SMA, Ti, and Brass, cut and drill quality
Version 2: New geometry, Experimental Verification, Fabrication of flow effectors out of Al, SMA, Ti, and Brass on materials
Version 3: Dimensional changes, Test bed set up
Version 4: Final version fabrication in Titanium, Challenges, WYKO Measurements, Fixture development, Surface finish, Tool wear, Observations with and without coolant.

NRC·CNRC
Integrated Manufacturing Technologies Institute

Flow Effector Version 1

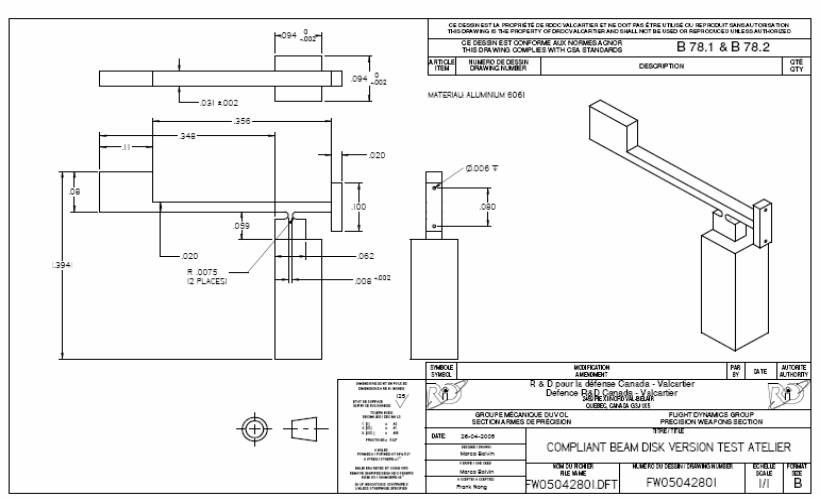

Geometric Specs determination, Post thickness, 250 µm supports requirements, processes – Laser, Micro-milling and Both, Samples prepared and evaluated. Laser Process too long. Materials Brass, Aluminum 7075, A number of trials conducted however samples were never tested.

NRC·CNRC
Integrated Manufacturing Technologies Institute

Al 7075 Edge and drill

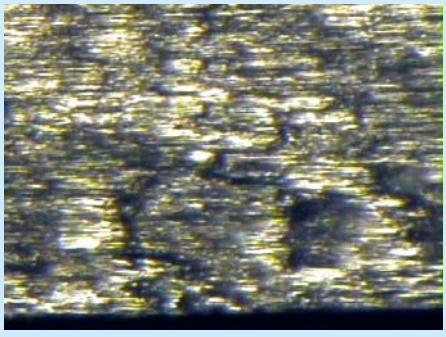

x 80

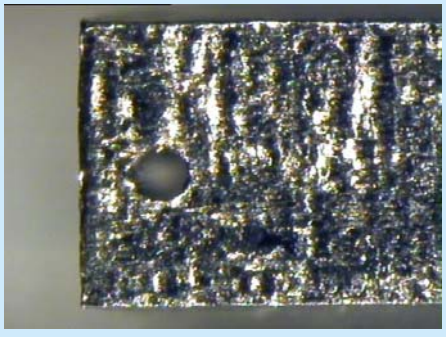

x 32

Micro milling / laser combined process

Brass Edge and Drill

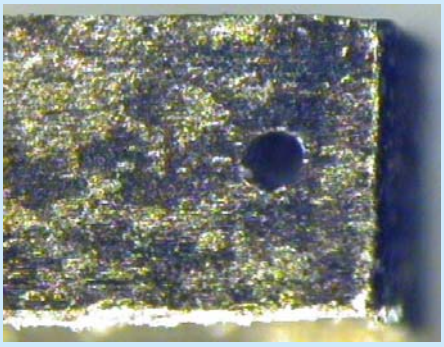

x 80

Micro milling / laser
combined process

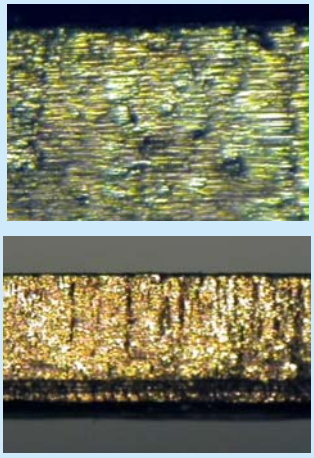

x 32

SMA Edge and Drill

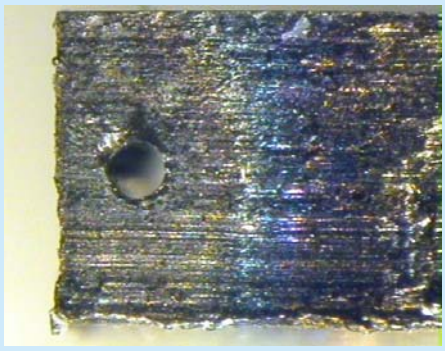

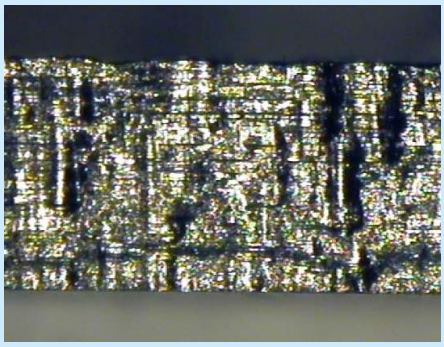

Micro milling / laser
combined process

NRC·CNRC Integrated Manufacturing Technologies Institute

Titanium Drill and Edge

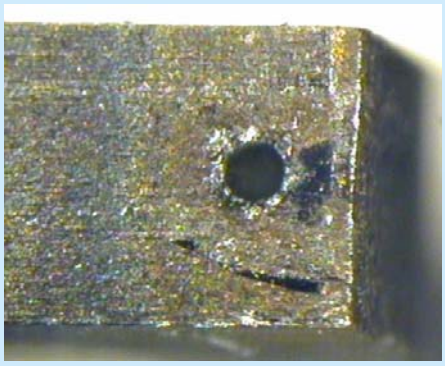

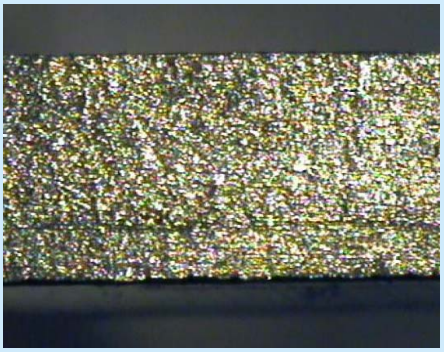

Micro milling / laser
combined process

NRC·CNRC Integrated Manufacturing Technologies Institute

Flow Effector Version 2

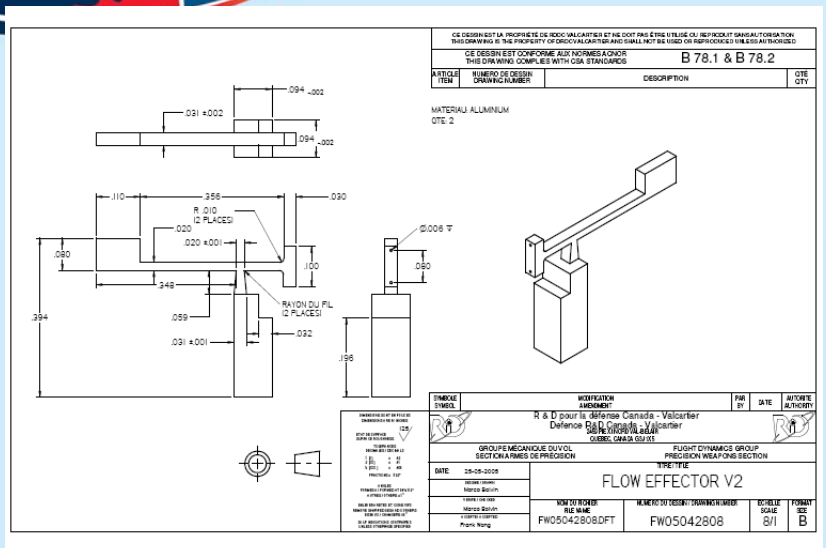

New geometry with triangular post, Samples for all materials prepared and tested/no consistency in dimensions of diff materials, Holes were made but laser drill was removing post material, conical entrance small exit debris not removed fully, shielding required below.

NRC·CNRC Integrated Manufacturing Technologies Institute

Flow Effectors Version 2

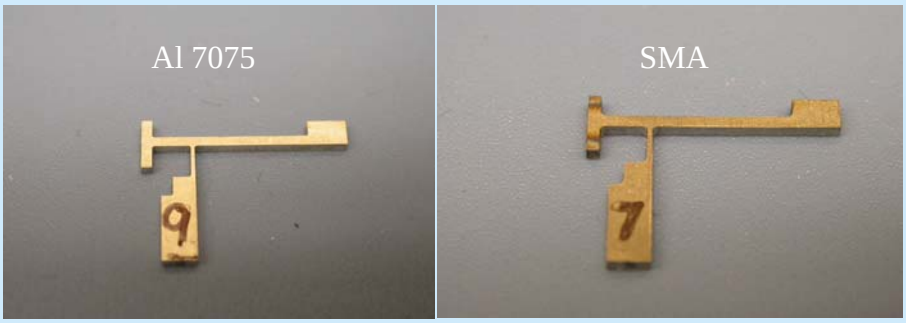

NRC·CNRC Integrated Manufacturing Technologies Institute

Flow Effectors Version 2

Brass

Ti

SMA

Al

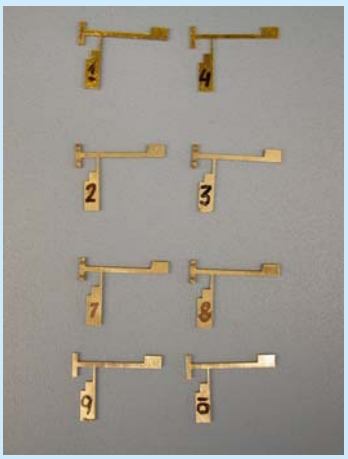

NRC·CNRC
Integrated Manufacturing Technologies Institute

Flow Effector Version 3

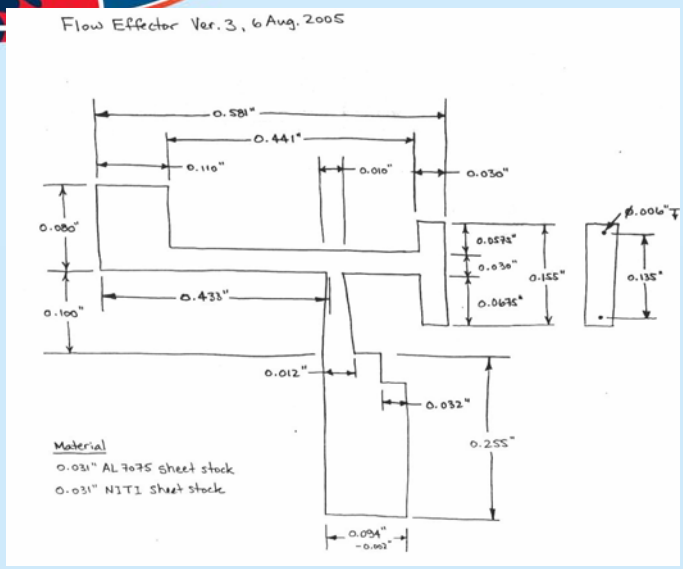

Conceptual version with several dimensional changes, measuring improvements. Never made samples and moved on to version 4

NRC·CNRC
Integrated Manufacturing Technologies Institute

Test Bed Setup Concept

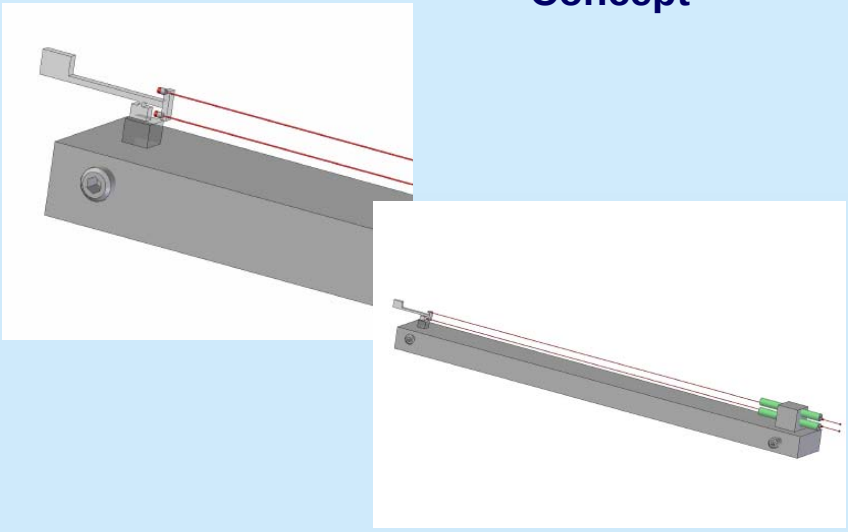

NRC·CNRC
Integrated Manufacturing Technologies Institute

Flow Effector Version 4

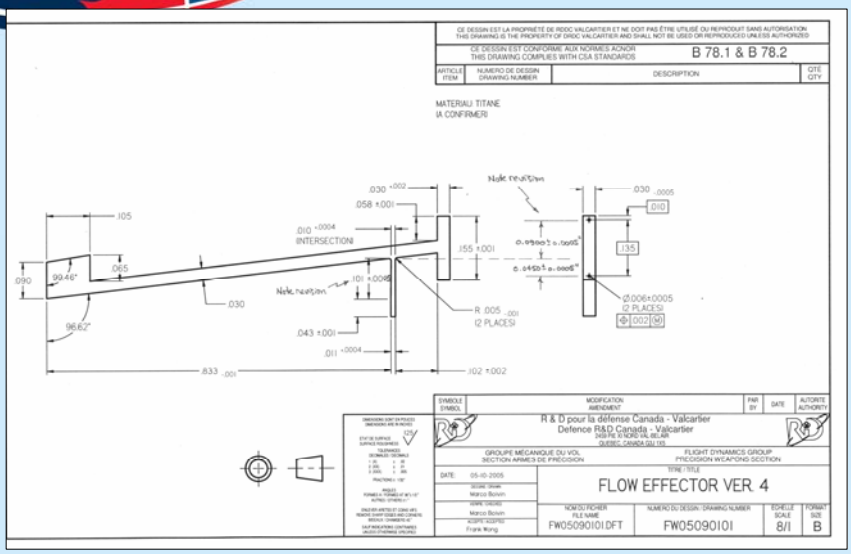

Main change was in length X2, angular shape, difficulty in measuring tolerances. Materials Ti and SMA. SMA was too thick, Very tight tolerances <0.0004", post with slight angle and then straight, Process used: Micromilling

NRC·CNRC
Integrated Manufacturing Technologies Institute

Fabrication Challenges

Fabrication Challenges:

- high accuracy: +0.0004" (+6.36 µm)
- high dimensional aspect ratio: 0.011":0.965" (1:87)
- high dimensional repeatability between parts
- low surface roughness
- verticality of machined sides

Micro-milling challenges:

- machinability of Ti / new "zero" / optimal process parameters / tool wear

General:

- Material Hardness – RC 23
- 10 + 2 parts Micro machined within tolerances
- Surface finish – along cutting direction Ra < 600nm
  across cutting direction Ra < 800nm

Successfully made 10+2 samples (in all 19 tested)

NRC·CNRC Integrated Manufacturing Technologies Institute

Flow Effectors Version 4

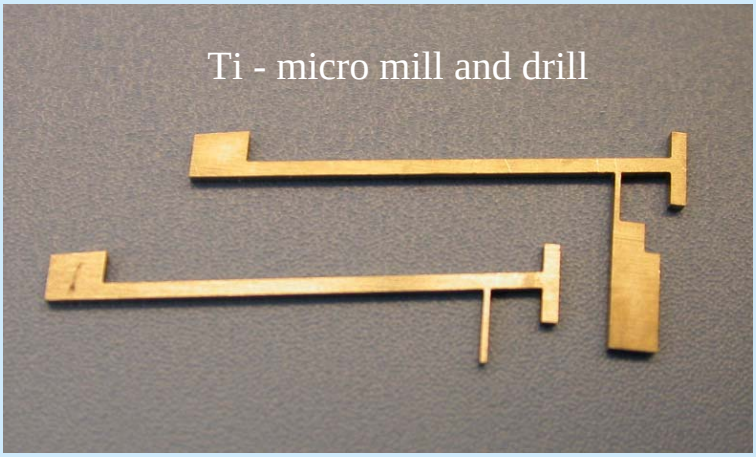

NRC·CNRC Integrated Manufacturing Technologies Institute

Micro-hole Drilling fixture

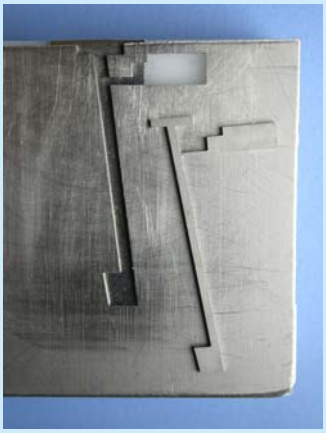

150 micron hole drilling

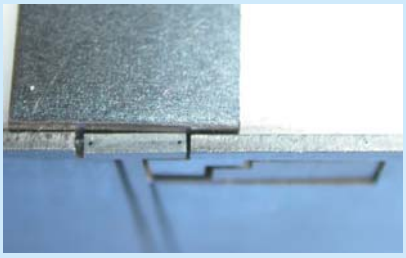

NRC·CNRC
Integrated Manufacturing Technologies Institute

Micro-hole Drilling on Titanium Flow Effector

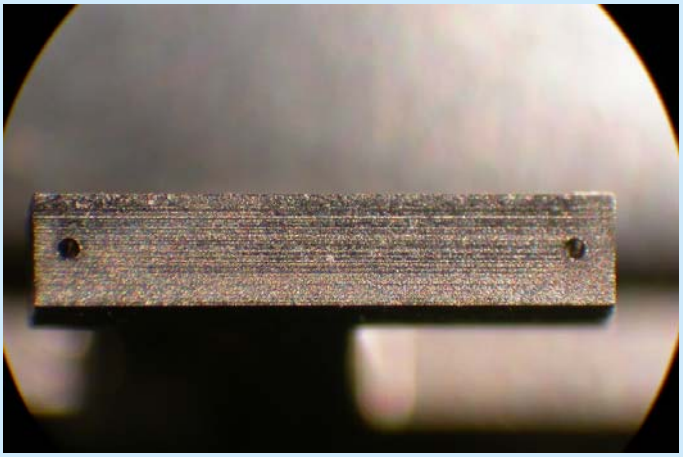

NRC·CNRC
Integrated Manufacturing Technologies Institute

Fabricated Flow Effectors

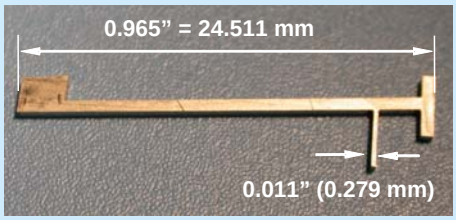

Flow Effector

Test Bench

Holes

NRC·CNRC
Integrated Manufacturing Technologies Institute

Measured Dimensions

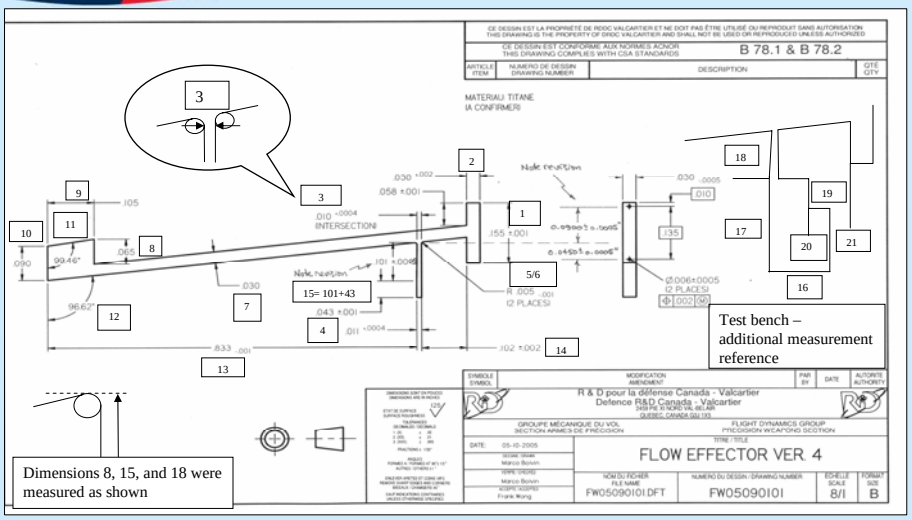

Total number of fabricated Flow Effectors: 19

NRC·CNRC
Integrated Manufacturing Technologies Institute

Measured Dimensions Flow Effector

Flow Effector Ver.4 (FW05090101)

	Part#	6	7	8	9	10	11	12	13	14	15	16	Method
Dim	Req	Mill 2	Mill 2	Mill 2	Mill 2	Mill 2	Mill 2	Mill 2	Mill 2	Mill 2	Mill 2	Mill 2	
1	155.00	154.75	154.75	154.95	154.85	154.75	154.65	154.70	154.90	154.95	154.45	154.90	Microscope
	+/-1.00	-0.25	-0.25	-0.05	-0.15	-0.25	-0.35	-0.30	-0.10	-0.05	-0.55	-0.10	
2	30.00	30.15	30.50	30.50	30.50	30.25	30.00	30.25	30.15	30.45	30.05	30.15	Microscope
	+2.00	0.15	0.50	0.50	0.50	0.25	0.00	0.25	0.15	0.45	0.05	0.15	
3	10.00	10.20	10.35	10.35	10.30	10.25	10.15	10.30	10.30	10.35	10.30	10.25	Microscope
	+0.40	0.20	0.35	0.35	0.30	0.25	0.15	0.30	0.30	0.35	0.30	0.25	
4	11.00	11.20	11.35	11.35	11.35	11.35	11.05	11.40	11.20	11.35	11.35	11.15	Microscope
	+0.40	0.20	0.35	0.35	0.35	0.35	0.05	0.40	0.20	0.35	0.35	0.15	
5 L	5.00	5.38	5.37	5.23	5.14	5.22	5.30	5.42	5.13	5.33	5.02	4.97	Vision Gauge
Rad	+/-0.5	0.38	0.37	0.23	0.14	0.22	0.30	0.42	0.13	0.33	0.02	-0.03	
6 R	5.00	5.03	5.04	5.06	5.11	5.07	5.24	5.15	5.05	5.03	4.95	4.96	Vision Gauge
Rad	+/-0.5	0.03	0.04	0.06	0.11	0.07	0.24	0.15	0.05	0.03	-0.05	-0.04	
7	30.00	29.40	29.90	29.90	29.60	29.55	29.40	29.65	29.60	29.70	29.65	30.05	Microscope
	+/-5.00	-0.60	-0.10	-0.10	-0.40	-0.45	-0.60	-0.35	-0.40	-0.30	-0.35	0.05	
8	65.00	64.40	64.55	64.50	64.30	64.40	64.50	64.45	64.50	64.20	64.60	64.60	Microscope
	+/-5.00	-0.60	-0.45	-0.50	-0.70	-0.60	-0.50	-0.55	-0.50	-0.80	-0.40	-0.40	
9	105.00	106.25	106.20	106.50	106.15	106.35	106.50	105.60	106.10	106.10	106.00	105.70	Microscope
	+/-5.00	1.25	1.20	1.50	1.15	1.35	1.50	0.60	1.10	1.10	1.00	0.70	
10	90.00	92.50	89.50	89.60	89.50	89.30	89.40	88.95	89.20	89.50	89.20	88.90	Microscope
	+/-5.00	2.50	-0.50	-0.40	-0.50	-0.70	-0.60	-1.05	-0.80	-0.50	-0.80	-1.10	
Angle	99.46	99.60	99.10	99.50	99.10	99.20	99.50	99.30	99.60	99.50	99.40	99.50	Vision Gauge
11		0.14	-0.36	0.04	-0.36	-0.26	0.04	-0.16	0.14	0.04	-0.06	0.04	
Angle	96.62	96.60	96.40	96.80	96.80	96.40	96.30	96.60	96.40	96.80	96.30	96.20	Vision Gauge
12		-0.02	-0.22	0.18	0.18	-0.22	-0.32	-0.02	-0.22	0.18	-0.32	-0.42	
13	833.00	832.40	832.60	832.10	832.15	832.30	832.55	832.10	832.35	832.90	832.45	832.25	Microscope
	-1.00	-0.60	-0.40	-0.90	-0.85	-0.70	-0.45	-0.90	-0.65	-0.10	-0.55	-0.75	
14	102.00	102.00	101.85	102.05	101.90	101.75	102.30	102.20	102.30	102.15	102.45	102.10	Microscope
	+/-2.00	0.00	-0.15	0.05	-0.10	-0.25	0.30	0.20	0.30	0.15	0.45	0.10	
15	144.00	143.10	143.05	143.00	143.20	143.15	143.05	143.20	143.25	143.05	143.50	143.20	Microscope
	+/-1.00	-0.90	-0.95	-1.00	-0.80	-0.85	-0.95	-0.80	-0.75	-0.95	-0.50	-0.80	
Mat. thickness		29.53	29.53	29.61	29.53	29.53	29.53	29.53	29.92	29.53	29.53	30.51	
Mag		x32	x32	x32	x32	x32	x32	x32	x32	x32	x32	x32	

NRC·CNRC
Integrated Manufacturing Technologies Institute

Measured Dimensions
Flow Effector

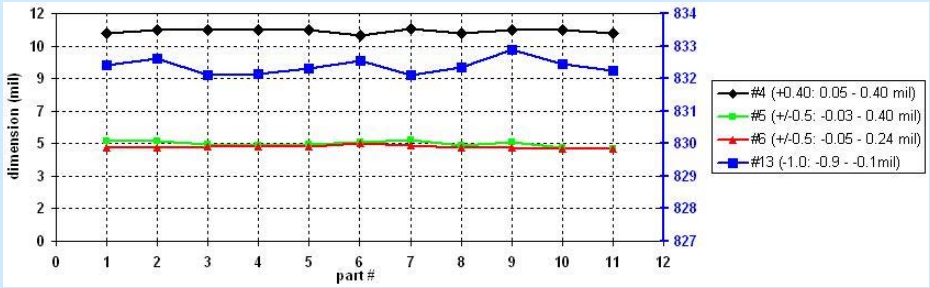

NRC·CNRC
Integrated Manufacturing Technologies Institute

Measured Dimensions
Holes

Holes									mark		new drill		
Edge	10.00	9.84	9.88	10.00	10.75	10.12	9.50	10.00	10.12	10.31	10.35	9.96	Microscope
Top	6.00	6.33	6.20	6.20	6.13	6.16	6.36	6.47	6.49	6.46	6.12	6.08	V. Gauge 64x
Dia	+/-0.50	0.33	0.20	0.20	0.13	0.16	0.36	0.47	0.49	0.46	0.12	0.08	
Sym		14.80	15.08	14.96	14.65	14.53	14.65	14.84	14.96	14.88	14.80	15.08	Microscope
		14.76	14.80	14.69	14.80	14.53	14.92	14.80	15.00	14.45	14.92	15.35	Microscope
Bott	6.00	6.26	6.36	6.29	6.27	6.13	6.44	6.34	6.45	6.49	6.08	6.11	V. Gauge 64x
Dia	+/-0.50	0.26	0.36	0.29	0.27	0.13	0.44	0.34	0.45	0.49	0.08	0.11	
Sym		14.96	15.24	14.76	15.24	14.57	14.76	14.96	15.04	15.04	14.65	14.84	Microscope
		14.57	14.57	14.88	14.65	15.00	14.96	14.65	14.96	14.21	14.88	15.51	Microscope
B.C.	135.00	134.84	135.15	135.00	135.20	135.05	135.10	135.05	135.15	135.10	135.05	135.15	Microscope

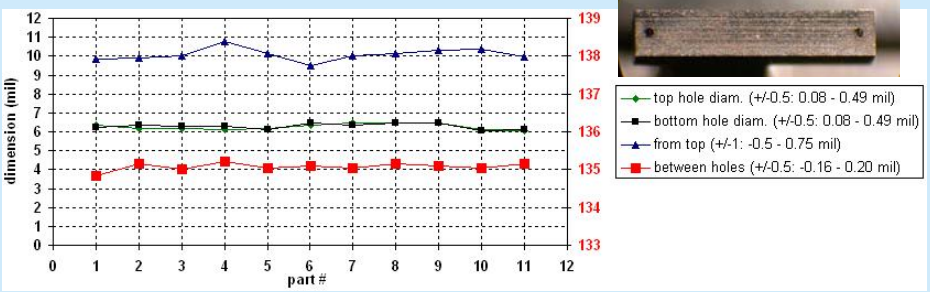

NRC·CNRC Integrated Manufacturing Technologies Institute

Measured Dimensions Test Bench

Flow Effector Ver 4.1 Test Bench (FW05090101_test_bench)

Dim	Part# Req	18 Mill 3	19 Mill 3	Method
1	155.00	154.90	154.70	Microscope
	+/-1.00	-0.10	-0.30	
2	30.00	30.30	30.45	Microscope
	+2.00	0.30	0.45	
3	10.00	10.35	10.00	Microscope
	+0.40	0.35	0.00	
4***	11.00	11.20	11.00	Microscope
	+0.40	0.20	0.00	
5 L	5.00	5.35	5.15	Vision Gauge
Rad	+/-0.5	0.35	0.15	
6 R	5.00	5.08	5.00	Vision Gauge
Rad	+/-0.5	0.08	0.00	
7	30.00	29.45	29.15	Microscope
	+/-5.00	-0.55	-0.85	
8***	65.00	64.35	64.45	Microscope
	+/-5.00	-0.65	-0.55	
9	105.00	105.80	106.35	Microscope
	+/-5.00	0.80	1.35	
10	90.00	89.15	89.45	Microscope
	+/-5.00	-0.85	-0.55	
Angle	99.46	99.60	99.50	Vision Gauge
11		0.14	0.04	
Angle	96.62	96.30	96.40	Vision Gauge
12		-0.32	-0.22	
13	833.00	832.50	833.00	Microscope
	-1.00	-0.50	0.00	
16	94.00	93.35	93.50	Microscope
	-2.00	-0.65	-0.50	

Dim	Part# Req	18 Mill 3	19 Mill 3	Method
16	94.00	93.35	93.50	Microscope
	-2.00	-0.65	-0.50	
17	255.00	255.25	255.20	Microscope
	+/-5.00	0.25	0.20	
18***	101.00	100.05	100.40	Microscope
	+/-1.00	-0.95	-0.60	
19	59.00	58.95	59.00	Microscope
	+/-5.00	-0.05	0.00	
20	32.00	31.35	31.50	Microscope
	+/-5.00	-0.65	-0.50	
21	19.00	19.70	19.70	Microscope
	+/-5.00	0.70	0.70	
Mat. thickness		30.51	30.51	
Mag		x32	x32	

Holes

Dim	Part# Req	18	19	Method
Edge	10.00	10.24	10.24	Microscope
Top Dia	6.00	6.13	6.15	Vision Gauge @64x
	+/-0.50	0.13	0.15	
Sym		15.35	15.24	Microscope
		15.28	15.24	Microscope
Bott Dia	6.00	6.20	6.10	Vision Gauge @64x
	+/-0.50	0.20	0.10	
Sym		15.08	15.24	Microscope
		15.16	15.24	Microscope
B.C.	135.00	135.25	135.25	Microscope

NRC·CNRC Integrated Manufacturing Technologies Institute

Tool Wear Study

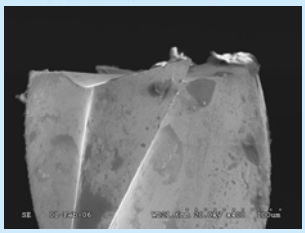
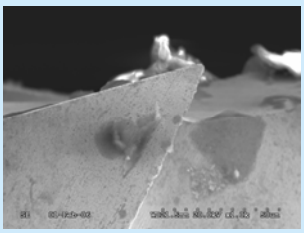
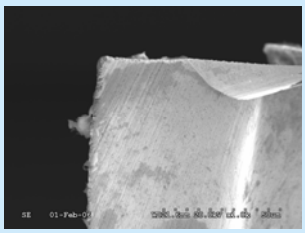

New micro mill tool

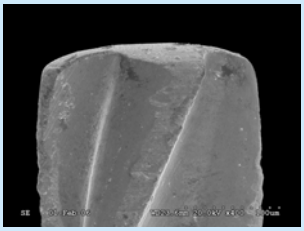
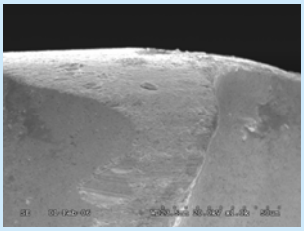
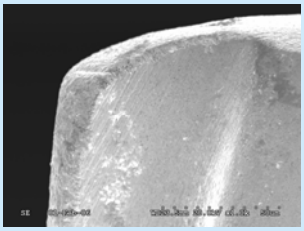

Tool after 11 parts machined

NRC·CNRC
Integrated Manufacturing Technologies Institute

Change in surface roughness

part #1 part #10 part #15

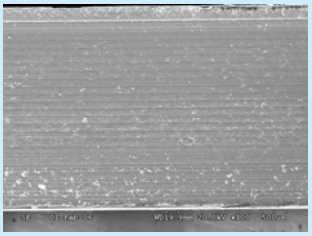
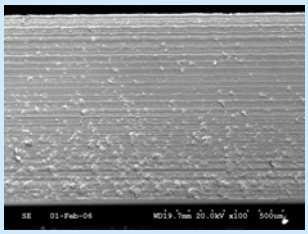
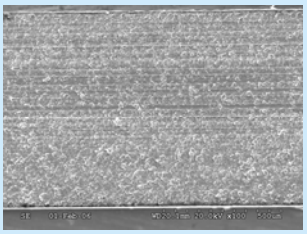

x100

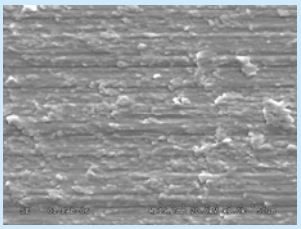
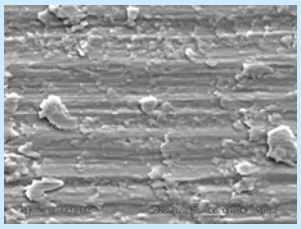
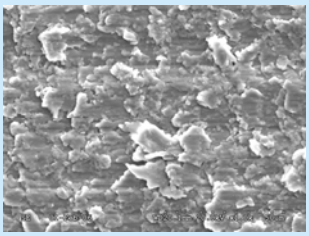

x1000

NRC·CNRC
Integrated Manufacturing Technologies Institute

WYKO Measurements

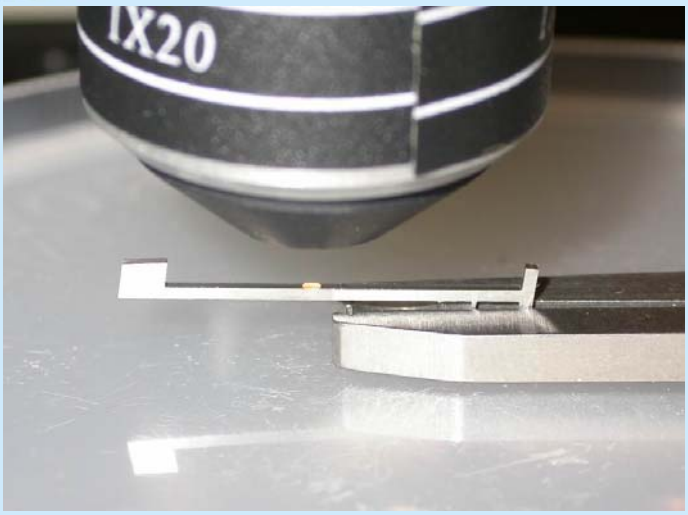

NRC·CNRC Integrated Manufacturing Technologies Institute

Change in surface roughness

part #1 part #10 part #15

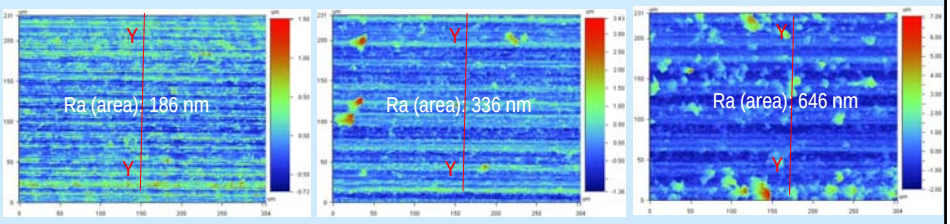

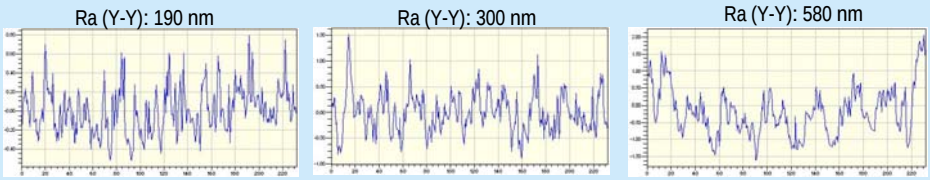

4-5 parts per tool

NRC·CNRC Integrated Manufacturing Technologies Institute

Change in surface roughness

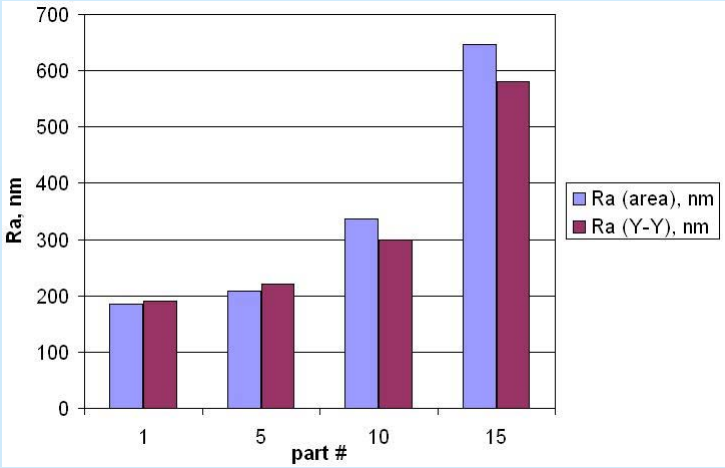

NRC·CNRC
Integrated Manufacturing Technologies Institute

Coolant Effect on Surface Quality

Flat Surface Test

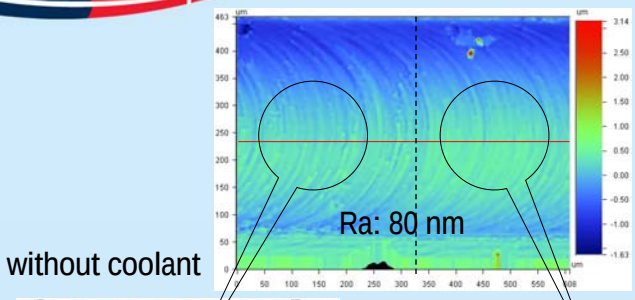

without coolant

with coolant

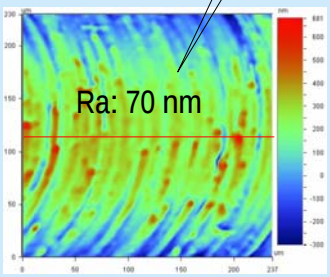

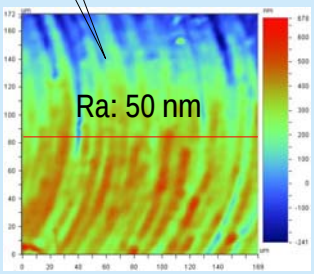

NRC·CNRC
Integrated Manufacturing Technologies Institute

Coolant Effect on Surface Quality

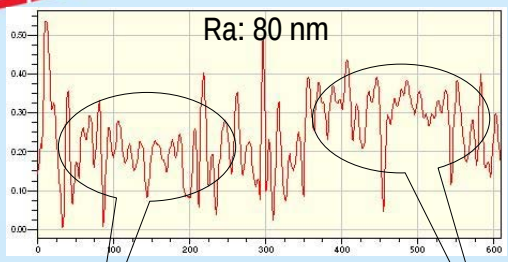

without coolant

with coolant

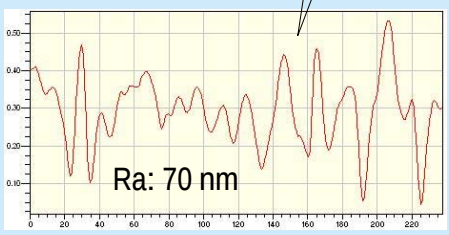

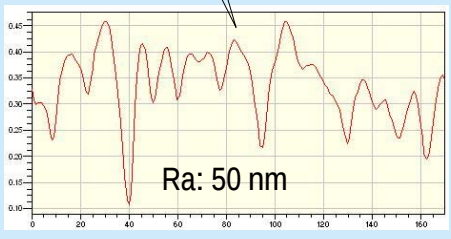

NRC·CNRC
Integrated
Manufacturing
Technologies
Institute

Acknowledgements

- Dr. Frank Wong, DRDC
- Dr. Evgueni Bordatchev, NRC-IMTI
- Mr. Hugo Reshef, NRC-IMTI

7. Control Synthesis

7.1 Position Control of SMA Actuation

presented by N. Léchevin, DRDC-Valcartier

A practical digital controller was designed with the objective of controlling the effector position of an SMA actuation mechanism over a range of 1 mm and within a bandwidth of [0 Hz, 1 Hz]. The plant under digital control comprised the compliant flow effector, the SMA wires, the power drive and the electronics. To meet the stringent positioning and rate requirements, a two-step variable structure set-point regulator was proposed. The controller is comprised of two parts. First, to guarantee fast transients, a bang-bang controller is activated whenever the regulation error is above a fixed threshold. Second, a linear digital controller is switched on when the error reaches the threshold. The linear digital controller provides smooth convergence of the closed-loop system to the steady state and prevents high frequency chattering, which is typical of bang-bang control.

Since the available micromechanical model of the SMA actuator was not intended for control studies, a discrete-time parameter identification of the actuated flow effector was carried out prior to control synthesis. With the discrete-time linear plant model obtained, the design of a digital controller followed. The closed-loop discrete-time control system had to satisfy 1) closed-loop pole-placement and 2) steady-state error requirements. Experimental results showed that the two-step variable structure controller satisfies the required specifications, providing response times below 0.3 sec with overshoot of about 5% of the steady state value.

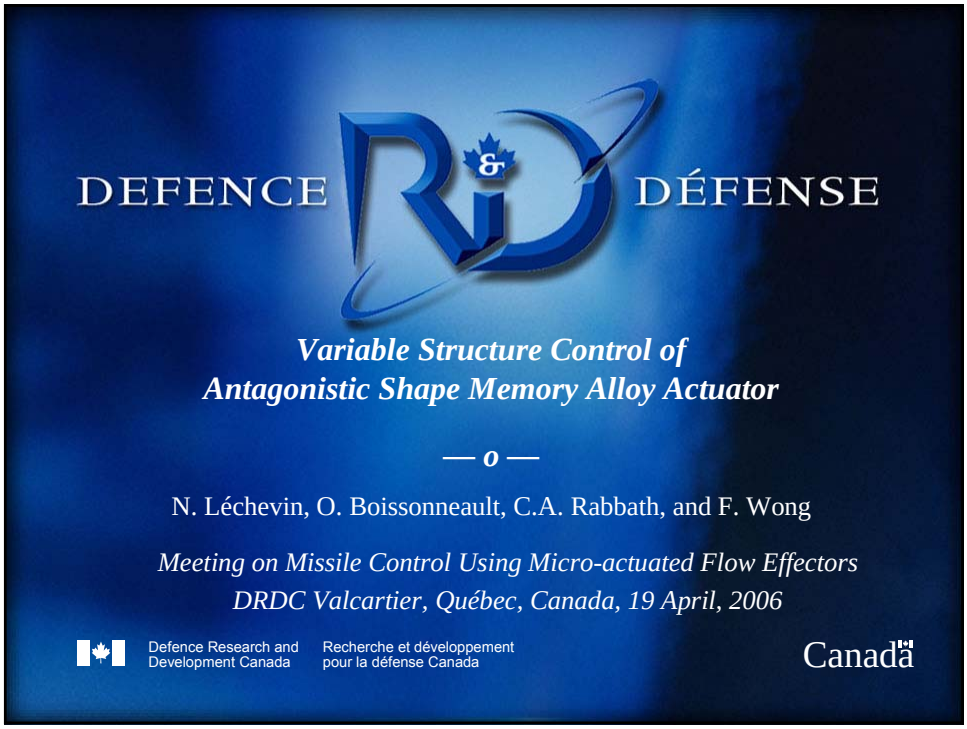

Outline

1. Control System for SMA-based Effector Positioning
2. Objectives
3. Previous Studies in Open Literature
4. Variable Structure Control Approach
5. Parameter Identification
6. DT Control
7. Experimental Results
8. Conclusions
9. References
10. List of Publications

1- Control System for SMA-based Effector Positioning

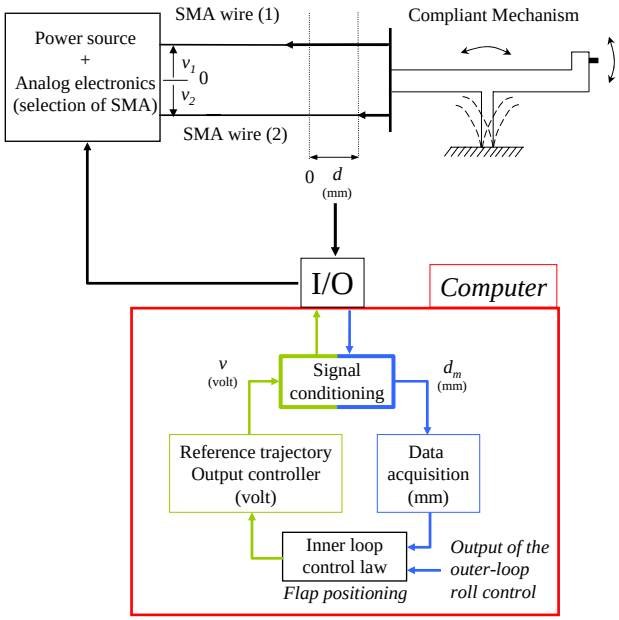

1- Control System for Effector Positioning (Cont'd)

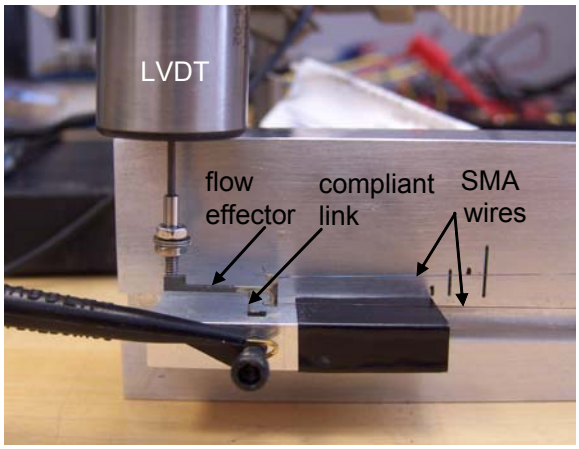

LVDT: linear variable displacement transducer;
SMA : shape memory alloy.

2. Objectives

- Robustness with respect to parametric uncertainties such as friction and the aerodynamic force.
- Compensate for the hysteretic behavior of the actuator;
- Good tracking performance within [0 Hz, 1 Hz];
- Zero steady-state error ⇒ avoid chattering;
- Displacement Range : 1 mm

3. Previous Studies in Open Literature

Hysteresis model-based Control: Preisach model and the like to compensate for hysteresic nonlinearity - [0,0.1Hz]

- Adaptive control : [Webb *et al*., 98], [Kokotovic *et al*., 96]
- Stochastic approach + PID controller + PWM: [Majima *et al*, 01];

Non-model-based Control

- Dissipativity-based PD controller: [Gorbet *et al.*, 97-01]
- Time-delay control: [Lee *et al.*, 04];
- Quasi-linearization by open-loop compensation with phaser: [Cruz-Hernandez and Hayward., 01, 05];
- Variable structure control: [Grant and Hayward., 97];

Drawbacks: o Sensitivity to model uncertainties;
o Mechanical load is not considered, [Gorbet, 01].

4- Variable Structure control

Quasipassive approach (2004/05)

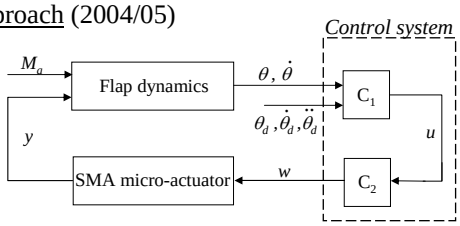

C_1: $u = U / b_1 \tanh(z/\varepsilon)$

C_2 : $w = k_p u + k_d \dot{u}$

Bang-bang + DT law (2005/06)

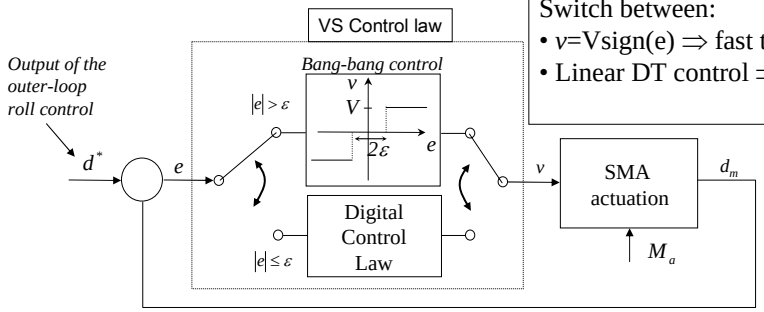

Switch between:
- v=Vsign(e) ⇒ fast transient
- Linear DT control ⇒ set-point regulation

4- Variable Structure Control

The design of the linear DT control law is based on a *linear approximation* with a *pure delay* of the SMA actuator.

- Quasilinearization by open-loop compensation with phaser: [Cruz-Hernandez and Hayward., 01, 05]

⇒ nonparametric identification: estimation of the phase lag in the Bode diagram;

⇒ design of a phaser to compensate for the delay;

- *1. Parameter identification* (ARX model)

2. *A LTI DT controller* is designed from *1*.

5- Parameter Identification

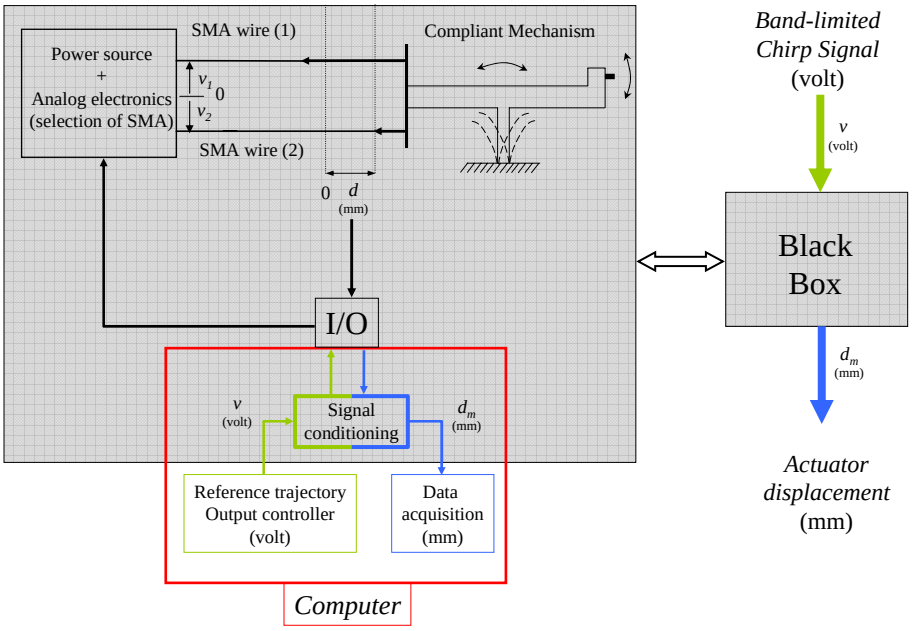

5- Parameter Identification (Cont'd)

a) Experiment

INPUT : *Band-limited Chirp Signal v* (volt) $0.3\,\text{Hz} \le f \le 1\,\text{Hz}$

- Each test is performed with a constant amplitude: V_a

OUTPUT: *Measured displacement (d_m) stored in the board*

> INPUT and OUTPUT are stored for each V_a
>
> V_a is swept from 1 V to 4.5 V

b) Off-line parameter identification

ARX model: $y(t) + a_1 y(t-1) + \ldots + a_{na} y(t-na) = b_1 u(t-nk) + \ldots + b_{nb} u(t-d-nb+1)$

y: d_m , *d: pure delay*
u: v , *na: number of poles* , *nb-1 : number of zeros*

FOR each V_a GET *(v, d_m)*
FOR na= 1:5
FOR na= 1:5
FOR d=1:15
(a_1,…,a_{na},b_1,…,b_{nb})=ARX(v, d_m,na,nb,d)
END END END END

> KEEP coefficients which provide a fitting ratio ≥ 80%

6- DT Control

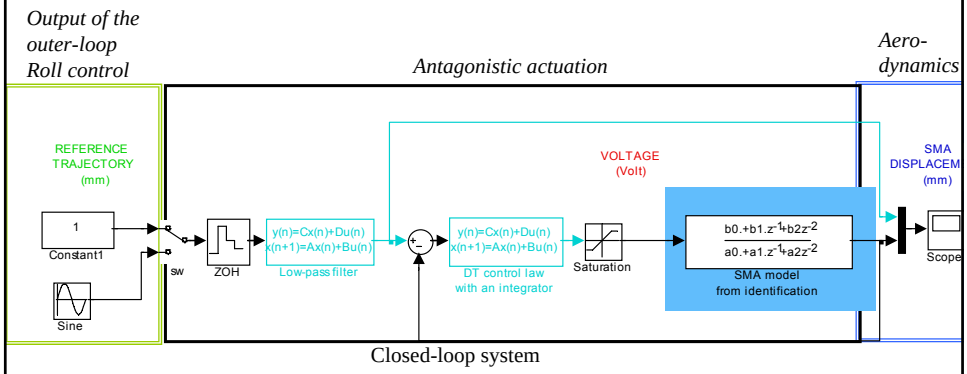

DT Control law objectives:

- ❑ Fast and Accurate set-point regulation
- ❑ Achieve smooth transition
  - ► Pole placement of the closed loop
  - ► Low-pass filter
  - ► Update initial condition of controller integrators

6- DT Control (Cont'd)

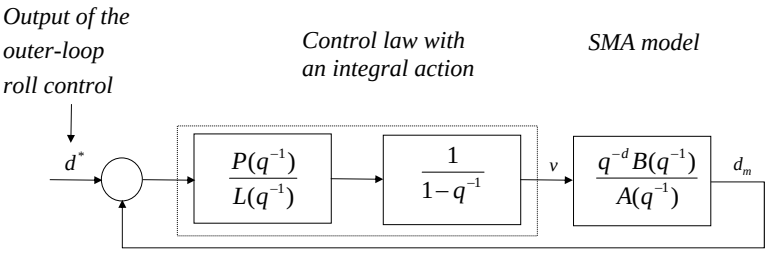

COMPUTATION of the Control Law matrices: direct digital method
[Astrom and Wittenmark, 90]

- ❑ Include an integrator in front of the plant;
- ❑ Closed-loop pole placement ;
- ❑ Solve a Diophantine equation system to obtain coefficients of polynomials $P(q^{-1})$ and $L(q^{-1})$.

7- Experimental Results

- Sample period : 5 ms (time constants of the heat transfer dynamics and of the compliant mechanism dynamics are larger than 100 ms);
- deg B = 1 , deg A = 2;
- Pole placement: $s_1 = s_2 = -3$, $s_3 = s_4 = s_5 = -30$;

$$\frac{v(k)}{e(k)} = \frac{1 - 1.5676q^{-1} + 0.5918q^{-2}}{3.4062 - 6.5593q^{-1} + 3.1582q^{-2}}$$

$$\varepsilon = 0.15 \text{ mm}$$

$$V = 3 \text{ volts}$$

- PWM voltage source control: f_{sw} = 400 Hz; $0V \le v \le 3$;
- SMA Wires: length = 5 in, diameter = 0.004 in;

- Set-point command: $0 \text{ mm} \le d^* \le 1 \text{ mm}$
  f = 0.25 Hz and 0.5 Hz.

7- Experimental Results

f = 0.25 Hz

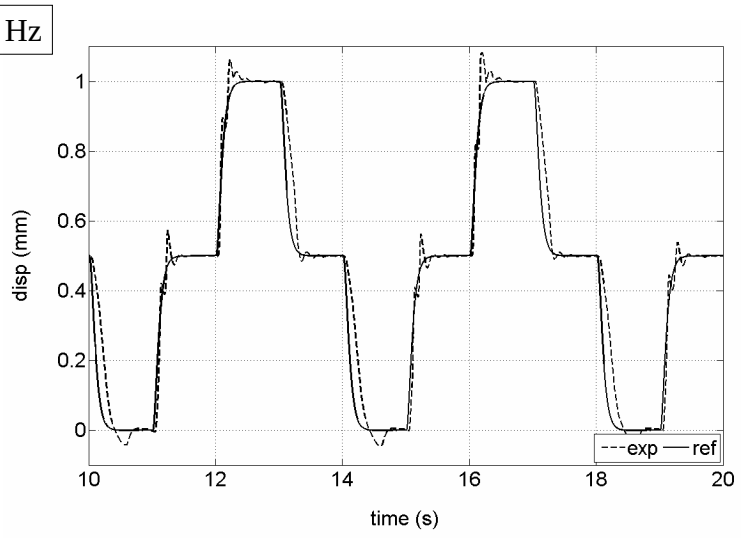

- Response time is less than 0.3 sec;
- Overshoot of about 5% of the steady state value;
- Zero steady-state error.

7- Experimental Results

f = 0.5 Hz

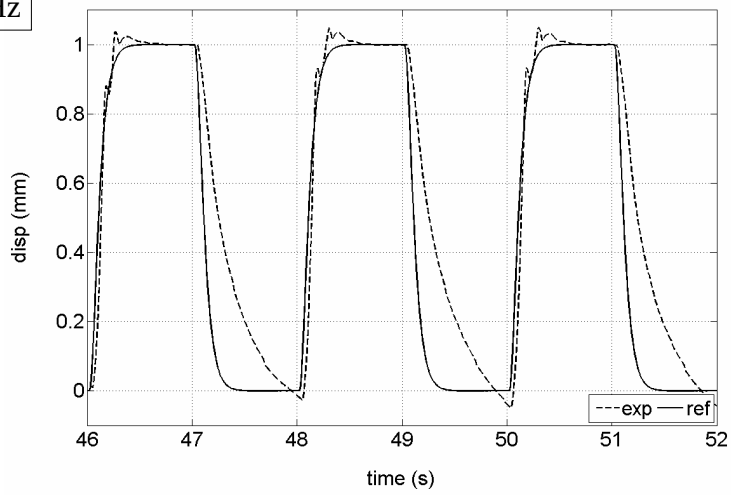

Difference between the rising and the descending phases caused by:

- Longer cooling time required by the SMA wires;
- Asymmetric moment arm.

8- Conclusion

- Variable Structure Controller is devised to achieve robust control and fast positioning of the effector;
- A linear Discrete-time law based on model identification is designed to achieve zero steady-state error without chattering.

Future Work: increase actuator response times

- Investigate cooling phase: smaller diameter wires
  $\Rightarrow$ tradeoff between diameter and mechanical load;
- Increase the moment arm of the bottom wire.

9. References

See references in: "71-NL-Quasipassive-apr2005, " *Missile flight control using micro-actuated flow effector – Review of fiscal year 2004/2005 progress* – Technical note TN 2005-282, April 2005.

[1] J.M. Cruz-Hernandez and V. Hayward, "Phase Control Approach to Hysteresis Reduction," *IEEE Transactions on Control Systems Technology*, Vol. 9, No. 1, pp. 17-26, January 2001.

[2] J. Cruz-Hernandez, M. and Hayward, "Position Stability For Phase Control Of The Preisach Hysteresis Model," *Transactions of the CSME (Special Edition)*, Vol. 29, No. 2, pp. 129-142, June 2005.

[3] Astrom, K.J. and Wittenmark, B., (1990) *Computer-Controlled Systems: Theory and Design*, Prentice Hall, NJ.

10. List of Publications

[1] N. Léchevin, C.A. Rabbath, F.C. Wong et O. Boissonneault, "Quasipassivity-based Robust Nonlinear Flap Positioning Control Using Shape Memory Alloy Micro-Actuators," *Transactions of the Canadian Society for Mechanical Engineering (Special Edition),* Vol. 29, No. 2, June 2005.

[2] N. Léchevin and C.A. Rabbath, "Quasipassivity-based Robust Nonlinear Control Synthesis for Flap Positioning Using Shape Memory Alloy Micro-Actuators," in *Proceedings of the 24th American Control Conference*, Portland, OR, June 2005.

[3] F.C. Wong, C.A. Rabbath, D. Corriveau, N. Hamel, N. Léchevin, O. Boissonneault, and S. Chen, "Missile Flight Control using Micro-actuated Nose-mounted Flow Effectors," *NATO Applied Vehicle Technology Panel (AVT) Symposium*, 15-18 May 2006, Amsterdam, The Netherlands.

7.2 Nonlinear Control Methods for Delta Wing Systems with SMA Actuator Dynamics

presented by B. Gordon, Concordia U.

This presentation investigates the application of various nonlinear control methods for delta wing systems using shape memory alloy (SMA) actuator models recently developed at DRDC. Radial basis function (RBF) neural network control, hybrid RBF control, receding horizon control (RHC), and linear parameter-varying (LPV) control approaches are applied to the system. The performance and robustness of the proposed control methods in the presence of uncertainty and SMA actuator time delays are examined. Furthermore, the applicability of the techniques to future experimental work and possible implementation issues are discussed.

Nonlinear Control Methods for Delta Wing Systems with SMA Actuator Dynamics

Mehrdad Pakmehr, Ming Yang, Hojjat Izadi, and B. W. Gordon

CIS Laboratory, Concordia University

April 2006

Overview

1. Delta Wing System
2. Objectives
3. LMI Approach for Stabilizing Adaptive Control
3. Hybrid Adaptive Neural Network Control
4. Vortex Control Combined with SMA Actuator Dynamics
5. Linear Parameter Varying Sliding Mode Control
6. Receding Horizon Control
7. Comparison of Vortex Control Methods
8. Conclusions and Future Work

Vortex Coupled Delta Wing System

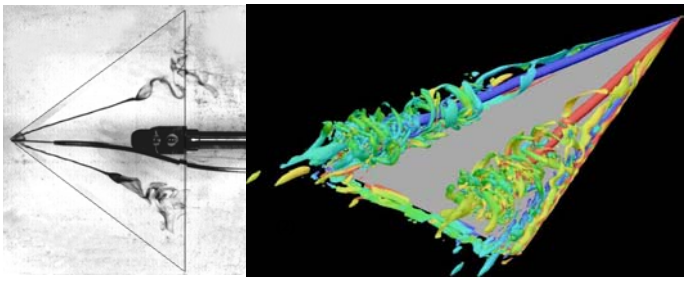

- Aerodynamic loads are dependent on the vortex breakdown location over the delta wing
- Left and right primary vortices need to be considered

$$X_{vbl} = X_{sl}(\phi(t)) + X_q(\dot{\phi}(t)) \cdot X_{sl}(\phi(t)) + \int_{t-T}^{t} X_u(t-\tau)\dot{\phi}(\tau)d\tau$$

$$X_{vbr} = X_{sr}(\phi(t)) + X_q(\dot{\phi}(t)) \cdot X_{sr}(\phi(t)) - \int_{t-T}^{t} X_u(t-\tau)\dot{\phi}(\tau)d\tau$$

3

Delta Wing State Space Model

- State space model (Liu and Gordon, 2004)

$$\begin{cases} \dot{x}_1(t) = c \cdot x_2(t) \\ \dot{x}_2(t) = -c \cdot x_1(t) + x_4(t) + x_4(t-T) \\ \dot{x}_3(t) = x_4(t) \\ \dot{x}_4(t) = -Cl(X_{vbl}, X_{vbr}) \cdot Q - f_c \cdot x_4(t) + 1/I \cdot u_3(t) \end{cases}$$

$$y(t) = x_3(t)$$

$$X_{vbl} = X_{sl}(x_3) + X_{sl}(x_3) \cdot k_q(t) \cdot x_4(t) + a(t) \cdot x_1(t) + u_1(t)$$

$$X_{vbr} = X_{sr}(x_3) + X_{sr}(x_3) \cdot k_q(t) \cdot x_4(t) - a(t) \cdot x_1(t) + u_2(t)$$

- 4th order nonlinear model with time delay *T*

4

Radial Basis Function (RBF) neural network for estimation of rolling moment coefficient Cl

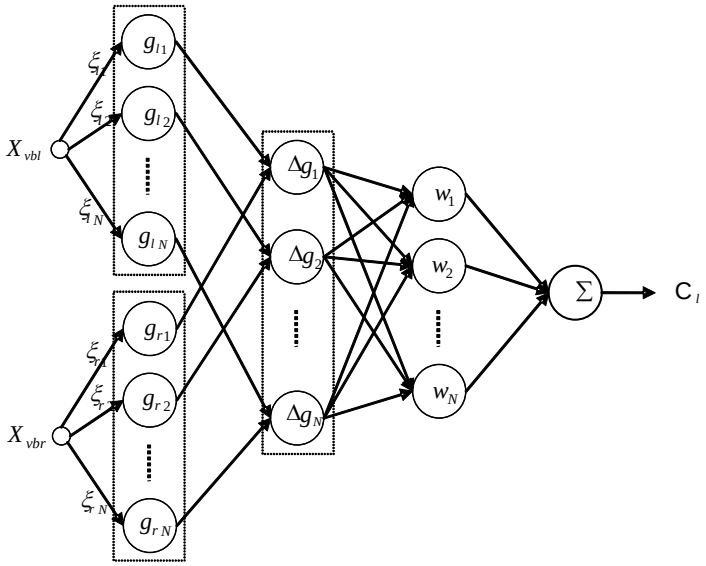

Uncertainty Bound for Neural Network Estimation of Cl

$$\Delta \le a + b\left\|x^*\right\|,\ \Delta = \left|c_l - \hat{c}_l\right|,\ x_i^* = x_i / x_{si}$$

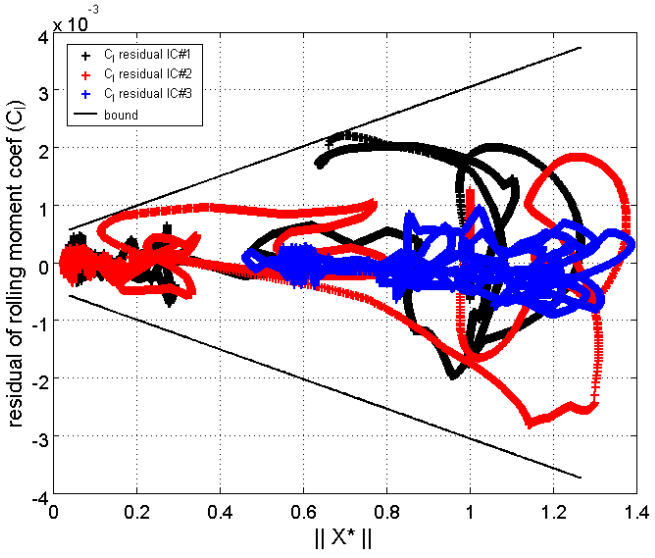

Objectives

- To develop nonlinear tracking controllers for vortex coupled delta wing dynamics
- Controller must compensate for unknown parameters, uncertainty, and time delays
- Combine the nonlinear control methods with shape memory alloy (SMA) actuator dynamics

7

Multiple Input Controller Structure

$$u_3(t) = u(t)$$

$$u_1(t) = \rho_{vbl} u(t)$$

$$u_2(t) = -\rho_{vbr} u(t)$$

- u(t) is the main control input which is the same as what has been presented in the previous section
- The other two control inputs have been defined as perturbations in the left and right vortex breakdown positions
- The relative weighting of the vortex inputs is given by ρ_{vbl}

8

Stabilizing Adaptive Control Approach

- A stabilizing adaptive controller was developed based on existing works (Foda, 1998)
- The controller is based on output measurements
- uncertainty bounds are assumed

$$\left.\begin{aligned}
&\dot{x}(t) = A_0 x(t) + D_0 x(t-\eta) + B_0[u_\rho^d(x_t,t) + h(x_t, Xvb, t)] \\
&u_\rho^d(x_t,t) = -\mu_d H_0 y(t) \\
&\dot{\mu}_d = -g\mu_d + \left\|H_0 y(t)\right\|^2 \qquad \mu_d(t_0) = \mu_d^+ \\
&x_{t_0}(\theta) = \nu(\theta) \quad \theta \in [-\eta, 0]
\end{aligned}\right\}$$

9

Output feedback Matrix H_0

1- In our case as the rows of C_0 are linearly independent so $(C_0 C_0^T)^{-1}$ does exist, and hence $(C_0 C_0^+) = 1$, so we can obtain H_0 as follows:

$$H_0 = B_0^T P_0 C_0^+$$

We can obtain H_0 only if the matching condition has a feasible solution.

2- Defining a constrained linear matrix inequality (LMI) as follows:

$$P_0 A_0 + A_0^T P_0 < 0$$

subject to constraints

$$H_0 C_0 = B_0^T P_0$$
$$P_0 = P_0^T > 0$$
$$H_{0\min} < H_0 < H_{0\max}$$

this can be solved using convex optimization tools, like YALMIP Toolbox, Matlab LMI Toolbox or LMITools, operating in Matlab environment.

10

Flowchart of practical application of delta wing stabilization control process

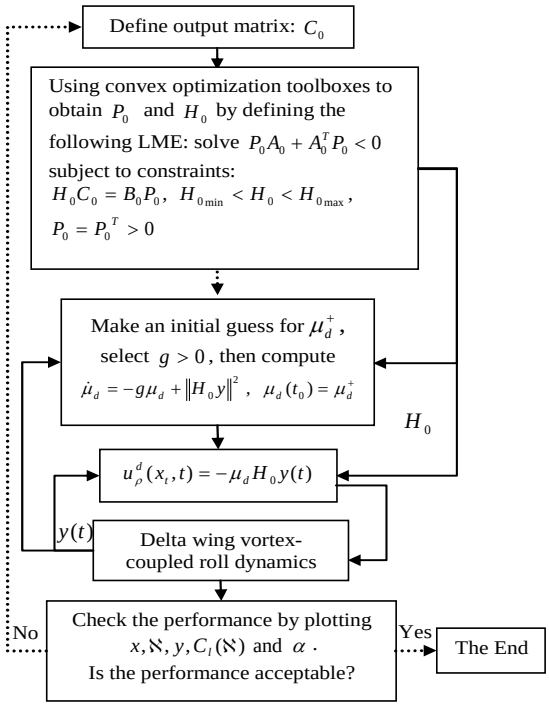

Schematic of the adaptive stabilizing controller

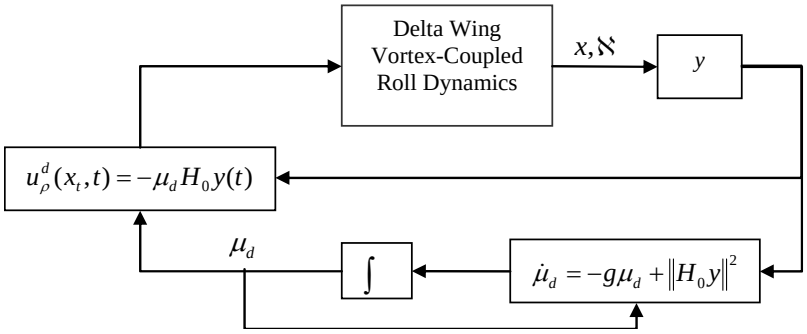

To improve the control task we define the following mechanisms for adaptation gain:

$$\begin{cases} if\ \mu_d < \mu_{\min}\ \&\ \dot{\mu}_d < 0 \Rightarrow \mu_d = \mu_{\min} \\ if\ \mu_d > \mu_{\max}\ \&\ \dot{\mu}_d > 0 \Rightarrow \mu_d = \mu_{\max} \end{cases}$$

12

Modelling Uncertainty Testing

To test the robustness of the method we defined the following disturbance in C_l:

$$\delta C_l = \Delta_{mean} \sin(\omega t)$$

where the Δ_{mean} is a mean value of Δ is

$$\Delta \le a + b\left\|x^*\right\|,\ \Delta = \left|c_l - \hat{c}_l\right|,\ x_i^* = x_i / x_{si}$$
$$a = 0.00047,\ b = 0.00258$$

13

Simulation Results for Stabilizing Controller

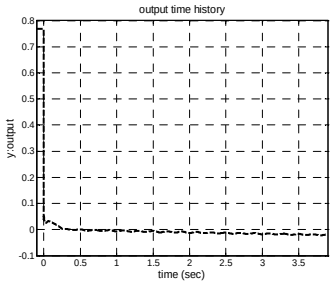

output time history (plant output)

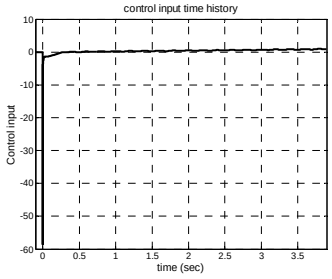

u (control input) time history

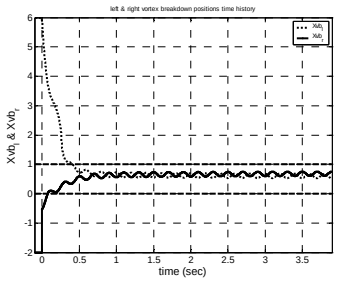

Left and Right vortex breakdown time history

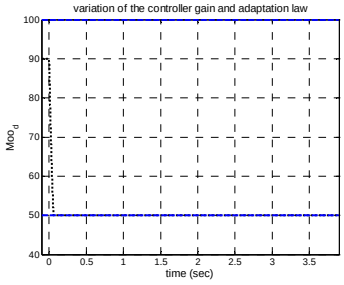

Variation of the controller gain

14

Hybrid Adaptive Neural Network Control

This approach is proposed to address the multiple equilibrium problem and estimation of CI from multiple experimental data sets

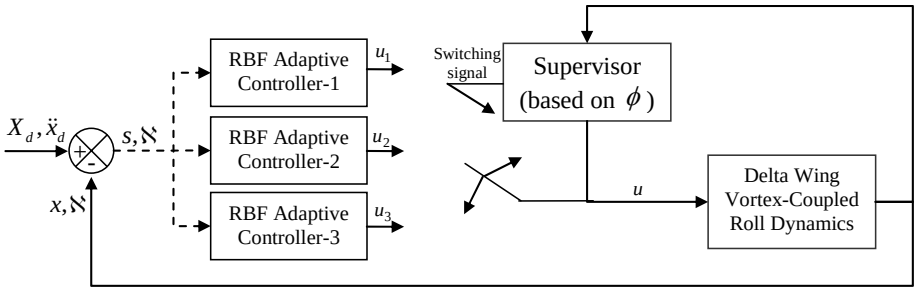

15

Hybrid automaton of the control system

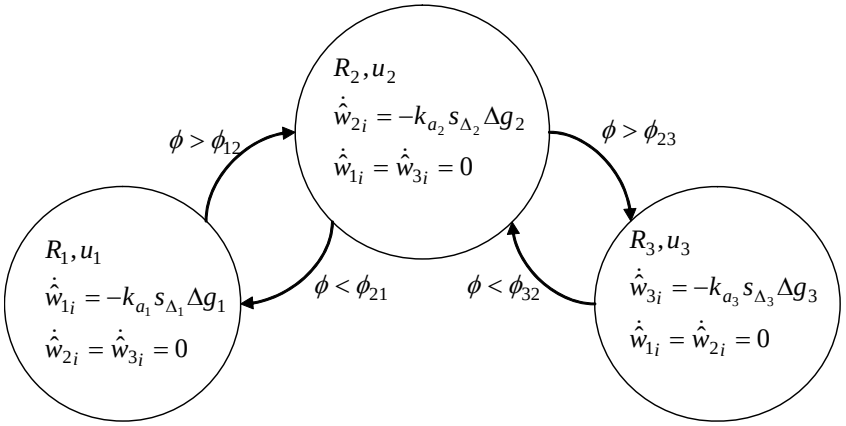

16

Hysteresis switching logic for hybrid control

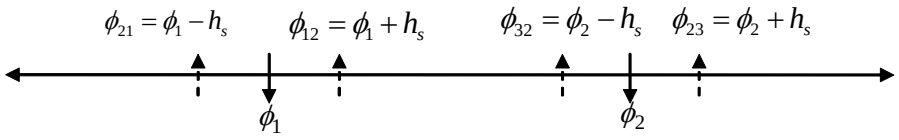

- Hysteresis switching logic is proposed to reduce chattering and limit cycling between the finite states of the hybrid system

17

Simulation Results for Hybrid Controller

$\phi_1 = -20$ [deg], $\phi_2 = 20$ [deg], $h_s = 4$[deg]

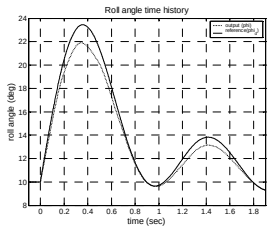

Roll angle time history (plant output)

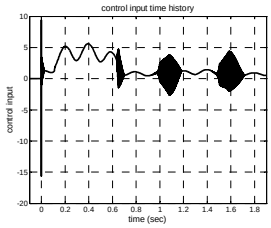

u (control input) time history

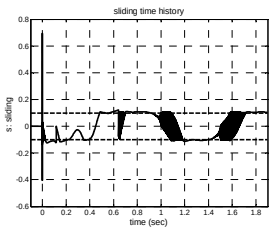

Sliding time history

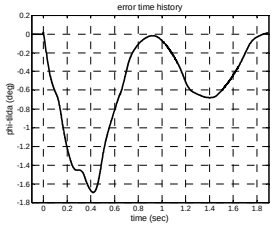

Error time history

18

Neural Network Adaptive Control Combined with SMA Model Developed at DRDC

Vortex coupled delta wing model:

$$\begin{cases} \dot{x}_1(t) = c\,x_2(t) \\ \dot{x}_2(t) = -c\,x_1(t) - \varepsilon_d\,x_2(t) + x_4(t) + x_4(t-T) \\ \dot{x}_3(t) = -\varepsilon_d\,x_3(t) + x_4(t) \\ \dot{x}_4(t) = -C_l(\aleph)Q - f_c\,x_4(t) + h_1 u_1(t)/I_w \end{cases}$$

$$\aleph = [X_{vbl}(t), X_{vbr}(t)]$$

$$X_{vbl}(t) = X_{sl}(x(t)) + X_{sl}(x(t))\,k_q(t)\,x_4(t) + a(t)\,x_1(t) + y_{smal}(t)$$

$$X_{vbr}(t) = X_{sr}(x(t)) + X_{sr}(x(t))\,k_q(t)\,x_4(t) - a(t)\,x_1(t) + y_{smar}(t)$$

$$y(t) = x_3(t)$$

19

Simulink block diagram of *continuous time* approximation of SMA control loop

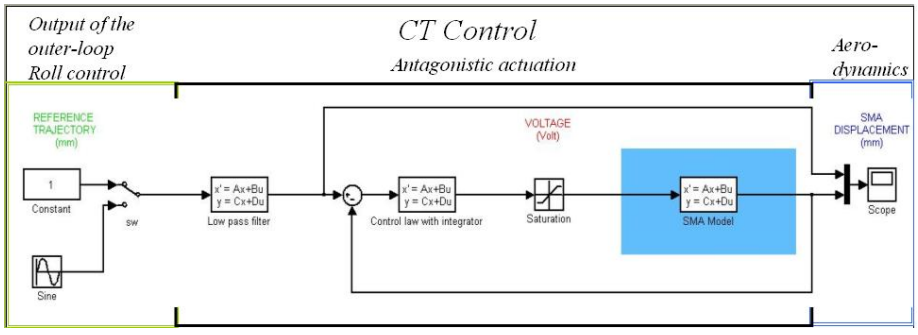

*Léchevin, N., Boissoneault, O., and Rabbath, C. A., "Control of Antagonistic Actuator by Means of Shape Memory Alloy - Identification-Based Control", Internal Report, Defence Research and Development Canada (DRDC), Valcartier, Quebec, Canada, January 5, 2006.

20

Continuous SMA Control System Model

Low pass filter

$$\dot{x}_{lpf}(t) = A_{lpf}x_{lpf}(t) + B_{lpf}u_i(t)$$
$$y_{lpf}(t) = C_{lpf}x_{lpf}(t) + D_{lpf}u_i(t)$$

$$u_i(t) = u_{1,2}(t)$$

Control law with an integrator

$$\dot{x}_{cont}(t) = A_{cont}x_{cont}(t) + B_{cont}u_{cont}(t)$$
$$y_{cont}(t) = C_{cont}x_{cont}(t) + D_{cont}u_{cont}(t)$$

$$u_{cont}(t) = (y_{lpf}(t) - y_{sma}(t))$$

Identified SMA model

$$\dot{x}_{sma}(t) = A_{sma}x_{sma}(t) + B_{sma}u_{sma}(t)$$
$$y_{sma}(t) = C_{sma}x_{sma}(t) + D_{sma}u_{sma}(t)$$

$$u_{sma}(t) = sat(y_{cont}(t))$$

21

Combined control system model

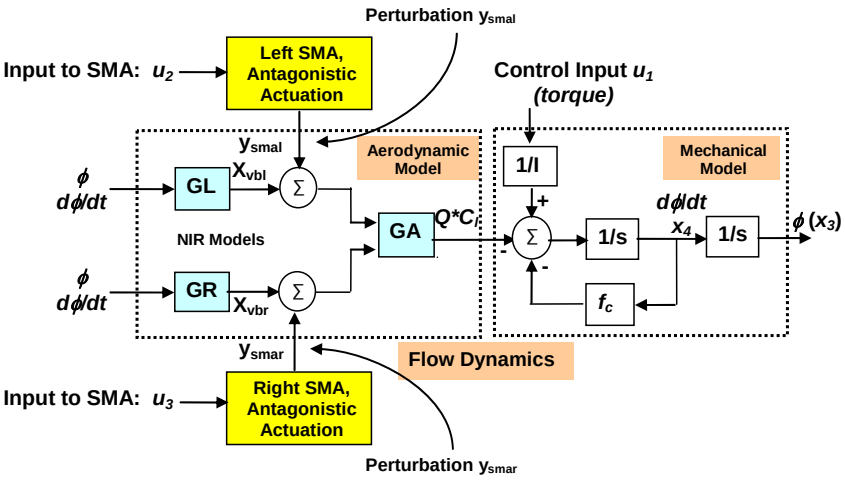

22

Simulation of the combined control system

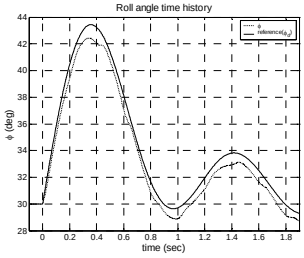

Roll angle time history (plant output and the command signal)

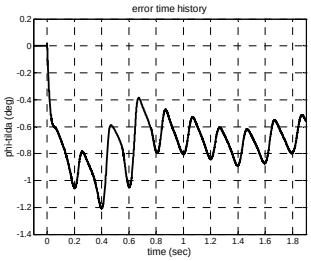

Error time history

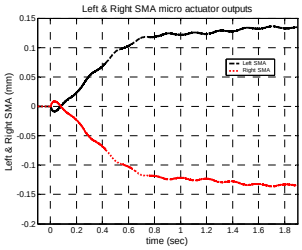

Left and Right SMA control loop output time history

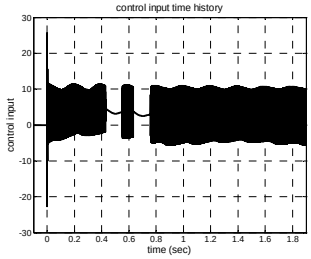

Overall control input time history

23

Linear Parameter Varying Sliding Mode Control (LPVSMC) Approach

LPVSMC drives the state trajectory of a state delayed system onto a parameter-varying sliding surface:

$$\mathbf{s}(\boldsymbol{\sigma}(t)) = \mathbf{H}(\boldsymbol{\sigma}(t))\,\mathbf{z}_w + \mathbf{L}(\boldsymbol{\sigma}(t))\,\mathbf{r} - \mathbf{L}(\boldsymbol{\sigma}(t))\,\hat{\mathbf{C}}(\boldsymbol{\sigma}(t))\,\mathbf{z}_1 + \mathbf{z}_2$$

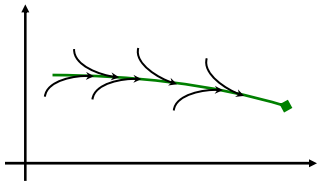

LPVSMC input: $$\mathbf{u}(\boldsymbol{\sigma}(t)) = \begin{cases} \mathbf{u}_{eq}(\boldsymbol{\sigma}(t)) - \mathbf{u}_n(\boldsymbol{\sigma}(t)), & \mathbf{s}(\boldsymbol{\sigma}(t))^T \hat{\mathbf{B}}(\boldsymbol{\sigma}(t)) > 0 \\ \mathbf{u}_{eq}(\boldsymbol{\sigma}(t)) + \mathbf{u}_n(\boldsymbol{\sigma}(t)), & \mathbf{s}(\boldsymbol{\sigma}(t))^T \hat{\mathbf{B}}(\boldsymbol{\sigma}(t)) < 0 \end{cases}$$

$$\mathbf{u}_n(\boldsymbol{\sigma}(t)) = \frac{k\left\|\mathbf{s}(\boldsymbol{\sigma}(t))\right\|}{\left|\mathbf{s}(\boldsymbol{\sigma}(t))^T \hat{\mathbf{B}}(\boldsymbol{\sigma}(t))\right| + \boldsymbol{\varepsilon}}$$

24

LPVSMC Approach

After the sliding surface is reached the state asymptotically approaches the desired trajectory

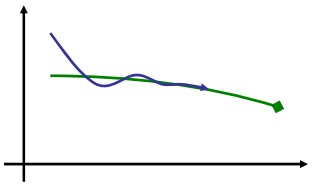

The stability of the state delayed system on the sliding manifold can be proven using a parameter dependant Lyapunov-Krasovskiĭ functional

$$V = V_1(\boldsymbol{\sigma}(t)) + V_2(\boldsymbol{\sigma}(t)) + V_3(\boldsymbol{\sigma}(t))$$

$$V_1(\boldsymbol{\sigma}(t), t) = \mathbf{z}^T(t)\mathbf{P}(\boldsymbol{\sigma}(t))\mathbf{z}(t)$$

$$V_2(\boldsymbol{\sigma}(t), t) = \int_{t-h}^{t} \mathbf{z}^T(\theta)\mathbf{R}(\boldsymbol{\sigma}(\theta))\mathbf{z}(\theta)d\theta$$

$$V_3(\boldsymbol{\sigma}(t), t) = \int_{t-h}^{t}\int_{s}^{t} \dot{\mathbf{z}}^T(\theta)\mathbf{Q}(\boldsymbol{\sigma}(\theta))\dot{\mathbf{z}}(\theta)d\theta ds$$

25

Simulation of LPVSMC with 1st order + delay approximation of SMA actuator dynamics

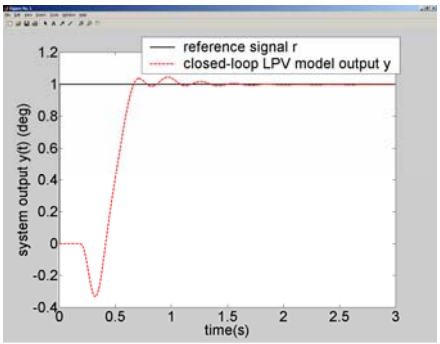

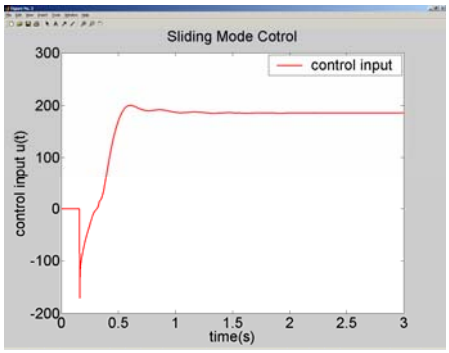

The LPVSMC approach is robust to model uncertainty and time delays

The performance is much better than regular LPV control for the vortex control problem

26

Receding Horizon Control Approach

nominal model: $\dot{x}(t) = f\left(x(t), u(t)\right) \qquad x(0) = x_0$

RHC optimization problem: $\min_{\mathbf{u}(.)} \int_t^{t+T} q(x(\tau), u(\tau))d\tau + V(x(t+T))$

Subject to input or state constraints: $lb_t \le S(x(t), u(t)) \le ub_t$

Closed loop RHC solution: $\dot{x}(\tau) = f\left(x(\tau), u^*(\tau)\right)$

$\tau \in [t, t+\delta), \quad 0 < \delta \le T$

RHC control is well suited to achieve high performance with systems subject to input saturation and other operating constraints

27

Simulation of RHC with 1st order + delay approximation of SMA actuator dynamics

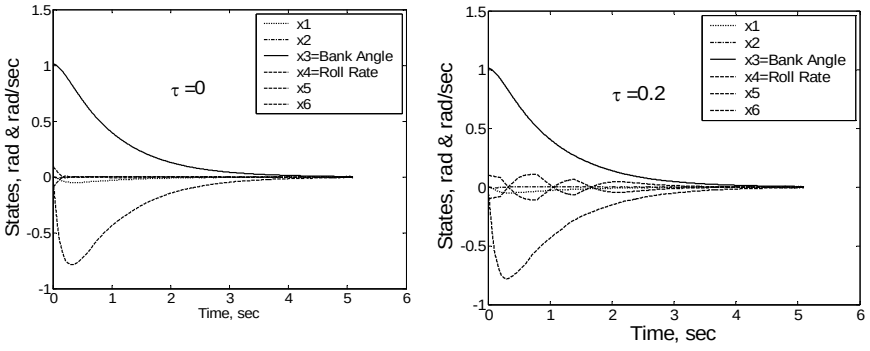

Simulation studies indicate RHC control is robust to model uncertainty and time delays for the vortex control problem

However, no theoretical guarantees are currently available for this class of problems

28

Comparison of Nonlinear Control Approaches

	Tracking performance	Saturation effects	Chattering effects	Robustness to model uncertainty	Robustness to time delays
LMI Adaptive Stabilization	good	high	none	high	high
Neural network adaptive control	excellent	medium	high	medium	medium
Hybrid neural network adaptive control	excellent	medium	high	medium	medium
Linear parameter varying sliding mode control	good	low	medium	high	high
Receding horizon control	excellent	none	none	medium*	high*

* Observed from simulations, but no theoretical guarantees currently exist

29

Conclusions and Future Work

- Nonlinear tracking controllers for vortex coupled delta wing dynamics were developed and tested on simulations
- The nonlinear control methods were combined with shape memory alloy (SMA) actuator dynamics

Possible Future Work:

- Full integration of the proposed vortex control methods with the SMA actuator control approach
- Experimental implementation and investigation
- CFD investigation

30

8. Participant Information

Name	Action List Name	E-mail	Telephone
Olivier Boissonneault	DRDC-ob	oliboiss@hotmail.com	(418) 844-4000 x.4525
Brandon Gordon	Concordia	bwgordon@me.concordia.ca	(514) 848-3175
Xing Zhong Huang	IAR-xzh	xingzhong.huang@nrc-cnrc.gc.ca	(613) 990-6796
Suzhen Chen	IAR-sc	Suzhen.Chen@nrc-cnrc.gc.ca	(613) 998-9685
Suwas Nikumb	IMTI-sn	Suwas.Nikumb@nrc-cnrc.gc.ca	(519) 430-7058
Daniel Corriveau	DRDC-dc	daniel.corriveau@drdc-rddc.gc.ca	(418) 844-4000 x.4156
Nicolas Hamel	DRDC-nh	nicolas.hamel@drdc-rddc.gc.ca	(418) 844-4000 x.4663
Camille Alain Rabbath	DRDC-car	camille-alain.rabbath@drdc-rddc.gc.ca	(418) 844-4000 x.4756
Frank Wong	DRDC-fw	franklin.wong@drdc-rddc.gc.ca	(418) 844-4000 x.4200
Nicolas Lechevin	DRDC-nl	lechevin@aei.ca	(450) 466-2911

9. Bibliography

Documents that have been produced in this Technology Investment Fund project have been categorized here by domain.

General

G1. Wong, F.C., Corriveau, D., Hamel, N., Rabbath, C.A., "Missile Flight Control using Microactuated Flow Effectors – Review of Fiscal Year 2003/2004 Progress", DRDC TN 2004-066, June 2004.

G2. Wong, F.C., Corriveau, D., Hamel, N., Rabbath, C.A., "Missile Flight Control using Microactuated Flow Effectors – Review of Fiscal Year 2004/2005 Progress", DRDC TN 2005-282, September 2005.

G3. Wong, F.C., Rabbath, C-A., Corriveau, D., Hamel, N., Lechevin, N., Boissonneault, O., Chen, S., "Missile Flight Control using Micro-actuated Nose-mounted Flow Effectors", AVT 135 Symposium on Innovative Missile Systems, Paper 21, May 2006.

G4. Wong, F.C., Corriveau, D., Hamel, N., Rabbath, C.A., "Missile Flight Control using Microactuated Flow Effectors – Review of Fiscal Year 2005/2006 Progress", DRDC TN 2006, to be published in September 2006.

Missile Aerodynamics

A1. Jeffrey, A., Wong, F.C., *Air-to-Surface Missile Control Authority Requirements for Actuated Micro-Surfaces*, DRDC Valcartier TM 2004-068, Oct. 2004.

A2. Wong, F.C., Lesage, F., *Exploratory Study of Static Microactuated Flow Effectors – Wind Tunnel Testing*, DRDC Valcartier TM 2004-140, Sept. 2004.

A3. Chen, S., McIlwain, S., Khalid, M., Hamel, N., Lesage, F., Wong, F., "A CFD Investigation on Flow Control using Microstructures", CFD2004, Ottawa, ON, May 2004.

A4. Corriveau, D., "Impact of Nose-Mounted Micro-Structures on the Aerodynamics of a Generic Missile", DRDC Valcartier, TM 2004-310, March 2005.

A5. Chen, S., Khalid, M., "A CFD Investigation of Flow Effector Control for Missile Flight at Supersonic Speed", NRC-IAR, LTR-AL-2005-0016, March 2005.

A6. Hamel, N., Corriveau, D., Wong, F.C., Rainville, P-A., "Numerical Investigation on the Leeside Vortex Manipulation of a Generic Missile", AIAA Paper 2005-4968, 23rd Applied Aerodynamics Conf., Toronto, 5-10 June 2005.

A7. Chen, S., Khalid, M., “Numerical Studies for Slender Body Flight Control using Flow Effectors”, CFD2005, St. John’s, Newfoundland, July 2005.

A8. Corriveau, D., “Impact of Nose-Mounted Micro-Structures on the Aerodynamics of a Generic Missile”, in proceedings of the 22nd International Symposium on ballistics, Vancouver, BC, Nov. 14-18, 2005.

A9. Chen, S., Corriveau, D., McIlwain, S., “Aerodynamic Investigations on Missile Yawing Control using Nose-Mounted Flow Effectors”, submitted to AIAA J., 2005

A10. Corriveau, D., Hamel, N., Wong F.C., “Side Force Generation Mechanism on a Missile with Nose-Mounted Micro-Structures”, AIAA Conference, expected June 2006.

A11. Hamel, N., Corriveau, D., “Study of Flow Behaviour for a Finned Missile Equipped with Nose-Mounted Flow Effectors”, DRDC Valcartier TM 2006, to be published in 2006.

A12. Corriveau, D., Hamel, N., “Impact of Nose-Mounted Micro-Structures on the Aerodynamics of a Finned Missile”, DRDC Valcartier TM 2006, to be published in 2006.

A13. Hamel, N., Corriveau, D., “CFD and Experimental Pressure Measurements on a Missile wiht Nose-Mounted Micro-Structures”, DRDC Valcartier TM 2006, to be published in 2006.

A14. Corriveau, D., Hamel, N., “Impact of Nose-Mounted Micro-Structures on the Aerodynamics of a Finned Missile”, AIAA Conference, Reno, to be published 2007.

Delta Wing Aerodynamics

D1. Huang, X.Z., “Comprehensive Experimental Studies on Vortex Dynamics over Military Wing Configurations in IAR,” AIAA Paper 2003-3940, June 2003. Also CASI Paper 357, 2003.

D2. Huang, X.Z., “Non-Linear Indicial Response / Internal State-Space Representation and Its Applications on Delta Wing Aerodynamics,” AIAA 2003-3944, June 2003. Also CASI Paper 358, 2003.

D3. Huang, X.Z., “Unsteady Behavior of Leading-Edge Vortex at Static and Dynamic Model Conditions,” ICAS 2004-2.9.2, 24th International Congress of the Aeronautical Sciences, 2004.

D4. Huang, X.Z., Y. Mebarki and A. Benmeddour, “Experimental and Numerical Configuration Study on UCAV's Aerodynamics”, ICAS 2004-P.7, 24th International Congress of the Aeronautical Sciences, 2004.

D5. Huang, X.Z., “Mini-Scale PIV Investigations on Wall-Bounded Flows and Wake Flows at Low Reynolds Number Flow Conditions”, AIAA Paper 2005-4606, 23rd Applied Aerodynamics Conf., Toronto, 5-10 June 2005.

D6. Huang, X.Z., Brown, T., Wong, F.C. and Berlivet, T., “A New Concept of Bi-Fold Five Component Balance,” IAR LR-AL-2005, to be published in 2006.

Shape Memory Alloy Actuation

S1. Wong, F.C., Boissonneault, O., Terriault, P., "Hybrid Micro-Macro-mechanical Constitutive Model for Shape Memory Alloys", SPIE Paper 5761-55, 12th SPIE Int. Symposia, Smart Structures and Materials and NDE for Health Monitoring and Diagnostics, 6-10 March 2005.

S2. Wong, F.C., Boissonneault, O., "Shape Memory Alloy-Based Micro-Flow Effector Development for Missile Flight Control", Cansmart 2005, Toronto, 13-14 Oct. 2005.

S3. Wong, F.C., Boissonneault, O., "Behavior of a Hybrid Constitutive Model for Shape Memory Alloy Micro-actuators", 13th SPIE Int. Symposia, Smart Structures and Materials and NDE for Health Monitoring and Diagnostics, Paper SPIE 6170-32, 26 Feb.-2 March 2006.

S4. Boissonneault, O., Wong, F.C., "Modèle numérique hybride macro-micro mécanique d'alliage à mémoire de forme", RDDC Valcartier, TR 2005, to be published in September 2006.

S5. Boissonneault, O., Wong, F.C., "Comportements dynamiques des micro-actuateurs d'alliage à memoire de forme sous une force constante", RDDC Valcartier, TM 2006, to be published in 2006.

S6. Boissonneault, O., Wong, F.C., "Comportements des micro-actuateurs antagonistiques d'alliage à memoire de forme", RDDC Valcartier, TM 2006, to be published in 2006.

S7. Wong, F.C., Rabbath, C.A., Lechevin, N., Boissonneault, O., "Prototype micro-actuated flow effector with closed-loop position control", DRDC Valcartier, TM 2006, to be published in 2006.

Control Synthesis

C1. N. Lechevin, C.A. Rabbath, F.C. Wong and O. Boissoneault, *Quasipassivity-based Robust Nonlinear Control for Flap Positioning Using Shape Memory Alloy Micro-Actuators*, Transactions of the Canadian Society for Mechanical Engineering, Volume 29 Issue 2, Special Edition, 2005, pp. 143-161.

C2. M. Pakmehr, B. W. Gordon and C. A. Rabbath, "Robust Adaptive Tracking Control of Delta Wing Vortex-Coupled Roll Dynamics Subject to Delay", IMECE2005-82196, *Proceedings of 2005 ASME International Mechanical Engineering Congress and Exposition,* Nov. 5-11, 2005, Orlando, FL.

C3. M. Pakmehr, B. W. Gordon and C. A. Rabbath, "Robust Adaptive Tracking Control of Delta Wing Vortex-Coupled Roll Dynamics Subject to Delay and SMA Actuator Dynamics", *Proceedings of IEEE Int. Conf. on Mechatronics and Automation*, Paper # 612, SU-A1-04, July 29 – Aug. 1, Niagara Falls, Ontario, 2005.

C4. M. Pakmehr, B. W. Gordon and C. A. Rabbath, "Robust Adaptive Tracking Control of Delta Wing Vortex-Coupled Roll Dynamics Using RBF Neural Networks", *Proceedings of IEEE Conference on Control Applications 2005,* Toronto, ON, 1039-1043.

C5. N. Lechevin and C.A. Rabbath, “Quasipassivity-based Robust Nonlinear Control Synthesis for Flap Positioning Using Shape Memory Alloy Micro-Actuators”, *Proceedings of American Control Conference 2005*, Portland, OR, June 8-10, 2005, 3019-3024.

C6. Pakmehr, M., Gordon, B.W., Rabbath, C.A., “Control-Oriented Modeling and Identification of Delta Wing Vortex-Coupled Roll Dynamics”, *Proceedings of the 2005 American Control Conference*, Portland, OR, June 8-10, 2005, 1521-1526.

C7. Izadi, H.A., Pakmehr, M., Gordon, B.W., Rabbath, C.A., “A Receding Horizon Control Approach for Roll Angle Tracking of Delta Wing Vortex-Coupled Dynamics”, 2006 American Control Conference, submitted.

C8. Pakmehr, M., Gordon, B.W. and Rabbath, C.A., “Control-Oriented Modeling and Identification of Delta Wing Vortex-Coupled Roll Dynamics”, Submitted to AIAA Journal of Aircraft, March 2006.

Micro-Fabrication

F1. Li, C., Nikumb, S., Wong, F., *An optimal process for femtosecond laser processing of NiTi shape memory alloy for fabrication of miniature devices*, Optics and Lasers in Engineering, 2005, in press or http://www.sciencedirect.com/science?_ob=ArticleURL&_aset=V-WA-A-W-A-MsSAYVW-UUA-U-AAVDDBVDCW-AAVCBACCCW-YUWVAVVWY-A-U&_rdoc=1&_fmt=summary&_udi=B6V4G-4H9PN5G-1&_coverDate=10%2F12%2F2005&_cdi=5758&_orig=search&_st=13&_sort=d&view=c&_acct=C000050221&_version=1&_urlVersion=0&_userid=10&md5=c77d39bc6b740ba86dac37fbd183797c, 3 April 2006.

Distribution list

Internal

Director General (printed pdf document only)
Document Library (3 printed pdf copies)
F.C. Wong (author, printed pdf document only)
N. Hamel (printed pdf document + CD)
D. Corriveau (printed pdf document + CD)
C.A. Rabbath (printed pdf document + CD)
F. Lesage (printed pdf document only)
Hd/PW Section (printed pdf document only)
N. Lechevin (printed pdf document + CD)

External

Director R&D Knowledge and Information Management (pdf file)
Directorate S&T Land (printed pdf document only)
Directorate S&T Land 5 (printed pdf document only)
Directorate S&T Air (printed pdf document only)
Directorate S&T Air 4 (printed pdf document only)
Directorate S&T Air 6 (printed pdf document only)
Directorate S&T Marine (printed pdf document only)
Directorate Air Requirements 5 (printed pdf document only)

Dr. B. Gordon (printed pdf document only)
Department of Mechanical & Industrial Engineering
Concordia University
Office: B-307 (2160b Bishop St.)
1455 de Maisonneuve Blvd. West
Montréal, Québec
H3G 1M8

Dr. S. Chen (printed pdf document + CD)
National Research Council Canada
U-66, 1200 Montreal Road
Ottawa, Ontario
K1A 0R6

Dr. X.Z. Huang (printed pdf document + CD)
National Research Council Canada
M10 rm 208, 1200 Montreal Rd
Ottawa, Ontario
K1A 0R6

Acting Director (printed pdf document only)
Institute of Aerospace Research
National Research Council Canada
M2, 1200 Montreal Road
Ottawa, Ontario
K1A 0R6

Dr. S. Nikumb (printed pdf document + CD)
Production Technology Research
Integrated Manufacturing Technologies Institute (IMTI)
National Research Council
800 Collip Circle
London, Ontario
N6G 4X8

Mr. G. Salloum (printed pdf document only)
Director General
Integrated Manufacturing Technologies Institute (IMTI)
National Research Council
800 Collip Circle
London, Ontario
N6G 4X8

Dr. J. Szabo (printed pdf document only)
Emerging Materials Section
DRDC – Atlantic
P.O. Box 1012
Dartmouth, Nova Scotia
B2Y 3Z7

Dr. C. Hyatt (printed pdf document only)
Emerging Materials Section
DRDC – Atlantic
P.O. Box 1012
Dartmouth, Nova Scotia
B2Y 3Z7

DOCUMENT CONTROL DATA

1. ORIGINATOR (name and address)	2. SECURITY CLASSIFICATION (Including special warning terms if applicable)
Defence R&D Canada - Valcartier 2459 boul. Pie XI North Quebec, QC, G3J1X5	UNCLASSIFIED

3. TITLE (Its classification should be indicated by the appropriate abbreviation (S, C, R or U)
Missile flight control using micro-actuated flow effectors - Review of fiscal year 2005/2006 Progress

4. AUTHORS (Last name, first name, middle initial. If military, show rank, e.g. Doe, Maj. John E.)
F.C. Wong

5. DATE OF PUBLICATION (month and year)	6a. NO. OF PAGES	6b .NO. OF REFERENCES
August 2006	150	37

7. DESCRIPTIVE NOTES (the category of the document, e.g. technical report, technical note or memorandum. Give the inclusive dates when a specific reporting period is covered.)
Technical Note

8. SPONSORING ACTIVITY (name and address)

9a. PROJECT OR GRANT NO. (Please specify whether project or grant)	9b. CONTRACT NO.
13eg16	

10a. ORIGINATOR'S DOCUMENT NUMBER	10b. OTHER DOCUMENT NOS
TN 2006-178	N/A

11. DOCUMENT AVAILABILITY (any limitations on further dissemination of the document, other than those imposed by security classification)

- [X] Unlimited distribution
- [ ] Restricted to contractors in approved countries (specify)
- [ ] Restricted to Canadian contractors (with need-to-know)
- [ ] Restricted to Government (with need-to-know)
- [ ] Restricted to Defense departments
- [ ] Others

12. DOCUMENT ANNOUNCEMENT (any limitation to the bibliographic announcement of this document. This will normally correspond to the Document Availability (11). However, where further distribution (beyond the audience specified in 11) is possible, a wider announcement audience may be selected.)

13. ABSTRACT (a brief and factual summary of the document. It may also appear elsewhere in the body of the document itself. It is highly desirable that the abstract of classified documents be unclassified. Each paragraph of the abstract shall begin with an indication of the security classification of the information in the paragraph (unless the document itself is unclassified) represented as (S), (C), (R), or (U). It is not necessary to include here abstracts in both official languages unless the text is bilingual).

Superior performance is a key goal in weapons design. Missiles must fly faster and farther, and be more agile, compact and lightweight. The United States have been very active in the development of smart structures for military applications such as missile guidance. For example, DARPA and the Air Force Office of Scientific Research are sponsoring the development of miniaturized active flow technologies to achieve far-term objectives for smart bombs and missiles. Their principal concepts for altering the flow around a body are centred on miniaturized devices that are embedded in the missile skin and/or airframe. The objective of this project is to demonstrate with hardware and software: 1) engineered micro-flow effectors of specific geometry and placement that are able to produce controllable aerodynamic forces on a missile under supersonic conditions or a delta wing under subsonic conditions, 2) microactuators that are able to meet the force, kinematic and thermal requirements set by the aerothermal environment and 3) control algorithms running on non-flightweight electronics and feedback sensors that take in command signals and output appropriate actuator drive signals to produce the desired aerodynamic force on a wind or water tunnel delta wing model. This report documents the progress made by the project members for fiscal year 2005/2006 in the areas of missile aerodynamics, delta wing aerodynamics, microactuator modeling, control synthesis and micro-fabrication.

14. KEYWORDS, DESCRIPTORS or IDENTIFIERS (technically meaningful terms or short phrases that characterize a document and could be helpful in cataloguing the document. They should be selected so that no security classification is required. Identifiers, such as equipment model designation, trade name, military project code name, geographic location may also be included. If possible keywords should be selected from a published thesaurus, e.g. Thesaurus of Engineering and Scientific Terms (TEST) and that thesaurus-identified. If it is not possible to select indexing terms which are Unclassified, the classification of each should be indicated as with the title.)

aerodynamics, active flow control, wind tunnel testing, flow effector, force balance, missile, delta wing, vortex control, PIV, CFD, shape memory alloy, modeling, microactuator, compliant mechanism, control synthesis, robust, micro-fabrication, laser machining, sampled-data control, nonlinear

Defence R&D Canada

Canada's Leader in Defence
and National Security
Science and Technology

R & D pour la défense Canada

Chef de file au Canada en matière
de science et de technologie pour
la défense et la sécurité nationale

WWW.drdc-rddc.gc.ca